



Groundwater Modelling for Urban Water Management in Gouda, the Netherlands

Weicheng Chen



Hoogheemraadschap van
Rijnland



**gemeente
gouda**

Groundwater Modelling for Urban Water Management in Gouda, the Netherlands

By

Weicheng Chen

in partial fulfilment of the requirements for the degree of

Master of Science
in Civil Engineering

at the Delft University of Technology,
to be defended publicly on Thursday March 29, 2018 at 13:30

Supervisor:
Thesis committee:

Dr. ir. Frans van de Ven	
Prof. dr. ir. Nick van de Giesen,	TU Delft
Dr. ir. Frans van de Ven,	TU Delft & Deltares
Prof.dr.ir. Mark Bakker,	TU Delft
Ir. Emiel Kruisdijk,	TU Delft
Ir. Neeltje Goeden,	Deltares
Drs. Mark Kramer,	Hoogheemraadschap van Rijnland

This thesis is confidential and cannot be made public until March 29, 2018.

An electronic version of this thesis is available at <http://repository.tudelft.nl/>.

Preface

This research is a small part of the project, Living Lab Land Subsidence, which is aiming to find a sustainable solution for the land subsidence problem in Gouda. This project is established by the water board of Rijnland, the municipality of Gouda, TU Delft, Deltares, and some other research institutions. Being involved in this project is a very special experience for me. I was able to meet and work with colleagues in different organizations and institutions. It gives me chances to have more insight to the Dutch landscape, urban water management system, as well as the groundwater system in the Netherlands. During my modeling procedures, I kept raising problems and solve problems. I enjoyed it and my interest on geohydrology is increasing. I am really grateful that I could have this opportunity to work on such a project. Though the thesis work is completed, I still have strong curiosity on geohydrologic topics like the simulation of the heterogeneity of the hydraulic properties of the subsurface, data-driven groundwater modeling and groundwater model calibration techniques. I am willing to work on geohydrology studies or related engineering programs in my future career life.

During my thesis work, I have gotten a lot of help in all aspects which I am really grateful. I would like to thank to my supervisor, Frans van de Ven, for his kindly patients, guidance and courage. It was not easy to construct a groundwater model for an urban area because of its high spatial and temporal heterogeneity, and I got stuck sometimes. He gave me a lot of support and inspiration in all aspects throughout my master research. I am also want to thank Neeltje Goorden, Mark Bakker and Mark Kramer for the advices and support I got on groundwater model set up and calibration. In addition, I would like to express my thanks to Arianne Fijan, Marjon ten Hagen, André 't Jong, Jan Prinsen for their kindly help and suggestion during my work.

At last, I would like to thank my parents, for their courage and concern. Pursuing a master degree in a country which is around 9000 km away from my hometown is quite hard for me at the beginning. Only with their courage I gradually get used to my school life and personal life here in the Netherlands. Now I am really glad that I finally conquered all the difficulties I met and I am ready to face the challenges in the future.

*Weicheng Chen
Delft, February 2018*

Contents

Abstract	1
Overzicht	1
1 Introduction.....	5
1.1. Land subsidence in Gouda	6
1.2. Groundwater modelling in urban scale.....	10
2 Objectives.....	12
3 Groundwater Modelling.....	14
3.1. Data Collection	14
3.1.1. Land surface elevation and subsurface structures.....	15
3.1.2. Land cover	16
3.1.3. Precipitation and Evapotranspiration.....	18
3.1.4. Surface water.....	19
3.1.5. Sewerage pipes.....	20
3.1.6. Phreatic groundwater level	21
3.2. Model Conceptualization and Construction	23
3.2.1. iMod.....	23
3.2.2. Selection of Boundary and Model resolution.....	25
3.2.3. Subsurface	27
3.2.4. Stresses.....	27
3.3. Calibration, validation and sensitivity analysis	34
3.4. Scenarios	36
4 Results	38
4.1. Model Calibration.....	38
4.1.1. Model parameters	38
4.1.2. Groundwater level at steady state	41
4.1.3. Time series at transient state	43
4.2. Model verification	48
4.3. Sensitivity Analysis	53
4.3.1. Conductance of canal bed	54
4.3.2. Conductance of Sewerage pipe walls.....	56
4.3.3. Hydrological conductivity of the upper phreatic aquifer layer	57
4.3.4. Hydrological conductance of the lower phreatic aquifer layer.....	59
4.3.5. Storage coefficient.....	60

4.3.6.	Vertical resistance	62
4.3.7.	Groundwater Recharge	63
4.4.	Scenario Analysis.....	65
4.4.1.	Scenario 1: Water tight sewerage pipes.....	65
4.4.2.	Scenario 2: Lower surface water level in the inner city	66
4.4.3.	Scenario 3: A new canal in Nieuwe Haven	67
4.4.4.	Scenario 4: A new canal in Nieuwe Haven + lower surface water level in the inner city.....	68
4.4.5.	Scenario 5: Infiltration Transportation pipes	69
5	Discussion	71
6	Conclusion.....	74
6.1.	Relevant hydrological processes	74
6.2.	Conceptualization and Construction of Groundwater model.....	75
6.3.	Groundwater model calibration and validation.....	76
6.4.	Sensitivity analysis.....	77
6.5.	Scenario analysis	77
7	Recommendation.....	79
	Bibliography.....	81
	Appendix 1: the mean value and the standard deviation of the level change in sensitivity test.....	85
	Appendix 2: the mean value and the standard deviation of the level change in scenario test.....	95

List of Figures

Figure 1 Dutch polder system (Source: http://redtandem.blogspot.nl/2015/08/five-provinces-in-five-days.html)	5
Figure 2 left: sluices around Gouda in the 15 th Century; right: a bird-view map of the old Gouda drawn in the 16 th Century (Sources: http://goudsvirtueelsluizenmuseum.nl/?page_id=305 ; https://www.sanderusmaps.com/en/our-catalogue/detail/163632/antique-map-of-gouda-by-braun--hogenberg/)	6
Figure 3 Canal Turfmarkt (Source: http://rijksmonumenten.nl/monument/16930/voormalige-synagoge-van-gouda/gouda/)	7
Figure 4 Ages and materials of the sewerage pipes in the inner city	8
Figure 5 Estimated average subsiding rate between 2017 and 2040	9
Figure 6 Comparison among the surface elevation, interference elevation and surface water level (source: https://gis.gouda.nl/gisviewer/viewer.do?appCode=bb3900e12b49685bada6eaf3e4a7407f&forceViewer=true&cmsPageld=1&cmsPageld=1)	9
Figure 7 Groundwater related hydrological processes	14
Figure 8 DTM map of Gouda (Unit: m NAP).....	15
Figure 9 Lithostratigraphy layers of Gouda (Van Laarhoven, 2017)	16
Figure 10 Basic Registration Large-scale Topography map	17
Figure 11 map of pavement materials.....	17
Figure 12 Weather Stations near Gouda.....	18
Figure 13 Monthly average fluxes of precipitation and potential evapotranspiration in Gouda (2000~2017)	19
Figure 14 Planned surface water level in the polders and the boezom.....	19
Figure 15 Sewerage system in Gouda.....	20
Figure 16 Back-stowed system (Wang, 2016).....	21
Figure 17 Observation wells	22
Figure 18 Average phreatic groundwater levels	22
Figure 19 Relationships between Package KDW and KHV, VCW and KVV (Vermeulen et al., 2016)	24
Figure 20 Groundwater extraction wells of Croda (Boleij, 2013).....	25
Figure 21 Change of the phreatic groundwater level after terminating the groundwater winning for best guess and worst case (Boleij, 2013)	26
Figure 22 Groundwater observation at Well 2-1.15.....	26
Figure 23 Comparison of measured surface water level and the planned one in the inner city (Source: http://rijnland.webgispublisher.nl/?map=Rijnland_viewer)	28
Figure 24 Back-stowed pipes and sewer level measurement point	29
Figure 25 Sewerage level observations in the inner city.....	30
Figure 26 Groundwater level observations at Well 1-1.05	30
Figure 27 Changing runoff coefficient according to the changing daily recharge	32
Figure 28 Map of recharge used in groundwater model at steady state (Unit: mm/d)	33
Figure 29 Cumulative frequency curve of Z value	33
Figure 30 Conductance of surface water (Unit: m ² /d).....	39
Figure 31 Conductance of sewerage pipes (Unit: m ² /d)	40
Figure 32 Deviations between the simulated groundwater levels at steady state and average observed sewerage level (Unit: m).....	41
Figure 33 Histogram of the deviation between the simulated value and observed value	41
Figure 34 Groundwater levels along cross sections	42
Figure 35 Calibration at Well 1-1.04 (RMSE = 0.05 m, R ² = 0.996, E = 0.68).....	44
Figure 36 Calibration at Well 1-1.08 (RMSE = 0.09 m, R ² = 0.991, E = -0.66)	44
Figure 37 Calibration at Well 1-1.12 (RMSE = 0.08 m, R ² = 0.988, E = -1.38)	45

Figure 38 Calibration at Well 1-1.14 (RMSE = 0.04 m, $R^2 = 0.996$, $E = 0.37$).....	45
Figure 39 Calibration at Well 2-1.05 (RMSE = 0.06 m, $R^2 = 0.998$, $E = -0.21$)	45
Figure 40 Calibration at Well 2-1.10 (RMSE = 0.20 m, $R^2 = 0.995$, $E = -9.96$)	46
Figure 41 Calibration at Well 2-1.14 (RMSE = 0.04 m, $R^2 = 0.999$, $E = -1.39$)	46
Figure 42 Calibration at Well 2-1.19 (RMSE = 0.10 m, $R^2 = 0.998$, $E = -6.91$)	46
Figure 43 Root mean square error of the groundwater level simulation at observation wells at calibration state (2015-2016)	47
Figure 44 R^2 of the groundwater level simulation at observation wells at calibration state (2015-2016)	47
Figure 45 Nash-Sutcliffe efficiency of the groundwater level simulation at observation wells at calibration state (2015-2016)	47
Figure 46 RMSE of the groundwater level simulation at observation wells at validation state (2016-2017).....	49
Figure 47 R^2 of the groundwater level simulation at observation wells at validation state (2016-2017)	49
Figure 48 Nash-Sutcliffe efficiency of the groundwater level simulation at observation wells at validation state (2016-2017)	49
Figure 49 Validation at Well 1-1.04 (RMSE = 0.06 m, $R^2 = 0.996$, $E = 0.74$)	50
Figure 50 Validation at Well 1-1.08 (RMSE = 0.09 m, $R^2 = 0.992$, $E = -0.75$).....	50
Figure 51 Validation at Well 1-1.12 (RMSE = 0.07 m, $R^2 = 0.993$, $E = -1.49$).....	50
Figure 52 Validation at Well 1-1.14 (RMSE = 0.05 m, $R^2 = 0.995$, $E = 0.28$).....	51
Figure 53 Validation at Well 2-1.05 (RMSE = 0.06m, $R^2 = 0.998$, $E = 0.09$).....	51
Figure 54 Validation at Well 2-1.10 (RMSE = 0.16 m, $R^2 = 0.995$, $E = -14.71$)	51
Figure 55 Validation at Well 2-1.14 (RMSE = 0.05 m, $R^2 = 0.999$, $E = -3.60$).....	52
Figure 56 Validation at Well 2-1.19 (RMSE = 0.08 m, $R^2 = 0.999$, $E = -2.30$).....	52
Figure 57 Validation at PB04 (RMSE = 0.11 m, $R^2 = 0.987$, $E = 0.21$)	52
Figure 58 Validation at PB05 (RMSE = 0.12 m, $R^2 = 0.983$, $E = -2.81$)	53
Figure 59 Validation at PB08 (RMSE = 0.05 m, $R^2 = 0.997$, $E = 0.747$)	53
Figure 60 Change of mean groundwater level after removing 50% of amount from canal conductance (Unit: cm).....	54
Figure 61 Change of mean groundwater level after adding 50% of amount to canal conductance (Unit: cm).....	55
Figure 62 Time series of sensitivity test at Well PB08 (canal conductance)	55
Figure 63 Change of mean groundwater level after removing 50% of amount from sewerage pipe conductance (Unit: cm)	56
Figure 64 Change of mean groundwater level after adding 50% of amount to sewerage pipe conductance (Unit: cm).....	56
Figure 65 Time series of sensitivity test at Well PB08 (pipe wall conductance).....	57
Figure 66 Change of mean groundwater level after removing 50% of amount from hydraulic conductivity of the upper phreatic aquifer layer (Unit: cm).....	57
Figure 67 Change of mean groundwater level after adding 50% to hydraulic conductivity of the upper phreatic aquifer layer (Unit: cm)	58
Figure 68 Time series of sensitivity test at Well PB08 (hydraulic conductivity at the upper phreatic aquifer).....	58
Figure 69 Change of mean groundwater level after removing 50% of amount from hydraulic conductivity of the lower phreatic aquifer layer (Unit: cm)	59
Figure 70 Change of mean groundwater level after adding 50% to hydraulic conductivity of the lower phreatic aquifer layer (Unit: cm).....	59
Figure 71 Time series of sensitivity test at Well PB08 (hydraulic conductivity of the lower phreatic aquifer).....	60
Figure 72 Change of mean groundwater level after removing 50% from storage coefficient (Unit: cm)	60
Figure 73 Change of mean groundwater level after adding 50% of amount to storage coefficient (Unit: cm).....	61
Figure 74 Time series of sensitivity test at Well PB08 (storage coefficient)	61

Figure 75 Change of mean groundwater level after removing 50% of value from vertical resistance (Unit: cm).....	62
Figure 76 Change of mean groundwater level after adding 50% of value to vertical resistance (Unit: cm).....	62
Figure 77 Time series of sensitivity test at Well PB08 (vertical resistance)	63
Figure 78 Change of mean groundwater level after removing 50% of calculated value from groundwater recharge (Unit: cm)	63
Figure 79 Change of mean groundwater level after adding 50% of calculated value to groundwater recharge (Unit: cm)	64
Figure 80 Time series of sensitivity test at Well PB08 (groundwater recharge)	64
Figure 81 difference of mean groundwater level between Scenario 1 and null scenario (Unit: cm)	65
Figure 82 Time series of scenario test at Well PB08 (Scenario 1).....	66
Figure 83 Difference of mean groundwater level between Scenario 2 and null scenario (Unit: cm)	66
Figure 84 Time series of scenario test at Well PB08 (Scenario 2).....	67
Figure 85 Difference of mean groundwater level between Scenario 3 and null scenario (Unit: cm)	67
Figure 86 Time series of scenario test at Well PB04 (Scenario 3).....	68
Figure 87 Difference of mean groundwater level between Scenario 4 and null scenario (Unit: cm)	68
Figure 88 Time series of scenario test at Well PB04 (Scenario 4).....	69
Figure 89 Difference of mean groundwater level between Scenario 5 and null scenario (Unit: cm)	70
Figure 90 Time series of scenario test at Well PB08 (Scenario 5).....	70
Figure 91 Simulated groundwater level along a cross-section on December 31, 2016 from 2 m × 2 m and 20 m × 20 m spatial resolution models	72
Figure 92 Average value of groundwater level change after removing 50% of amount from canal conductance.....	85
Figure 93 Standard Deviation of groundwater level change after removing 50% of amount from canal conductance.....	85
Figure 94 Average value of groundwater level change after adding 50% of amount to canal conductance	86
Figure 95 Standard Deviation of groundwater level change after adding 50% of amount to canal conductance	86
Figure 96 Average value of groundwater level change after removing 50% of amount from sewerage pipe conductance	86
Figure 97 Standard Deviation of groundwater level change after removing 50% of amount from pipe conductance	87
Figure 98 Average value of groundwater level change after adding 50% of amount to sewerage pipe conductance	87
Figure 99 Standard Deviation of groundwater level change after adding 50% of amount to sewerage pipe conductance	87
Figure 100 Average value of groundwater level change after removing 50% of amount from hydraulic conductivity of the upper phreatic aquifer layer	88
Figure 101 Standard Deviation of groundwater level change after removing 50% of amount from hydraulic conductivity of the upper phreatic aquifer layer	88
Figure 102 Average value of groundwater level change after adding 50% to hydraulic conductivity of the upper phreatic aquifer layer	88
Figure 103 Standard Deviation of groundwater level change after adding 50% to hydraulic conductivity of the upper phreatic aquifer layer	89
Figure 104 Average value of groundwater level change after removing 50% from hydraulic conductivity of the lower phreatic aquifer layer.....	89
Figure 105 Standard Deviation of groundwater level change after removing 50% from hydraulic conductivity of the lower phreatic aquifer layer.....	89

Figure 106 Average value of groundwater level change after adding 50% to hydraulic conductivity of the lower phreatic aquifer layer.....	90
Figure 107 Standard Deviation of groundwater level change after adding 50% to hydraulic conductivity of the lower phreatic aquifer layer.....	90
Figure 108 Average value of groundwater level change after removing 50% from storage coefficient	90
Figure 109 Standard Deviation of groundwater level change after removing 50% from storage coefficient	91
Figure 110 Average value of groundwater level change after adding 50% of amount to storage coefficient	91
Figure 111 Standard Deviation of groundwater level change after adding 50% of amount to storage coefficient	91
Figure 112 Average value of groundwater level change after removing 50% of value from vertical resistance.....	92
Figure 113 Standard Deviation of groundwater level change after removing 50% of value from vertical resistance.....	92
Figure 114 Average value of groundwater level change after adding 50% of value to vertical resistance.....	92
Figure 115 Standard Deviation of groundwater level change after adding 50% of value to vertical resistance.....	93
Figure 116 Average value of groundwater level change after removing 50% of calculated value from groundwater recharge.....	93
Figure 117 Standard deviation of groundwater level change after removing 50% of calculated value from groundwater recharge	93
Figure 118 Average value of groundwater level change after adding 50% of calculated value to groundwater recharge.....	94
Figure 119 Standard deviation of groundwater level change after adding 50% of calculated value to groundwater recharge	94
Figure 120 Mean value of groundwater level increase between Scenario 1 and null scenario .	95
Figure 121 Standard deviation of the level difference between Scenario 1 and null scenario...	95
Figure 122 Mean value of groundwater level decrease between Scenario 2 and null scenario	96
Figure 123 Standard deviation of the level difference between Scenario 2 and null scenario...	96
Figure 124 Mean value of groundwater level increase between Scenario 3 and null scenario .	96
Figure 125 Standard deviation of the level difference between Scenario 3 and null scenario...	97
Figure 126 Mean value of groundwater level decrease between Scenario 4 and null scenario	97
Figure 127 Standard deviation of the level difference between Scenario 4 and null scenario...	97
Figure 128 Mean value of groundwater level decrease between Scenario 5 and null scenario	98
Figure 129 Standard deviation of the level difference between Scenario 5 and null scenario...	98

Abstract

Since the 12th Century, polder systems started to be built to control the water levels in the Netherlands so that this country can create more arable land and prevent inundation. Gouda is a city lying on a peatland in the Rhine-Meuse Delta. Because of the water draining and the increasing loads because of human activity, this city has been subsiding for centuries. Land subsidence in Gouda causes a lot of problems and costs, for example, the maintenance of the infrastructure and houses, the protection of cultural heritage. In the meantime, Gouda is under a high vulnerability of flooding and inundation, especially the north-western part of the inner city. The freeboard at a canal in that area, Turfmarkt, is now extremely limited (in centimetres), for which the area nearby can be easily inundated due to the insufficient drainage. The groundwater level in that area is also close to the land surface, indicating a high risk of groundwater inundation. Land subsidence makes these flooding hazard increase.

To solve the land subsidence problem, anthropogenic layers consisting of clay and sand were put on the top of the peatland, while the controlled surface water level in Gouda was gradually adapted to the lowering land level. However, simply lowering the surface water level and keep putting anthropogenic layer on land surface are not sustainable ways to solve the problem. When the surface water level is reduced, the lowered groundwater level in Gouda can accelerate the land subsidence; in the meanwhile, some part of the wooden piles of the houses built in the 19th and 20th Century could get exposed to the air and become affected by the fungi. Moreover, many houses in the historical center of Gouda are built without piles ('on steel'), hence sink with the land subsidence; raising the land surface by putting additional anthropogenic layers on top would cause entrance problem for these houses.

Facing these challenges, a project called Living Lab Land Subsidence, is established to study on the land subsidence in the historic city center of Gouda by the Water Board of Rijnland, the Municipality of Gouda, TU Delft, Deltares and some other research institutions, aiming to "build a strong city on soft land". Being a part of this project, this research is aiming to build a high-resolution dynamic groundwater model for the inner city and Korte Akkeren, the urban district next to the city center of Gouda that is located in a lower polder, to simulate the groundwater level at local details. This model should be sufficient to be linked to a land subsidence model for further study on land subsidence in Gouda.

This groundwater model is built based on an existing coarse regional groundwater model with fixed head boundaries. The subsurface structure is reconstructed in the new model according to the fieldwork and lithostratigraphy summary by Van Laarhoven (2017). The first 30 meters of the subsurface is divided into four layers: the upper phreatic aquifer consists of the recent anthropogenic layer and the upper part of the historical anthropogenic layer; next the lower part of the historical anthropogenic layer as a lower phreatic aquifer, the aquitard composed of clay and peat, and the first aquifer that consists of coarse sands. The parameters such as the resistance of the aquitard, the hydraulic conductivity and storage coefficient of the aquifers are calibrated later. The spatial heterogeneity of the effective groundwater recharge is very large because of the high heterogeneity of land cover. Thus the land surface in Gouda is divided into six types: impervious area, pervious pavement, grasslands/lawns, trees, backyards, and water. The recharge is estimated for every land cover type under every possible weather conditions. To capture spatial heterogeneity cell sizes of 2 x 2 m were applied in the model area. Some sewerage pipes in the historical city center of Gouda are leaky. To maintain the groundwater level in Gouda, they are constructed as back-stowed pipes, in which the water level in the pipes is controlled by a weir. The opening and closing actions of the weir is indicated with the monitoring data of the water level in the sewer system and the groundwater level nearby. The leakiness of these pipes is indirectly related to their ages. Firstly, the disjunction between the pipes caused by land subsidence is one cause of the leaky pipes. The older the pipes are, the higher the possibility that pipe disjunction would happen. Secondly, the material used to make sewerage pipes have been changed from weak materials such as bricks to strong materials such as fiberglass reinforced concrete. Newer pipes are less and less likely to be cracked and leaky. Therefore, the conductance of the pipes is calibrated in four groups according to their ages. When simulating the interaction between the surface water and groundwater,

the surface water level is assumed to be constant since the groundwater doesn't react fast when the surface water level changes, and, more importantly, the surface level controlled in the polder system doesn't deviate much from the target level. The conductance of the canal bed and river bed is to be calibrated.

The model is calibrated first in steady state then in transient state. The calibrated result in steady state is used as the initial state of the transient state calibration. Because of the limitation of the data availability, this model is calibrated using the groundwater observation in period 2015~2016, and validated with the data in period 2016~2017. The groundwater level observations of 8 wells (four in the inner city and four in Korte Akkeren) are used to calibrate the model with the patterns of the observed groundwater level; the observations at 3 new wells in the inner city are added to analyse model performance in validation period. Root mean squared error, coefficient of determination and Nash-Sutcliffe efficiency between the simulated phreatic groundwater level and the daily average value of the measurements at every observation wells are calculated to make sure that the simulation quality in all the wells is acceptable. When calibrating the groundwater model, the results of Wang's fieldwork (2016) are regarded as references. Generally speaking, this groundwater model is able to give an acceptable estimation of the groundwater level in the study area though larger deviation between simulated values and observed values were found at a few locations. Among all the parameters, the groundwater is most sensitive to the conductance of the canal bed and leaky pipes, while least sensitive to the storage coefficient of the aquifer and the resistance of aquitard.

To conclude this modelling effort, the effects of some scenarios were analysed and discussed:

- Scenario 1: All the leaky pipes are changed into water-tight ones. In this scenario, the yearly average groundwater level raises a lot in the north western part of the inner city where the oldest, most leaky pipes locate. The groundwater level significantly rises in dry periods.
- Scenario 2: Decreasing the surface water level in the inner city by 20 cm. The groundwater level reduces a lot in this scenario, and the level decrease is similar in the dry period and wet period.
- Scenario 3: A new canal in Nieuwe Haven. The area influenced by this canal is limited, and the groundwater level increases more in dry periods than that in wet periods.
- Scenario 4: A new canal in Nieuwe Haven + decreasing the surface water level in the inner city by 20 cm. The groundwater level drop near the new canal in the dry periods is reduced, while the level drop in the other area is still significant.
- Scenario 5: Replacing all the back-stowed pipes with Infiltration transportation pipes. In this scenario, the yearly average groundwater level in the inner city, especially the north-western part, is increased significantly, while the yearly average in the eastern part of Korte Akkeren reduces. The groundwater level becomes more stable and closer to the surface water level along the time series.

Samenvatting

Sinds de 12e eeuw worden in Nederland polders aangelegd om de waterstanden onder controle te houden, zodat inundatie wordt voorkomen en meer (akker)land ter beschikking komt. Gouda is een stad in een veengebied in de Rijn-Maas Delta. Door de ontwatering van het veen en de toenemende belasting door menselijke activiteit is deze stad al eeuwen aan het verzakken. Bodemdaling in Gouda veroorzaakt veel problemen en kosten, bijvoorbeeld met het onderhoud van infrastructuur en huizen, en problemen met de bescherming van cultureel erfgoed. Tegelijk is de binnenstad van Gouda kwetsbaar voor overstromingen en wateroverlast, vooral het laaggelegen noordwestelijke deel. Bij de Turfmarkt, een kanaal in dat gebied, is de drooglegging nu uiterst beperkt (centimeters), waardoor het gebied in de buurt gemakkelijk overstroomt raakt door onvoldoende ontwatering. De grondwaterstand in dat gebied staat dicht bij maaiveld, wat wijst op een hoog risico van overstroming van het grondwater. Door bodemdaling wordt de kans op overstroming steeds groter.

Om het bodemdalingsprobleem op te lossen, zijn antropogene lagen van klei en zand aangebracht bovenop de veengronden, terwijl ook het peil van het oppervlaktewater geleidelijk is aangepast aan het dalende maaiveld. Het simpelweg verlagen van het oppervlaktewaterpeil en het blijven aanvullen van de antropogene laag door ophoging van het maaiveld zijn echter geen duurzame manieren om het probleem op te lossen. Wanneer het oppervlaktewaterpeil wordt verlaagd kan de verlaagde grondwaterstand in Gouda de bodemdaling versnellen, terwijl intussen een deel van de houten palen van de huizen uit de 19^e en 20^e eeuw aan de lucht kan worden blootgesteld en aangetast kan worden door schimmels. Bovendien zijn in het historische centrum van Gouda, zijn veel huizen op staal (dus zonder palen) gebouwd; Die woningen dalen dus mee met het maaiveld, waardoor ophoging van het gebied leidt tot problemen met de toegankelijkheid van de panden.

Geconfronteerd met deze uitdagingen, is door Gemeente Gouda, Hoogheemraadschap van Rijnland, TU Delft, Deltares en enkele andere onderzoeksinstituten het project Living Lab Bodemdaling opgezet om onderzoek te doen naar de bodemdaling in het historische centrum van Gouda, gericht om " Stevige stad op slappe bodem ". Als onderdeel van dit project, is dit onderzoek gericht op het bouwen van een hoge resolutie dynamisch grondwatermodel voor de binnenstad en Korte Akkeren – een woonwijk gelegen in een lagere polder net naarst het stadscentrum van Gouda - om het grondwater niveau te simuleren op lokale details. Dit model zou geschikt moeten zijn om gekoppeld te kunnen worden aan een bodemdalingsmodel voor nader onderzoek naar bodemdaling in Gouda.

Dit grondwatermodel is gebouwd op basis van een bestaand grof regionaal grondwatermodel met vaste stijghoogten op de randen. De opbouw van de ondergrond is in het nieuwe model gereconstrueerd aan de hand van de uitkomsten van het veldwerk en de lithostratigrafie-samenvatting door Van Laarhoven (2017). De eerste 30 meter van de ondergrond is verdeeld in vier lagen: De bovenste freatische watervoerende laag bestaat uit de recente antropogene ophooglaag en het bovenste deel van de historische antropogene ophooglaaglaag. Daaronder ligt het onderste deel van de historische antropogene ophooglaag als een onderste freatische watervoerende laag, dan de aquitard die is samengesteld uit klei en veen, en het eerste watervoerende pakket dat bestaat uit grof zand. De parameters zoals de weerstand van de aquitard, de hydraulische geleidbaarheid en de opslagcoëfficiënt van de watervoerende lagen worden later gekalibreerd. De ruimtelijke heterogeniteit van de natuurlijke aanvulling van het grondwater is erg groot vanwege de hoge heterogeniteit van de landbedekking. Daarom is het landoppervlak in Gouda verdeeld in zes typen: ondoorlatend gebied, doorlatende bestrating, grasvelden / gazons, bomen, achtertuinen en water. De aanvulling van het grondwater wordt geschat voor elk type landbedekking onder alle mogelijke weersomstandigheden. Vanwege de ruimtelijke heterogeniteit in het landgebruik zijn in het modelgebied cellen van 2 x 2 m gemodelleerd. Sommige rioolbuizen in het historische centrum van Gouda zijn lek. Om de grondwaterstand in Gouda te handhaven kunnen ze worden 'opgeboeid', waarbij het waterniveau in de leidingen wordt geregeld door een stuw. Alle openings- en sluitingsacties van de stuw zijn waargenomen in de meetgegevens van het waterniveau in het rioelstelsel en de grondwaterstand in de buurt. De lekkage van deze pijpen is indirect gerelateerd aan hun leeftijd. Ten eerste zijn losse verbindingen tussen de buizen,

veroorzaakt door bodemdaling, een oorzaak van de lekkende leidingen. Hoe ouder de leidingen zijn, hoe groter de kans dat buisverbindingen lek raken. Ten tweede is het materiaal dat wordt gebruikt om rioleringsbuizen van te maken veranderd van zwakke materialen zoals baksteen in sterke materialen zoals met glasvezel versterkt beton. De nieuwere leidingen zijn steeds minder snel lek. Daarom is de intree weerstand (*conductance*) van de buizen in vier groepen gekalibreerd, naar hun leeftijd. Bij het simuleren van de interactie tussen oppervlaktewater en grondwater wordt verondersteld dat het oppervlaktewaterniveau constant is, omdat het grondwater niet snel reageert wanneer het oppervlaktewaterniveau verandert en vooral ook omdat het oppervlaktewaterniveau nauwelijks fluctueert in de tijd. De intree weerstand (*conductance*) van het de waterbodembodem van de grachten en rivier moet in het model worden gekalibreerd.

Het model wordt eerst stationair en vervolgens dynamisch gekalibreerd. Het stationair gekalibreerde model wordt gebruikt als de vertrekpunt voor de kalibratie van het dynamische model. Vanwege de beperking van de beschikbaarheid van gegevens, is dit model gekalibreerd met behulp van de grondwaterobservatie in de periode 2015 ~ 2016 en gevalideerd met de gegevens in de periode 2016 ~ 2017. De waarnemingen van grondwaterstanden van 8 meetpunten (vier in de binnenstad en vier in Korte Akkeren) zijn gebruikt om het model te kalibreren op de waargenomen grondwaterstanden; voor de modelvalidatie zijn de waarneming bij 3 nieuwe meetpunten in de binnenstad aan de analyse toegevoegd. De root mean squared error, de determinatiecoëfficiënt en de Nash-Sutcliffe-efficiëntie tussen het gesimuleerde freatische grondwaterstand en de daggemiddelde waarde van de metingen is berekend bij elke observatieput om ervoor te zorgen dat de kwaliteit van de simulatie in alle putten aanvaardbaar is. Bij het kalibreren van het grondwatermodel zijn de resultaten van het veldwerk van Wang (2016) beschouwd als referenties. Over het algemeen levert het grondwatermodel een aanvaardbare schatting van het grondwaterpeil in het studiegebied, hoewel op een paar plaatsen een grotere afwijking tussen gesimuleerde waarden en waargenomen waarden werd gevonden. Van alle modelparameters is het grondwater het meest gevoelig voor de intree weerstand (*conductance*) van de waterbodembodem het aanwezige oppervlaktewater en de weerstand van lekkende leidingen, terwijl het model het minst gevoelig is voor de opslagcoëfficiënt van de watervoerende laag en de weerstand van aquitard.

Ter afsluiting van de modelstudie zijn de effecten van enkele scenario's berekend en besproken

- Scenario 1: alle lekkende leidingen worden vervangen door waterdichte. In dit scenario stijgt het jaarlijkse gemiddelde grondwaterpeil veel in het noordwestelijke deel van de binnenstad waar de oudste, lekke leidingen zich bevinden. De grondwaterstand neemt significant toe in droge perioden.
- Scenario 2: verlaging van het oppervlaktewaterpeil in de binnenstad met 20 cm. De grondwaterstand daalt veel in dit scenario en de daling in droge en natte perioden is vergelijkbaar.
- Scenario 3: een nieuwe gracht in Nieuwe Haven. Het gebied dat door dit kanaal wordt beïnvloed, is beperkt en de grondwaterstand neemt meer toe in droge perioden dan in natte perioden.
- Scenario 4: Een nieuwe gracht in Nieuwe Haven + verlaging van het oppervlaktewaterpeil in de binnenstad met 20 cm. De daling van de grondwaterstand in de buurt van de nieuwe gracht in droge perioden wordt verminderd, terwijl de niveauperlaging in het andere gebied nog steeds aanzienlijk is.
- Scenario 5: Alle opgeboeide riolen vervangen door infiltratie-transport(IT)riolen. In dit scenario neemt de gemiddelde jaarlijkse grondwaterstand in de binnenstad aanzienlijk toe, met name het noordwestelijke deel, terwijl het jaargemiddelde in het oostelijk deel van Korte Akkeren sterk daalt. De grondwaterstand wordt stabiel en blijft over de hele simulatieperiode dicht bij het oppervlaktewaterpeil.

1 Introduction

Land subsidence can be defined as ground surface settling. It can be either a gradual progress or a sudden one (USGS, 2016). The cause of land subsidence varies, for example, exploitation of groundwater, increasing load on land surface, or even earthquake (Arkansas Geological Survey, 2015). In numerous delta areas, peat soil is a main culprit of subsiding (Deverel & Leighton, 2010; Stanley, 1988; Törnqvist et al., 2008). Peat is a highly organic material, which is fibrous, waterlogged and highly compressible (Koster, Erkens, & Zwanenburg, 2016). The cause of peat land subsiding varies, like increasing of loading and lowering the groundwater table.

The western part of the Netherlands was originally a marshy delta of the rivers Rhine and Meuse which covered with widespread peatlands (Querner, Jansen, & Kwakernaak, 2008). Nowadays, there is approximately 27% of the nation is below the sea level (Rosenberg, 2018). Over 60% of the population of the nation lives in this area. What is worse, this percentage may increase due to the rising sea level and land subsidence. The Dutch polder system was constructed to protect this area from inundation. The polders are land units that enclosed by dikes so that there is no connection with the surface water outside. As a result, the surface water in the polder can be managed actively.

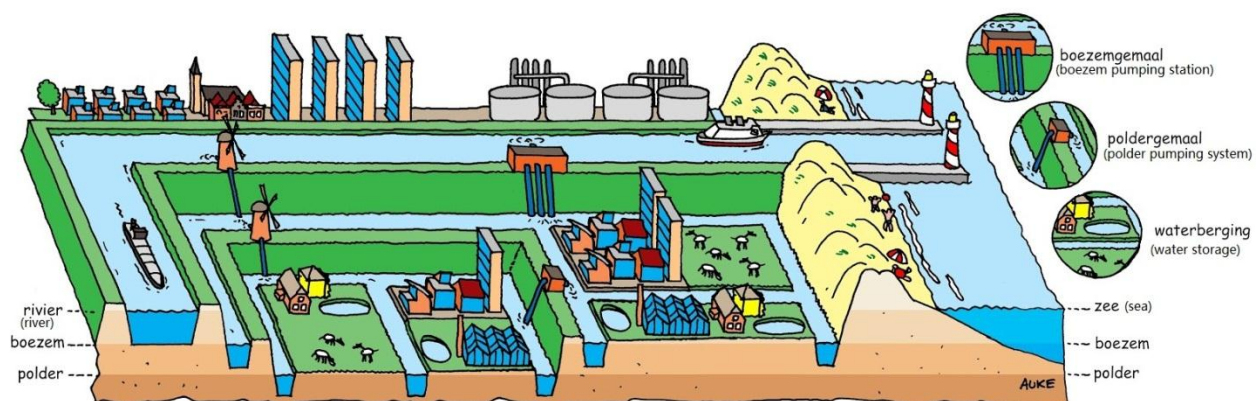


Figure 1 Dutch polder system (Source: <http://redtandem.blogspot.nl/2015/08/five-provinces-in-five-days.html>)

The traditional polders in the Netherlands were firstly formed in the 12th Century, aiming to the create arable land in the area “Green Heart of the Netherland” (Van Schoubroeck, 2010). At that time, the delta swamps were drained into the rivers nearby. Since the groundwater became lower than before, the air was able to penetrate into the deeper peat soil, which caused further peat oxidation and shrinking (Van den Akker et al., 2010). Then the surface level gradually descended below the river level (Cuenca & Hanssen, 2007). To adapt the agricultural system to the lowering surface level and inundation, Dutch people built windmills, making use of their natural resources as their energy to bring the water from polders uphill into boezem areas then into rivers (most of them are replaced by modern pumps later), forming the so-called “polder systems” (Van Schoubroeck, 2010) (See [Figure 1](#)). The boezem area is the places where the surface water level is intermediate between the polders in the region and the rivers. Its existence is meant to detain water in case that the discharge to the river is limited because of a high river level. In the polder system, there is a dense network of canals and ditches, in which the water level is controlled by storage, gates, sluice, and pumps. At the location of major towns and industrial areas, for example, Gouda, anthropogenic

layers consist of clay and sand are put on the top of the peatland (Stafleu, Maljers, Gunnink, Menkovic, & Busschers, 2011).

1.1. Land subsidence in Gouda

Gouda, the “wettest” city in the Rhine-Meuse Delta, is strategically situated on the Hollandse IJssel and the Gouwe, an artificial channel linked to the Oude Rijn (Nienhuis, 2010). Around the year 1000, the area where the city locates was a peatland covered by a marsh forest. The Gouwe was a narrow peat-river, along whose bank the early peak extraction was started from approximately 9th Century. During the 11th and 12th Centuries, Gouda witnessed the first settlement on a raised outcrop along the bank of the Gouwe (Nienhuis, 2010). Around 1225, a new canal linked the Gouwe with the Oude Rijn. The estuary of the Gouwe was transformed into a harbor (Nienhuis, 2010). To manage the surface water level in the inner city from the tidal influence from the Hollandse IJssel, a sluice is also installed in the inner city in the 13th Century (Nienhuis, 2010). This harbor attracted a lot of traders travelling between Flanders and France in the south, and between the Holland and the Baltic Sea in the north. This brings the Gouda to prosperity in the 14th Century. A map of sluices around Gouda in the 15th Century and a bird-view map of the old Gouda drawn in the 16th Century are shown in **Figure 2**. Gouda became a factory city with a relatively large amount of labor from 1870. After the arrival of the company Croda in 1858 and the Royal Gold Maiden Machinale Garespinnerij NV in 1861, the city is expanded to Korte Akkeren (Wikipedia, 2017).



Figure 2 left: sluices around Gouda in the 15th Century; right: a bird-view map of the old Gouda drawn in the 16th Century (Sources: http://goudsvirtueelsluisenmuseum.nl/?page_id=305; <https://www.sanderusmaps.com/en/our-catalogue/detail/163632/antique-map-of-gouda-by-braun--hogenberg/>)

This city, location above the peat soil, has been suffering from land subsidence for centuries (Coalitie: 'Stevige stad op slappe bodem', 2015b). Since the thickness of the anthropogenic layer in Gouda is in meters, and the elevation of the phreatic groundwater table in Gouda is above the top of the peat layer, the peat layer is now located in the saturated zone. Thus, there is barely any subsidence caused by oxidation anymore in the urbanized area. The subsidence in this area nowadays is mainly because of the rising effective stress on the subsurface. These are three causes of the increasing effective stress, dewatering urbanization, and additional filling. Firstly, the aquifers are frequently associated with compressible layers of fine-grained sediments (such as clay and silt), which is compressible. When the groundwater level is reduced because of dewatering, the effective stress increases from the top through the sediment column in the meantime. The increased effective stress compressed this fine-grain sediment layer, and, even more, the peat layers in the subsurface, causing a land subsidence. In the meantime, urbanization brings an increasing number of population and construction to the city, which also increases the loading on top of the soil, which compressed the fine-grained deposits in the subsurface. To keep the land on a certain level, residents correct the subsiding land level by land filling. This of course increases the top load and hence the effective stress, thus inducing more and accelerate the land subsidence.

This brings a lot of challenges to the city, for example, the maintenance of the infrastructure and houses, the protection of the cultural heritage, as well as water management. Damages to the infrastructure can be both above the ground (like buildings, pavements) and below the land surface (like sewerage pipes, or electricity networks) due to the uneven sinking (Boersma, 2015; Van den Born, 2016). Also, the high vulnerability of flooding and inundation brought by the land subsidence also troubles Gouda. As shown in **Figure 3**, the canal called Turfmarkt in the northwestern part of the inner city can be a typical example. The freeboard of this canal is extremely limited (in centimeters), for which the area nearby is easily be inundated due to the insufficient drainage. What makes the situation worse is that some historical houses having been there before 1902 are built without any piles (Coalitie: 'Stevige stad op slappe bodem', 2015a). These houses are sinking with the ground. This fact increases the risk of both surface water and groundwater inundation even inside of the houses.



Figure 3 Canal Turfmarkt (Source: <http://rijksmonumenten.nl/monument/16930/voormalige-synagoge-van-gouda/gouda/>)

Uneven subsidence is even more problematic. As the depth of different soil layers in the subsurface varies from place to place, the effect of change in effective stress is different, too. This causes uneven settlement. Uneven settlement causes damages to the infrastructure in the city, including the sewerage pipes, the aged sewer pipes in Gouda are leaky (Wang, 2016). This leakiness is mainly due to the disjunction between the pipes and cracks on the pipe. Thus, besides the degree of uneven subsidence, the leaky extent of these sewers also depends on the material of the pipes. The material used to construct sewerage pipes differs during different period (See [Figure 4](#)). In the very beginning, the sewerage pipes are made of bricks, which is easy to be cracked. Concrete sewerage pipes first occur in 1869 and starts prevailing gradually. These concrete pipes are stronger than the brick sewerage pipes. In early 20th Century, pipes made of cast iron and stoneware started to be used in the sewerage system. Then occur the plastic and fiberglass reinforced materials, which would hardly to be cracked. Generally speaking, the materials of the sewerage pipes are growing stronger and stronger through the passing time. To avoid permanent drainage of groundwater via the leaky pipes, a back-stowed system is constructed making use of these aged pipes. In this system, several weirs are installed to control the sewerage water head in the leaky pipes. Thus, the drainage flux via the sewerage pipes can also be controlled.

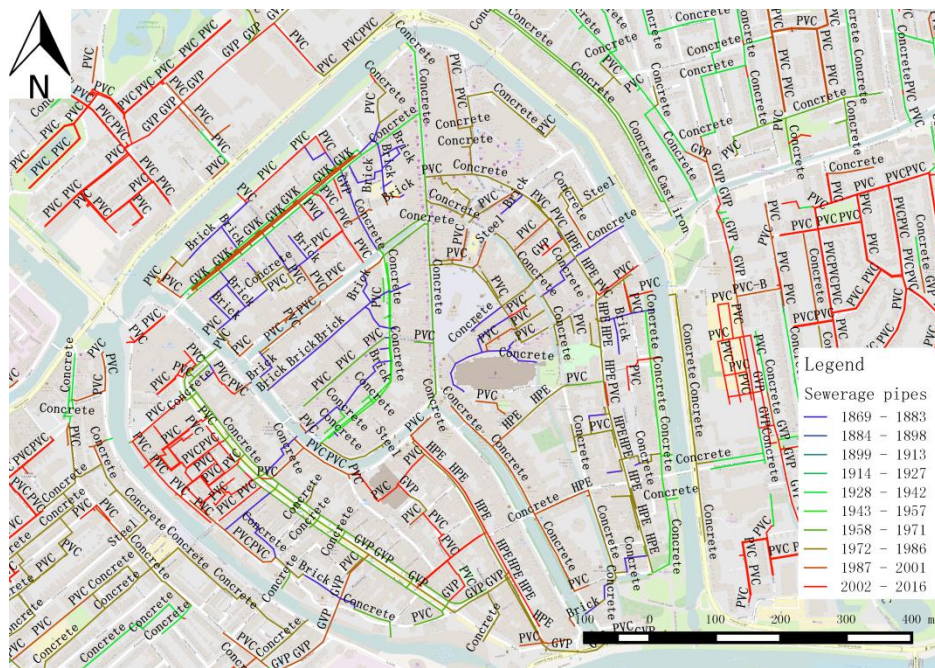


Figure 4 Ages and materials of the sewerage pipes in the inner city

Land subsidence in Gouda is continuing. [Figure 5](#) shows the average setting rate of the ground between 2017 and 2040 estimated by Fugro. Although land subsidence in Gouda is a slow progress, the historic part of the city is already in a fragile state. [Figure 6](#) shows the comparison among the surface elevation (measured in 2017 and estimated for 2040), management interference elevation (“ingrijphoogte” in Dutch) as well as the planed surface water level for the polder system (“polderpeil” in Dutch) and in Gouda. As shown in the figure, the land surface in some locations is already below the surface water level in the canals, and the number will continue rising in next decades. Just lowering the groundwater table is no longer a solution for Gouda. Firstly, as mentioned, the lower groundwater table may accelerate the land subsidence through the additional effective stress caused by dewatering. Moreover, decreasing the groundwater levels can cause maintenance problem to these houses with wooden piles. Since the beginning of the 20th Century, houses in the historical center started to being built with piles. Until the 1950s, wood is used as the material for the

piles (Coalitie: 'Stevige stad op slappe bodem', 2015a). Once the groundwater is drained, and part of the wooden piles is exposed to the air, fungi could grow on the exposed part of the wooden piles and affect it, which could cause severe damage to the building.

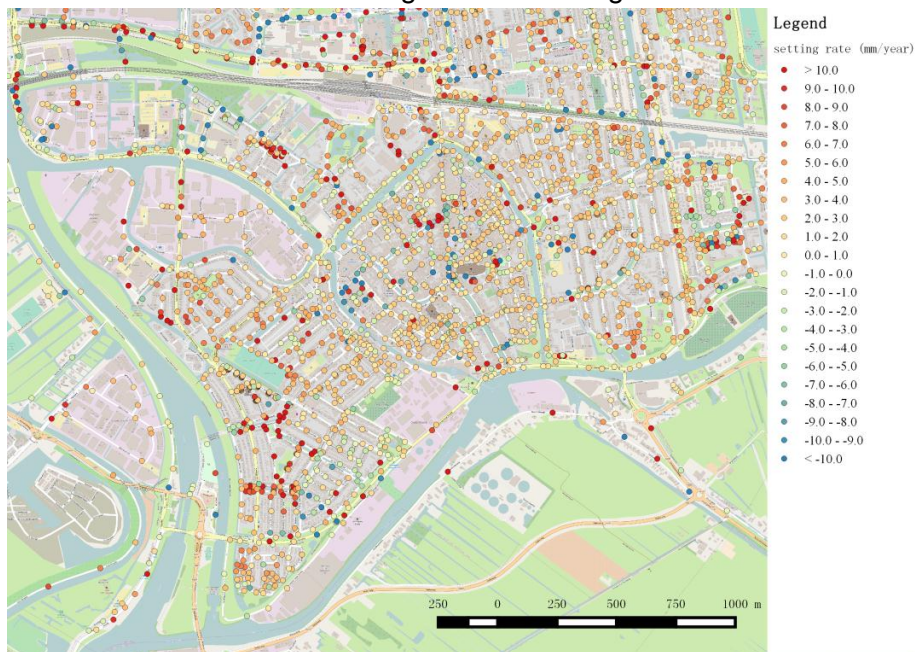


Figure 5 Estimated average subsiding rate between 2017 and 2040

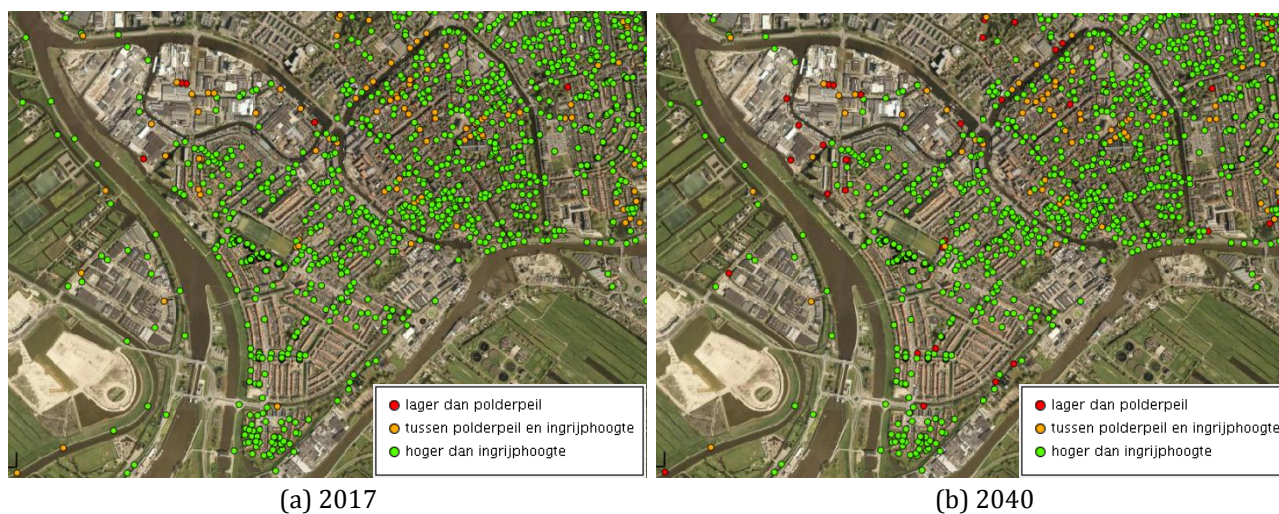


Figure 6 Comparison among the surface elevation, interference elevation and surface water level (source: <https://gis.gouda.nl/gisviewer/viewer.do?appCode=bb3900e12b49685bada6eaf3e4a7407f&forceViewer=true&cmsPageId=1&cmsPageId=1>)

These decades have witnessed an increasing awareness of the climate change. According to the Fifth Assessment Report of the Intergovernmental Panel on Climate Change, global warming can increase the frequency, intensity, and duration of extreme weather events such as heavy rainfall, droughts, and dry spells (IPCC, 2014). The increased frequency and amount of precipitation during extremely wet weather will lead to growing flooding hazard in Gouda. In the meantime, the occurrence of the extreme dry spells may also result in lower groundwater level in the dry period, because of the effect of evapotranspiration. A low groundwater level could bring damage to the wooden piles of some historic houses and might accelerate the subsidence.

Facing these challenges, a project, Living Lab Land Subsidence, is established to study on the land subsidence in the historic city center of Gouda by the Water Board of Rijland, the Municipality of Gouda, KCAF, TU Delft, Rijkswaterstaat, Deltares and some other research institutions in 2014, aiming to “build a strong city on soft land” (Hoogheemraadschap van Rijland, 2014). Being a part of the “Living Lab” project, this research studies on the behavior of the groundwater system in two areas in Gouda, the inner city and Korte Akkeren. Korte Akkeren is an independent polder, while the inner city is located at the boezem area lying on the north of a river, de Hollandse IJssel. The inner city is the focus area of “Living Lab”. It is a highly valued historical area with numerous historical houses built since 16th Century. The lower part of the inner city suffers from the high risk of both surface water and groundwater inundation in Gouda. To understand the groundwater system in Gouda, more observation wells have been installed to improve the observation network on groundwater level since May 2015. Korte Akkeren is the reference area for “Living Lab”. It is also a representative area for city district with is built from the 1860s on. As shown in [Figure 5](#), the land surface is sinking at a significant rate in Korte Akkeren, especially in the southwestern part, resulting in high cost of the maintenance for the infrastructure. This research is intended to investigate and simulate the hydrological processes relevant to the groundwater level in Gouda via a groundwater model, both for managing the surface and stormwater in the wet season to protect the city from highly frequent inundation, as well as controlling the groundwater level in the dry sea to prevent the acceleration of the land subsidence and damages to the wooden piles.

1.2. Groundwater modelling in urban scale

Urbanization brings lots of impacts on all aspects such as ecology, economy as well as water management. Some of these impacts on urban groundwater are positive, like a higher efficient use of land resources, more effective public transport and centralized water treatment, which reduce per capita emissions of contaminants (Schirmer, Leschik, & Musolff, 2013). In the meanwhile, urbanization also brings a significant pressure on the environment via changes in water balance, poorly regulated contaminant emissions and some other human activities (Fletcher, Andrieu, & Hamel, 2013). Facing the climate change nowadays and the increasing environmental stresses brought by human beings, urban groundwater became a distinct branch of geohydrology (Vázquez-Suñé, Sánchez-Vila, & Carrera, 2005). Nowadays, researches on urban groundwater are mostly focused on the impact of anthropogenic influences on groundwater quality and quantity, such as changes in groundwater regime caused by land use change (Dams, Woldeamlak, & Batelaan, 2008), salt intrusion problem after groundwater exploitation in coastal area (Zhou, Chen, & Liang, 2003), pollution problem due to point or non-point source (Nas & Berkday, 2010), and integral sustainable urban water management (Carneiro & Carvalho, 2010; Vázquez-Suñé & Sanchez-Vila, 1999).

When studying the groundwater in urban areas, there are two necessary steps involved, identifying the most influential factors in the water balance and (or) groundwater flow of urban geohydrological cycle and developing/applying methodologies to quantify these factors (Vázquez-Suñé et al., 2005). Due to the urbanization and industrialization, the natural geohydrological cycle in the urban areas is disturbed human activity, the knowledge on the water balance is crucial for urban geohydrological study. Studying the magnitude, relative importance and dependence upon hydrological parameters are required when trying to understand the water balance. Zhang and Kennedy (2006) studied the sustainable yield of the aquifer in Beijing, China, by balancing the water flow within the city. Their

study on groundwater balance involves processes such as groundwater extraction, seepage from surface water, leakage from water mains and sewerage pipes, precipitation and estimation on evapotranspiration. Vázquez-Suñé et al. (2005) also included seepage into (subway) tunnels in water balance analysis. It is well recognized that due to the construction of urban areas, direct recharge from precipitation and evapotranspiration is often reduced, while indirect recharge increases due to the leakage from water mains, sewerage system, and, if there is any, storm water detention infrastructures like soakaways. Extends to the changes vary in different sites, and the estimation on their contributions on water balance is complicated to analyze (Lerner, 2002).

Groundwater modeling is an important method to study groundwater quantity and quality problems in urban areas. Some of the urban groundwater models are constructed similarly to those in a non-urban regional model when they are aimed to study the groundwater problems for large cities which overlays on important aquifers. In these models, the small-scale features are negligible (Carneiro & Carvalho, 2010). However, when a groundwater model is aimed to simulate the groundwater for a smaller area, detailed local information like underground car parks, tunnels cannot be neglected anymore, requiring higher resolution (Carneiro & Carvalho, 2010). What's more, the heterogeneities of the urban surface and geological subsurface structure is more emphasized in high resolution small scale models when compared to those in a larger urban regional model (Carneiro & Carvalho, 2010; Miles et al., 2007). This detailed information promotes the resolution of the model high enough to study on more local problems or adopt as an assessment tool for urban managing and decision making (Vázquez-Suñé & Sanchez-Vila, 1999). To construct a model with a high resolution, various sources of information is required, such as a sufficient groundwater observation network, detailed spatial information on land use, water mains and sewerage system networks, surface water. The development of geographic information system, digital terrain models, and computational capacity allows us to process this large volume of information for groundwater modeling. 3D model of lithology or even hydrological properties can be built based on knowledge of lithostratigraphy and core log with various approaches, such as geostatistical and stochastic methods to describe the geological heterogeneity (Bierkens, 1996; Stafleu et al., 2011), or Markov chain approaches (Elfeki & Dekking, 2001). spatial variance of land cover could be described with the information of urban planning, as well as the distribution of water supply and sewerage system. However, the high requirement on the data availability for characterizing the heterogeneity gives the challenge to construct a high-resolution groundwater model for the urban area. Several urban groundwater study cases are typically focusing on a specific construction problem (Miracapillo & Howard, 2007; Vázquez-Suñé & Sanchez-Vila, 1999) or rely on a large-scale urban groundwater model with less local details (Taylor et al., 2006). There are only a few researchers constructed the very detailed groundwater model for a small urban region for urban water management purpose (Beretta, Avanzini, & Pagotto, 2004; Epting, Huggenberger, & Rauber, 2008).

This research describes the construction method on a high-resolution groundwater model for a small region of urban area in Gouda, which takes the heterogeneity of land surface, subsurface structure, and underground infrastructure into consideration. This model is constructed basing on a large regional model with a coarse resolution and can be used as a tool for assessing the influence of urban water management strategies to provide suggestions and information both for groundwater managing and land subsidence model.

2 Objectives

The groundwater level in Gouda should neither be too high nor too low. The low groundwater level may accelerate land subsidence and harm the wooden piles of the buildings while the high groundwater level can result in inundation from surface water and groundwater. To increase the resilience of the city, this research is aimed at providing a dynamic model including the inner city and Korte Akkeren to simulate the groundwater level at local details. Several water management strategies will be tested in the model to observe their effects on the groundwater levels. Then this model can be linked to a land subsidence model for further study on land subsidence under different (ground)water management scenarios.

To achieve this goal in the end, the following research steps are taken:

- Investigate the hydrological processes relevant to the groundwater;
- Establish a “high resolution” groundwater model, to sufficiently include the local details;
- Calibrate and validate the model with the existent data;
- Analyze the sensitivity of the parameters;
- Analyze the effects of new canals and other groundwater management methods on the groundwater level;

As a first step, a groundwater model at steady state is constructed with time-averaged inputs. The outputs of the model illustrate the groundwater flow and levels. The levels would arise when the system has equilibrated to all boundary conditions and defined stresses (Barnett et al., 2012). The steady solution calculated with a groundwater model fails to show the temporal variation of the groundwater level. The aim of this research is to understand the groundwater regime and the behavior of the groundwater levels under different time-varying stresses, both the high groundwater level occurs in wet seasons and the low groundwater happens in dry seasons are essential. Thus, building a groundwater model at the transient state rather than the steady state is necessary in this research. Besides, the heterogeneity of the groundwater level is high in Gouda because of the high spatial heterogeneity of urban surfaces, subsurface structures, and infrastructures which also need to be taken into consideration. As a result, the model should be capable of representing the significant differences in the groundwater table regime at a very small scale, which brings a big challenge to this research. The high heterogenetic stresses make it hard to calibrate a high-resolution groundwater model.

In the context of the Living Lab Land Subsidence Gouda, a very detailed groundwater monitoring network was installed in the northern part of the inner city early summer 2016, while a dense monitoring network was already available all over the city. Availability of these data allowed us to study groundwater dynamics in high resolution indeed. The observation network took as many factors as possible, such as land cover, plant types, historical leaking pipes, surface water as well as crawl spaces (Wang, 2016). According to the observation, it is found that the surface water, leaking sewerage pipe and land cover are major influential factors for the groundwater level in the inner city (Wang, 2016). The surface water and leaking sewerage pipes influence the groundwater level via water exchange between the groundwater and surface water system or the sewerage system. The land cover affects the groundwater level because of the spatial variation of infiltration and evapotranspiration. During a precipitation event, the infiltration of the rainwater happens in

permeable surfaces (like grassland) and semipermeable surfaces (like brick pavement), while no infiltration can occur in the impermeable surfaces. The actual amount of infiltration rate depends on the amount of vegetative cover, soil properties, like moisture and hydraulic conductivity, as well as the effective precipitation intensity (Chu, 1978; McGinty, Smeins, & Merrill, 1979; Thrash, 1997). Surface runoff starts to be generated when the effective precipitations rate exceeds the infiltration capacity. This surface runoff can be discharged into the canal, sewer system or stay at the surface. Besides, the irrigation can also be a water source supplying soil moisture in the vegetated area. In the impermeable regions, there is hardly any infiltration during the precipitation event; the generated surface runoff can be discharged to the sewer system, the canals nearby or infiltrated in the permeable areas. The evaporation exists at the wet surfaces and pervious areas when the water vapor in the air is unsaturated, while transpiration occurs where vegetation exists. Vegetation put down the roots which extract soil water as well as nutrients to the stem and leaves. Some of the water goes back to the atmosphere. The transpiration rate varies widely depending on the weather conditions (such as temperature, relative humidity, solar radiation, and wind velocity.), soil properties and moisture, and type of plants (Penman, 1950; Rawson, Begg, & Woodward, 1977). Usually, the soil water used for transpiration is extracted from the root zone (unsaturated zone). However, when the groundwater table is shallow, the water in the saturated zone can also supply water for transpiration through capillary rise.

In the following chapters, more details of the modeling attempts are discussed. The geological information and the data of influential factors are introduced in Chapter 3. Based on the collected information, the groundwater model is conceptualized and constructed on the basis of a regional model. The calibration and validation strategies as well as the (ground)water management scenario are also discussed in Chapter 3. Chapter 4 provides a discussion on the methodology of the groundwater modeling in this research. Chapter 5 shows the results of the calibration and validation according to the calculated root mean square error at every observation well and the comparison of the time-series at some specific locations. Conclusions of this research are made in Chapter 6 while some recommendations are given in Chapter 7.

3 Groundwater Modelling

When developing a conceptual model, there is always a trade-off among realism, generality and precision. It is not possible to maximize all these three simultaneously (Barnett et al., 2012; Levins, 1993). Thus, before conceptualization and constructing the groundwater model, it is important to investigate the pattern of the phreatic groundwater level to get a better understanding of the key behavior of the groundwater system. Wang (2016) established a groundwater observation network along Nieuwe Haven and Turfmarkt in the inner city and investigated the influence of the different stresses on the groundwater level. It is found that the leaking sewerage pipes, spatial difference of infiltration and evapotranspiration caused by different kinds of land cover, as well as surface water have obvious influences on the groundwater system, while the influence of the buried harbor quay wall buried under Nieuwe Haven is negligible because the elevation of the top of the quay walls are beneath the groundwater table. In this research, only the influential factors will be included in the groundwater model.

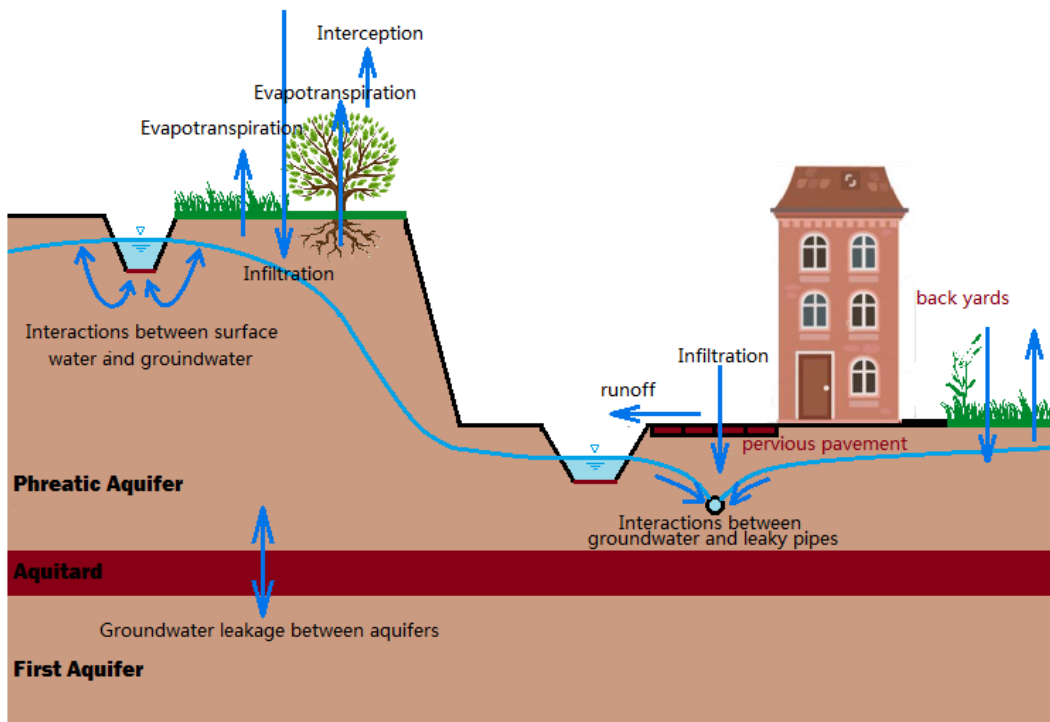


Figure 7 Groundwater related hydrological processes

3.1. Data Collection

Before constructing a groundwater model for Gouda, the geological information is collected so that the subsurface structure in the study area can be conceptualized. The information of the essential elements on groundwater according to Wang's results (2016), such as land use map, precipitation and potential evapotranspiration data, as well as surface water and sewerage pipe distribution, are

collected for stress simulation. Moreover, the phreatic groundwater observations are also gathered for model calibration and verification.

3.1.1. Land surface elevation and subsurface structures

The Digital Terrain Model (DTM) map of Actueel Hoogtebestand Nederland (AHN, a digital elevation map of the Netherlands) is collected as the land surface elevation data (<https://www.pdok.nl/nl/ahn3-downloads>). However, this DTM data set is not continuous (*Figure 8*). It excludes objects like trees and houses. As a result, the DTM is interpolated to produce a continuous map of the ground surface elevation. The ground elevation of the inner city is approximately 1 m higher than the polder Korea Akkeren.

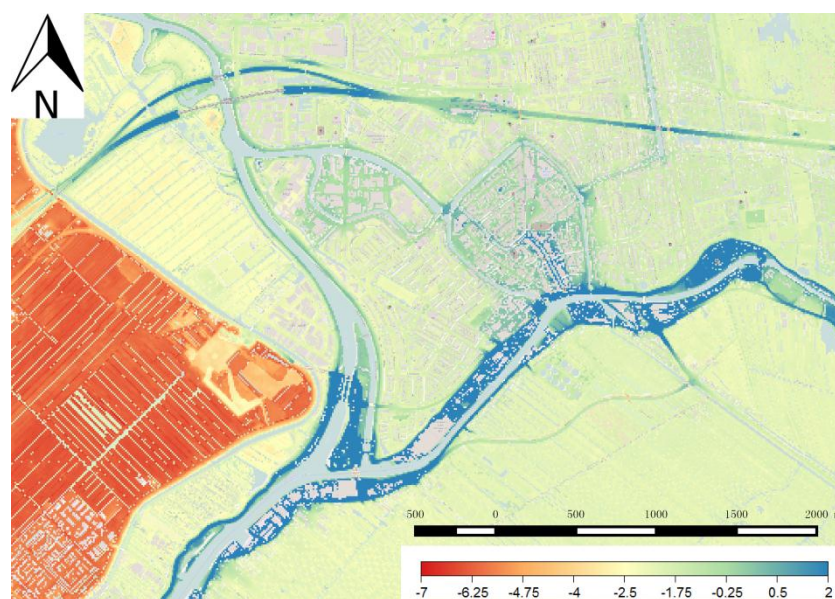


Figure 8 DTM map of Gouda (Unit: m NAP)

Borehole information is used to characterize the subsurface structure. A first source of borehole information comes from the boreholes of the dense network of groundwater monitoring wells (see also *Section 3.1.6*). The lithology logs at every groundwater monitoring wells can be found in the data portal of Wareco. The depths of these lithology logs of these observation wells are approximately 2.5 m, which only shows a superficial geology structure of Gouda. Thus, besides the lithology logs of the groundwater monitoring wells, the observation from Van Laarhoven (2017), as well as his summation on the lithostratigraphy, is used here to construct the subsurface structure of the groundwater model. The depth of his observation wells is between 6 m and 10 m, which are sufficient enough to reach the low-permeable peat layer lies deeper in the underground.

As mentioned in *Section 1.1*, the town has been sinking during the development and increasing residential settlement for centuries. To solve this problem, besides lowering the water level in the canals, the government continues manually lifting the streets. Thus, on top of the peat layer, the phreatic layer is composed of the elevating materials. According to the lithology log of the observation wells, the composition of the lifting materials is complex, from clay sand to silty sand or even gravels. Van Laarhoven (2017) summarized the lithostratigraphy in the inner city and Korte Akkeren. He found that the anthropogenic layer can be generally divided into two sub-layers, a recent layer and a historical one (See *Figure 9*). The recent layer is mostly composed of clean

marine sand and gravels, while the historical one consists of regional materials like sandy clay and plenty debris of archeological admixture. This fact indicates that the hydraulic conductivity of the recent layer could be larger than that of the historical layer. Under the anthropogenic layer follows the recent fluvial deposits, composed by sandy channel and fluvial channel fill consisting of silty clay. This layer embedded in the underlying peat layer by two rivers (Gouwe and de Hollandse IJssel). As for the peat layer, since Gouda was firstly founded in the inner city then expanded from the inner city to Korte Akkeren hundreds years later, the inner city has experienced a longer period of land subsidence than Korte Akkeren. Thus, the compaction degree of the peat soil in the inner city is more significant than that in Korte Akkeren, which means that the resistance of the peat layer between two aquifers in the inner city could be larger. Below the peat layer, follows the Holocene fluvial deposits from the Gouderak and Zuidplas channel belt. The Holocene floodplain and natural levee of this layer is clayey while the channel bed consists of sands, overlaying on the sandy deposits of Pleistocene age.

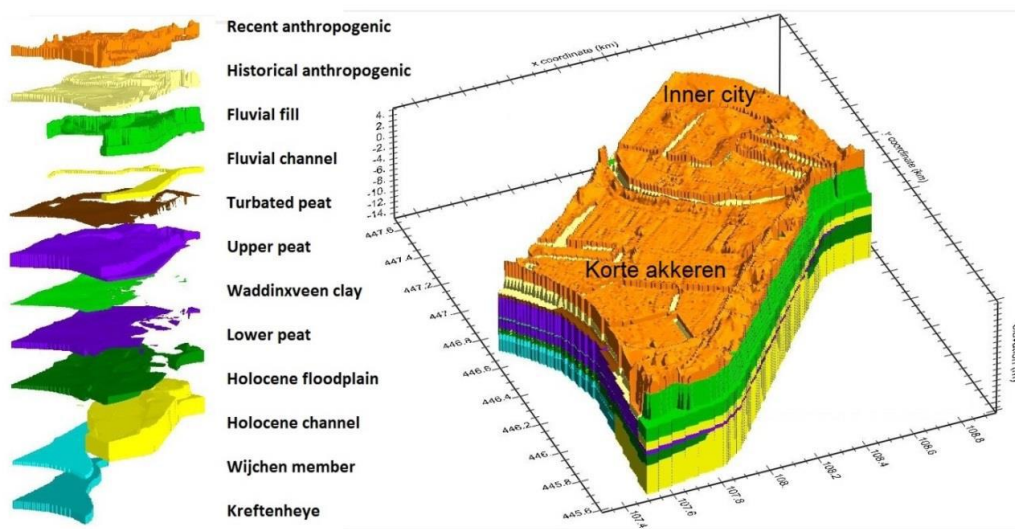
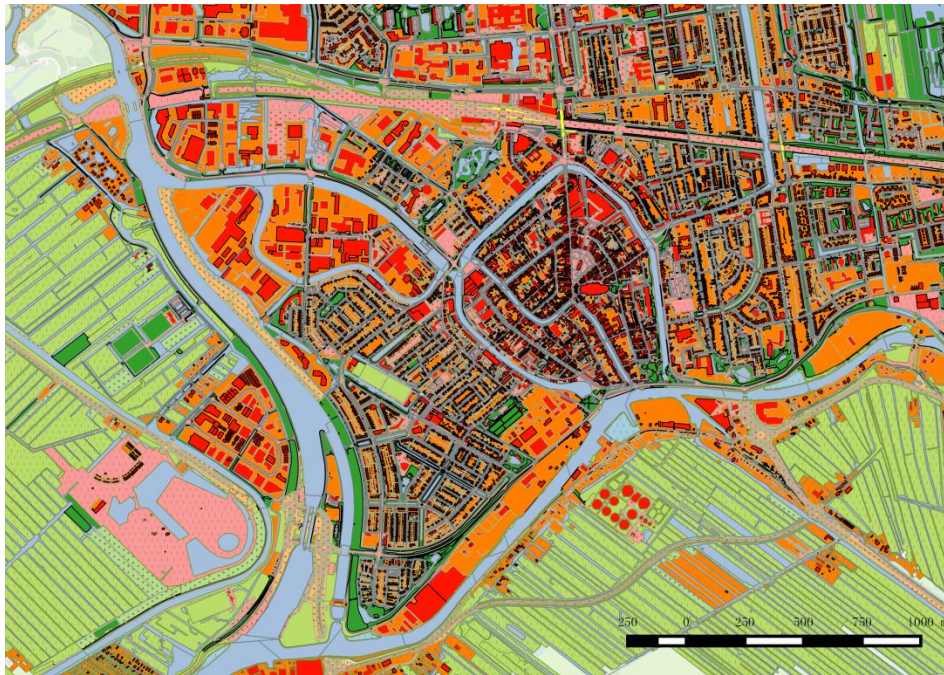


Figure 9 Lithostratigraphy layers of Gouda (Van Laarhoven, 2017)

3.1.2. Land cover

The land cover influences the spatial variation of the infiltration and evapotranspiration. Thus it is important to collect the detailed land cover data of Gouda. The Basic Registration Large-scale Topography map (“Basisregistratie Grootschalige Topografie”, in Dutch) provided in the GIS system of the municipality of Gouda (<https://gis.gouda.nl/gisviewer/viewer.do?appCode=e286ba8b873c74cf27b726bb8d753747&forceViewer=true&cmsPageld=1&cmsPageld=22>) shows the general usage of the areas in Gouda in details (Figure 10). This figure shows the location of every houses, gardens and agricultural area. For example, it is clear that the inner city is an urbanized area with a larger density of houses when compared with Korte Akkeren, where less infiltration and evapotranspiration are expected. However, the detailed land cover of areas like the bare ground is still unknown. Thus, this land use map should be improved by specifying the land cover for areas like bare ground. Also, a map showing the information of the pave material data is collected from the municipality of Gouda (Figure 11). It is because the infiltration in the pavements also varies among the pavement materials. For example, no infiltration would occur in impervious pavement area (asphalt pavement and cement concrete pavement), while infiltration can occur through elements pavement like bricks and tiles. In addition,

these pave material data is collected from the municipality of Gouda After integrating all the information so that the spatial variation of the infiltration and evaporation could be calculated.

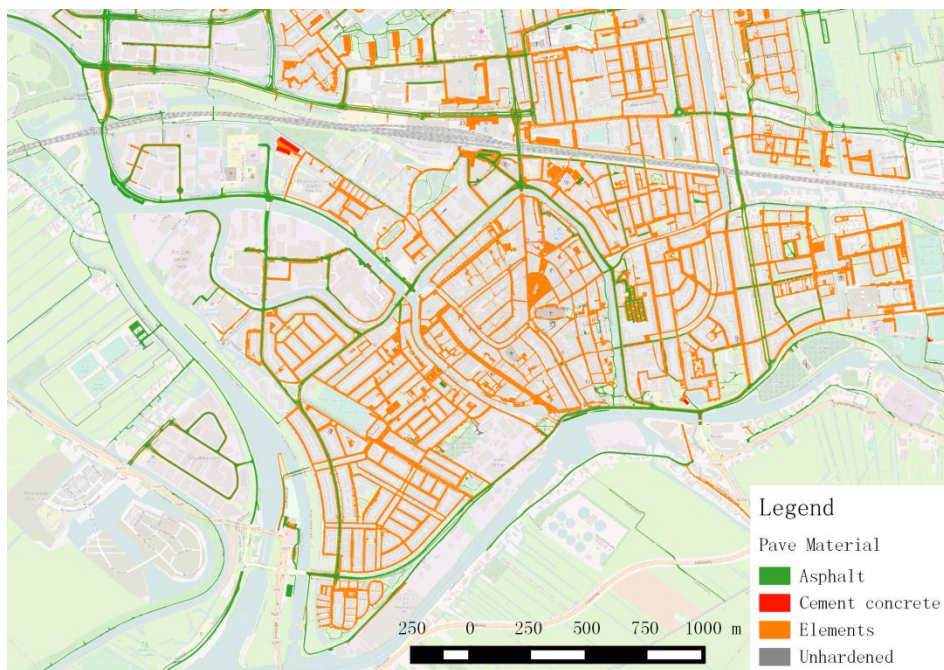


Legend

Land Cover

- Andere bronhouder vlak (Other source holder)
- begroeid terreindeel kenmerkpunt (Extensive ground)
- hoogspanningsmast op maaiveld vlak (High-voltage mast at ground level)
- kunstwerkdeel vlak (Artwork)
- onbegroeid terreindeel vlak (Bare ground)
- onbegroeid terreindeel vlak decompositie (Bare ground decomposition)
- ondersteunend waterdeel vlak (Water supporting construction)
- overbruggingsdeel vlak (Bridging part)
- overig bouwwerk vlak (Other construction)
- overkapping op maaiveld vlak (Covering at ground level)
- pand op maaiveld vlak (Houses)
- scheiding vlak decompositie (Saperation decomposition)
- vlak grasland agrarisch (Agricultural grassland)
- vlak grasland overig (Other grassland)
- vlak groen (The greens)
- vlak kademuur (Quay walls)
- vlak muur (Walls)
- vlak trap (Staircase)
- vlak onbegroeid terreindeel onverhard (Unpaved bare ground)
- vlak overig opstal geen IMGEO (Other superstructure not classified in IMGEO)
- vlak weg maaiveld (Roads)
- vlak weg maaiveld niet in beheer gemeente (Roads not under the control of municipality)
- waterdeel vlak (Water)

Figure 10 Basic Registration Large-scale Topography map



Legend

- Pave Material
- Asphalt
- Cement concrete
- Elements
- Unhardened

Figure 11 map of pavement materials

3.1.3. Precipitation and Evapotranspiration

Since time step of the groundwater model is one day, the daily temporal resolution would be enough for the precipitation and evapotranspiration data. KNMI provides daily precipitation and potential evaporation observation data as open sources (<http://www.knmi.nl/nederland-nu/klimatologie-metingen-en-waarnemingen>). There is a precipitation observation spot located in Gouda. The observation at that location is used to represent areal precipitation because this precipitation station lies just outside the inner city and the total area of Gouda is small which make the spatial variation of the precipitation limited. However, there is no evapotranspiration observation point in Gouda. The observation from the nearest weather station Cabauw (See **Figure 12**) is used to represent the potential evapotranspiration in Gouda. The potential evapotranspiration is not measured directly. It is calculated with Makkink's Equation (Jacobs & De Bruin, 1998; McMahon, Malano, & Schultz, 2015):

$$L_v E = c_1 \frac{s}{s + \gamma} K^\downarrow + c_2$$

Where L_v represents the latent heat of vaporization, s means the slope of the saturation water vapor – temperature curve at air temperature, K^\downarrow is the incoming solar radiation, γ is the psychrometric constant, while c_1 and c_2 are empirical constants.

Figure 13 shows the monthly average value of precipitation and potential evapotranspiration. April has the lowest average precipitation value while August has the highest one. The monthly average value of potential evapotranspiration shows a regulation: higher in summer and lower in winter. When compared the average precipitation and evapotranspiration, it can be indicated from the graph that the December and January are the wettest months since the average precipitation is way more than potential evapotranspiration. The value of average potential evapotranspiration exceeds average precipitation from April to July, while the difference in April is the highest one.



Figure 12 Weather Stations near Gouda

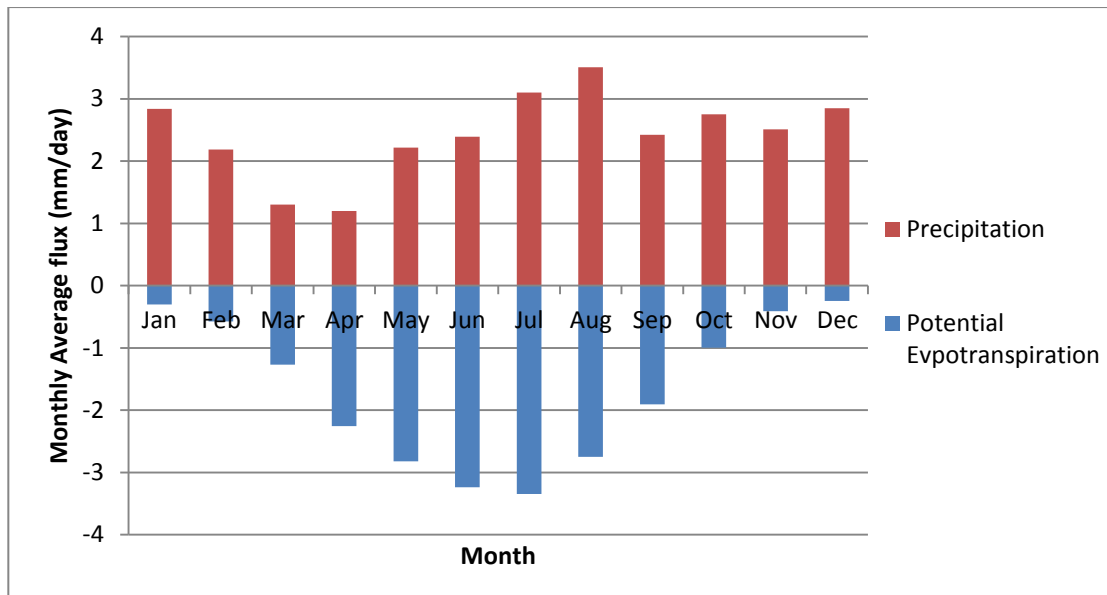


Figure 13 Monthly average fluxes of precipitation and potential evapotranspiration in Gouda (2000~2017)

3.1.4. Surface water

Both the surface water level in the inner city and Korte Akkeren are managed by water board Hoogheemraadschap van Rijnland actively, while the surface water level in the polders on the southwest and south side of the study areas are managed by another water board, Hoogheemraadschap van Schieland en de Krimpenerwaard. The information of the canals like their location, planned water level, and depth of the canals within the model boundary are provided by both the water boards. *Figure 14* shows the planned surface water elevation of the polders and boezom. Since the inner city lies at the boezem area, the surface water level in the inner city is the highest ones among all the polders nearby, including Korte Akkeren. The surface water level in the inner city is approximately 1.5 m higher than that in Korte Akkeren. Besides, on the south of the study area lays a tidal river, the Hollandse IJssel, the average level of which is approximately 0.37m NAP according to the monitoring data from Hoogheemraadschap van Rijnland.

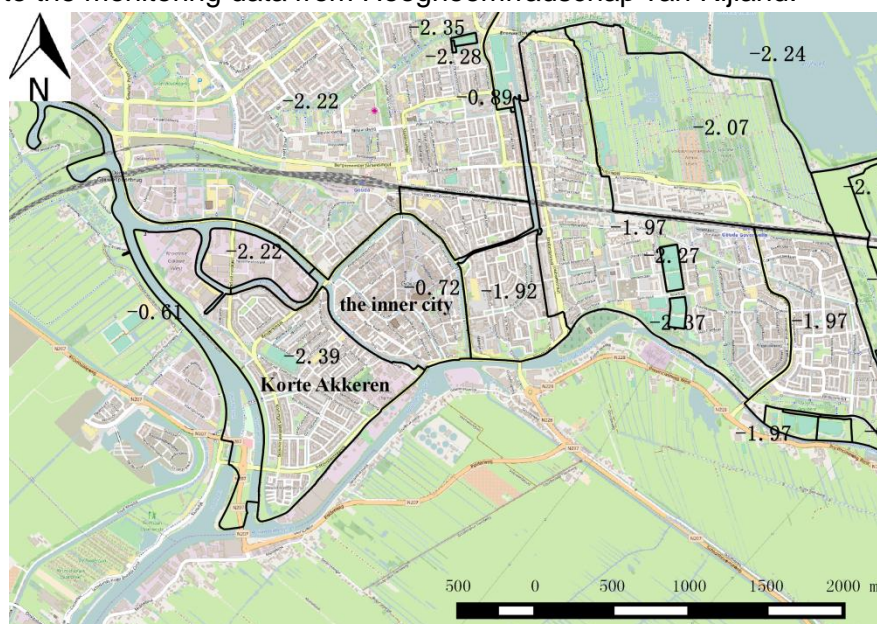


Figure 14 Planned surface water level in the polders and the boezom

3.1.5. Sewerage pipes

The data of the material, age, elevation of the pipes in the sewerage system in Gouda can be downloaded from the web GIS system. This sewerage system is mixed with both combined sewer system and separated sewer system, See **Figure 15**. The sewer pipes are mostly from the combined system in the inner city while approximately half of Korte Akkeren has installed a separate sewer system. Among these sewerage pipes, there are two types of pipe influencing the groundwater level, infiltration transportation pipe (IT-Riool) and the historic back-stowed pipe (Opgeboeid) (Meliefste, 2014; Shot, 2011).



Legend

Sewerage system

Separated system

- Bemalen (Pipe Linked with Pump)
- IT-Riool (Infiltration Transportation Pipe)
- Opgeboeid (Back-stowed Pipe)
- Overstortleiding (Overflow Pipe)
- Regenwaterriool (Storm Water Pipe)
- Regenwaterriool_vgs (Storm Water Pipe_Improved Separated System)

- Spoelleiding (Flushing Pipe)
 - Vuilwaterriool_vgs (Wastewater Pipe_Improved Separated System)
- ##### Combined system
- Bemalen (Pipe Linked with Pump)
 - Opgeboeid (Back-stowed Pipe)
 - Overstortleiding (Overflow Pipe)
 - Spoelleiding (Flushing Pipe)

Figure 15 Sewerage system in Gouda

● Back-stowed Pipe (Opgeboeid)

Owing to the unevenly land subsidence in Gouda, pipes in the historical combined sewerage system are suffering from problems like disjunction and cracks. This leads to the water leakage between the sewerage system and groundwater. Thus, to prevent too much leakage from groundwater into the sewer system, these pipes are transformed into a special system, Back-stowed system (“Opgeboeid” in Dutch). Two weirs are placed at the beginning and the end of the back-stowed system, respectively, to maintain the sewerage water level in the pipes (see **Figure 16**). During the dry weather, the sewerage water level in the back-stowed system is kept to be similar to the surface water level (approximately 10 cm lower). However, once it is indicated that there would be a rainfall event, the weir at the end of the system will be opened so that the water in the pipes can be discharged away. Then these sewerage pipes now are transformed to be drainage pipes – the groundwater may leak into these pipes and be discharged away through the sewer

system. When the weirs are closed again, the sewerage water level in the pipes will be raised again. Though the back-stowed system can help to manage the groundwater level in Gouda, it may cause some pollution to the groundwater and soil. Since most of the pipes in the back-stowed system are from the combined sewer system, they transport both wastewater and rainwater. Once the groundwater level is lower than the sewerage water level in the back-stowed system, water in these pipes, as well as the pollution from wastewater, leaks out.

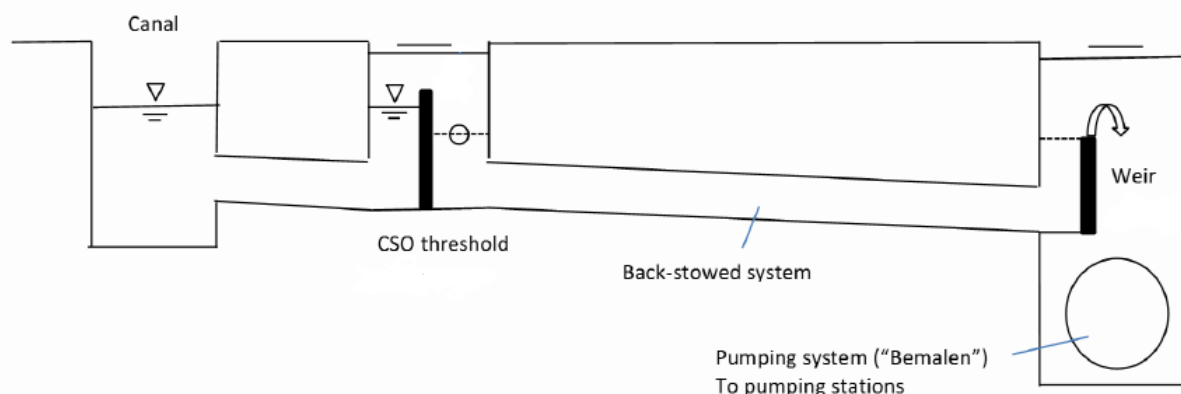


Figure 16 Back-stowed system (Wang, 2016)

- Infiltration Transportation Pipe (IT-Riool)

To protect the groundwater and soil from the negative environmental impact caused by the back-stowed pipes, the municipality of Gouda is separating the combined system. As far as feasible, stormwater is collected in the infiltration transportation pipes while the wastewater and the remainder of the stormwater are collected by watertight pipes that carry the water to the wastewater treatment plant and, in situations of extreme loading, t combined sewer overflows. The water-tight pipes are used to prevent the leakage from the pipes, while the infiltration transportation pipes are installed to manage the groundwater level. The wall of these infiltration transportation pipes is permeable, and these pipes are connected to the open water nearby. Thus, the sewerage water levels in these infiltration transportation pipes are approximately equal to the surface water level. During the dry seasons, when the groundwater level is lower than the sewerage water head, water in the infiltration transportation pipes will leak into the groundwater. During the wet seasons, the pipes can also act like subsurface drainage pipes: they could drain the groundwater to the surface water when its level is higher than the water head in the pipes.

3.1.6. Phreatic groundwater level

Since January 2015, high-tech devices for measuring the groundwater level have been installed by Wareco in varies location in Gouda. These devises measure and log the groundwater level in the phreatic aquifer with a high frequency, hourly, which gives a more comprehensive picture of the behavior of groundwater level. In May 2016, some additional groundwater observation wells are introduced in the northern part of the inner city in Gouda, where the ground surface is lower than the southern part of the inner city and has a large vulnerability of floods and inundation, to monitor the groundwater level and observe the major influential factors. The log of the groundwater level in all the observation wells (*Figure 17*) can be downloaded from the portal of Wareco. The average groundwater levels observed by these devices are shown in *Figure 18*.

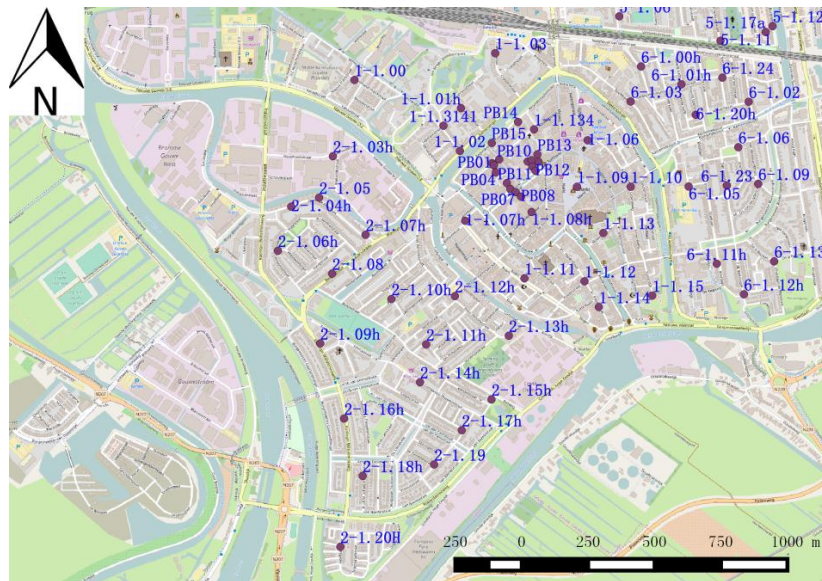


Figure 17 Observation wells

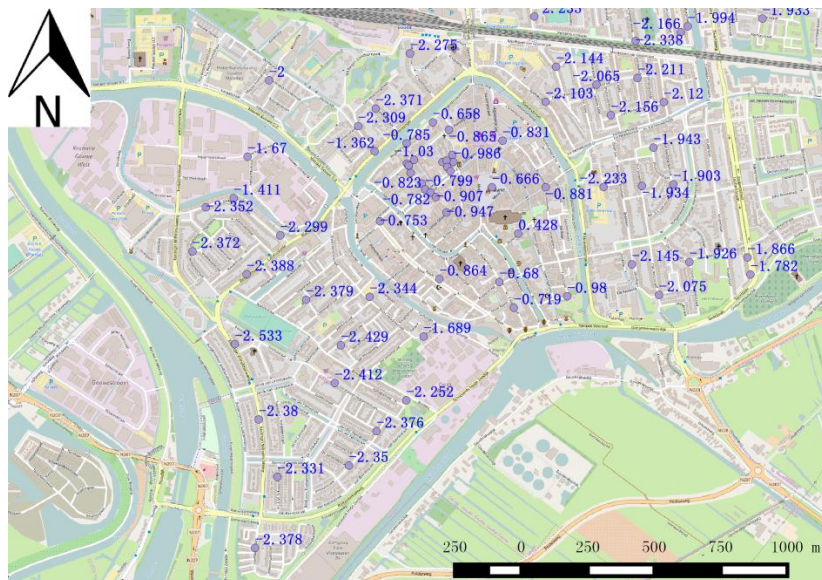


Figure 18 Average phreatic groundwater levels

The groundwater level in the inner city is generally below the surface water level, indicating infiltration from the canals. However, some observation wells show that the groundwater level is higher than the surface water level, for example, some locations in the southern part of the inner city. This can be caused by the infiltration from the Hollandse IJssel. Besides, the average groundwater level in Well 1-1.13 is approximately 1m higher than the surface water level in the inner city, which is strange but may be caused by the thinner phreatic aquifer.

Among the observation wells in Korte Akkeren, the average groundwater levels are mostly above the surface water level, while some are lower than the surface water level. The reason can be the infiltration from groundwater into the leaking sewerage pipes or the groundwater leakage to the lower aquifers. Also, it is observed that there is a large deviation between the groundwater level in the phreatic aquifer and the first aquifer, indicating that the resistance of the aquitard in between is relatively high.

3.2. Model Conceptualization and Construction

3.2.1. iMod

In this research, the groundwater model is constructed with the help of the modelling software, iMod, developed by Deltares on the basis of ModFlow by USGS (Vermeulen, Burgering, & Minnema, 2016). This tool helps modeler to build finite differential groundwater model with a fine resolution. The iMod approach allows varies resolutions, sizes of the input maps. It will perform rescaling whenever the resolution of the input data is different with the simulation resolution (Vermeulen et al., 2016).

In this research, only the major influential factor is included in the model. Thus, the following packages are used:

- BND: Boundary conditions
- SHD: Starting head
- TOP: Top of aquifers
- BOT: Bottom of aquifers
- KHV: Horizontal permeability
- VCW: Vertical resistances
- RIV: River package
- RCH: Recharge package
- OLF: Overland flow package
- STO: Storage coefficient

Among all the packages, the boundary conditions and starting head are compulsory. The river package consists of multiple raster maps as input data while others only require one (or even a constant value). The detail of some of the modelling package is described in the following.

BND Boundary conditions

The input map (or constant value) defines whether the grid cell (or area) is included in the model or whether the head at the grid cell is fixed in the simulation. If the grid cell is specified with a value less than zero, the head in the grid cell is fixed in the simulation. A value larger than zero denotes that the grid cell is included in the simulation and the head is computed during iteration. When the value of the grid cell equals to zero, this grid cell is excluded in the simulation. In a groundwater model, it is essential to have at least one fixed boundary condition; either can be grid cells with values less than zero or making use of the head-dependent components such as a river.

KHV Horizontal Permeability and VCW Vertical resistance

The horizontal permeability package should be used in combination with package TOP and BOT. Then the transmissivity of the aquifer is calculated with the horizontal permeability and the thickness of the aquifer during the model simulation. Alternatively, these packages can be replaced by the package KDW (Transmissivity of the aquifer). The vertical resistance package corresponds to the resistance of the aquitards. It also can be replaced with the combination of other three packages, TOP, BOT and KVV (vertical permeability) package (See [Figure 18](#)).

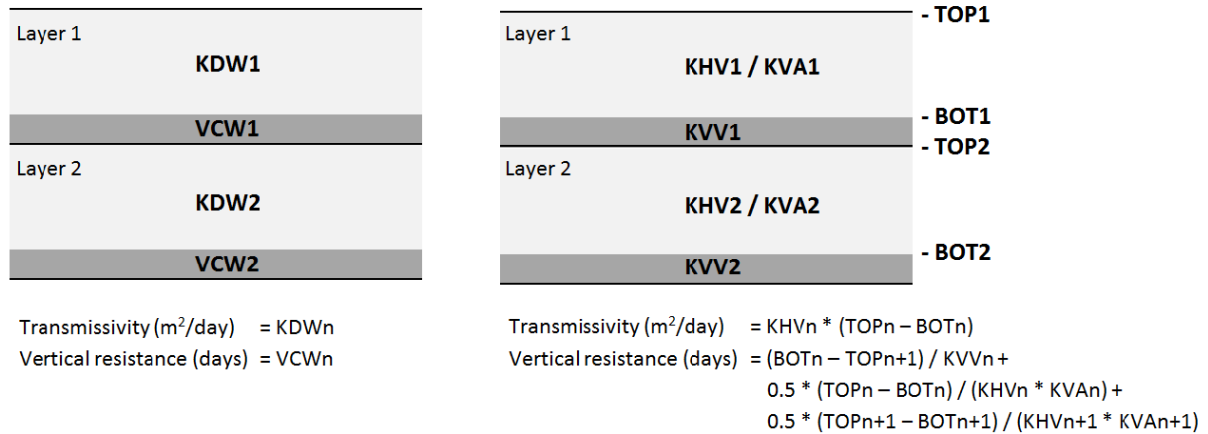


Figure 19 Relationships between Package KDW and KHV, VCW and KVV (Vermeulen et al., 2016)

RIV River package

This package consists of the raster maps specifying water level, the bottom level, the conductance of the bed and the infiltration factor as input. The river package represents the presence of permanent water from which water may infiltrate to the groundwater and/or to which water may leak from the groundwater. The infiltration factor represents the presence of the infiltration flux whenever the head is less than the bottom. When the value in the grid cell of the infiltration factor map is larger than zero, infiltration through the bottom is allowed even though the groundwater level is lower than the river bottom.

OLF Overland flow package

In this package, the elevation is above which outflow of groundwater will occur when the phreatic groundwater level exceeds it. The overland flow is discharged out of the model and does not return to the subsurface again. This elevation can be assigned a few centimeters above the surface elevation to simulate the shallow ponding on the land surface. The flow rate of this package is calculated assuming a fixed resistance against the outflow of 1 day.

STO Storage coefficient

In this package, the storage coefficient is specified to the grid cells under confined condition while the specific yield is assigned to the grid cells under the unconfined condition for each aquifer. The value of the storage coefficient depends on the lithology of the aquifer. Usually, the specific yield of the unconfined aquifer differs from 0.1 to 0.2, while the storage coefficient in confined aquifer varies between 10⁻⁵ and 10⁻³.

3.2.2. Selection of Boundary and Model resolution

There are several methods to decide the boundary condition since the surface water level in the canals around Gouda is in control of the water board Hoogheemraadschap van Rijnland and is measurable, the first idea is making use of the canals around the inner city of Gouda and Korte Akkeren. However, since the bed of the canals around the polders does not always reach the bottom of the phreatic aquifer, there would be still some groundwater flux underneath the canals which affects the accuracy of the model. Thus, using the canals around the study area as the boundary conditions is insufficient. Alternatively, methods, like calculating the spreading length or estimating the boundary with an existing model, are feasible. In this research, the later solution is adopted. The boundary is selected based on a regional 9-layer model with relatively coarse resolution (100 m × 100 m) developed by Deltares. Since this research only focuses on the simulation of the groundwater level in the phreatic aquifer. Both the horizontal and vertical boundary can be selected based on the sensitivity. Firstly, the groundwater level at steady state is calculated with a fixed head at the boundary. Then, a certain value is added or subtracted to the fixed head at each boundary cell to observe its effects on the groundwater level in the study area at steady state with different numbers of vertical layers. If the deviation is acceptable, then the boundary is also sufficient.

In addition, Croda, a company located in Korte Akkeren (See [Figure 20](#)), had been extracting the groundwater in the first and second aquifer since the 1950s. The water extraction stopped permanently in the winter of 2015. Before the company stopping the extraction, Royal Haskoning DHV studied the influence its influence on the groundwater level in Gouda with a groundwater model (Boleij, 2013). The calculated change of the phreatic groundwater level after terminating the groundwater winning for best guess and worst case is shown in [Figure 21](#). For the best guess, there is seldom any change in phreatic groundwater level in both the inner city and Korte Akkeren. For the worst case, there is some level change occurs in the eastern part of Korte Akkeren, but the level change is within 10 cm. And according to the groundwater level observation well near the groundwater extraction points (Well 2-1.15), no obvious level drop is observed during the winter of 2015 ([Figure 22](#)). These facts indicate that the resistance of the aquitard is so large that the sensitivity of phreatic groundwater level to the groundwater extraction is relatively small. Thus, to speed up the simulation, the groundwater level in the first aquifer is set to be a constant value as an additional boundary.



Figure 20 Groundwater extraction wells of Croda (Boleij, 2013)

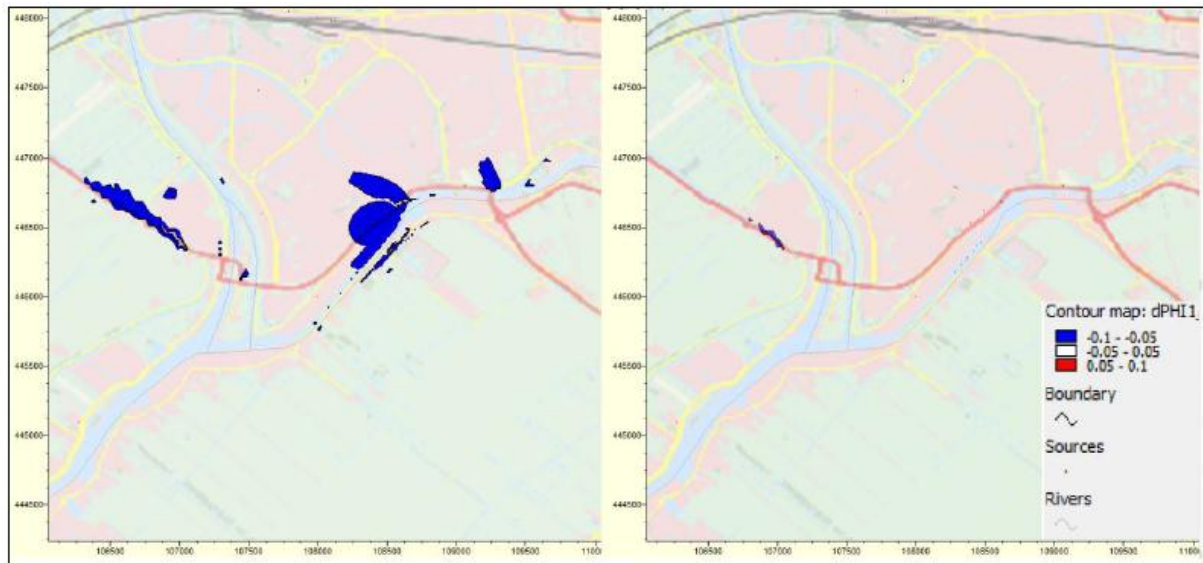


Figure 21 Change of the phreatic groundwater level after terminating the groundwater winning for best guess and worst case (Boleij, 2013)

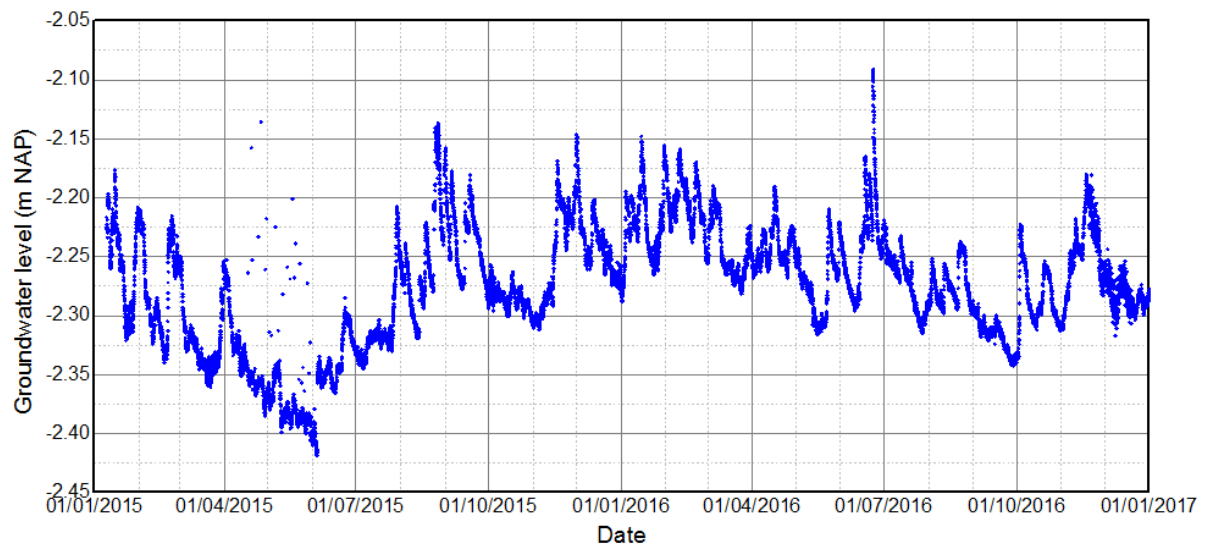


Figure 22 Groundwater observation at Well 2-1.15

Choosing an appropriate data resolution according to the intended use of the model is important for model construction. It is true that having a very high model resolution does help to increase the accuracy of the model, however, this also increases the size and the simulation time. In this research, the model is established mainly to support the further study on the land subsidence and groundwater regime in Gouda. Both of them are relative slow progresses. Thus, the temporal resolution for this model can be relatively low, daily resolution could be enough. In the meanwhile, since the model is also aimed to simulate the groundwater level to protect the wooden piles of historical houses, the spatial resolution should be high enough to include local details like different kinds of land covers. Based on the data availability, the spatial resolution of this model is $2\text{ m} \times 2\text{ m}$. Vertically, the top and the bottom elevation of the phreatic aquifer is modeled in a high resolution, while the resolution of the other layers is coarser.

3.2.3. Subsurface

In this research, the subsurface structure is constructed based on the coarser model provided by Deltares. More details at first 5 m are included in the model, based on the lithology logs and lithostratigraphy concluded by Van Laarhoven (2017). The elevation of the subsurface structure of the model is concluded in **Table 1**. In this research, the peat layer and the fluvial deposits are combined to be conceptualized as one aquitard, while the anthropogenic layers are simulated as the phreatic aquifer. Because the lithological components of the two anthropogenic layers are different, the hydrological properties of these two layers may also differ. As a result, the phreatic layer is divided into two separated aquifers with an extremely low resistance in between. However, errors can occur when the groundwater level is lower than the bottom of the upper phreatic layer. As a result, the bottom of this layer is set to be lower enough to avoid this problem. As for the peat layer, because the peat soil in the inner city experienced a more extended period of compression than that in other areas, a higher aquitard resistance in the inner city is expected.

Table 1 Conceptualization of subsurface structure for groundwater model

Layers		Top elevation (m NAP)	Bottom elevation (m NAP)	Lithostratigraphy
Phreatic aquifer	Upper	8.2~-6.7 5.1~-1.3 (The inner city) 2.0~-2.7 (Korte Akkeren)	2.8~-7.4 0.7~-4.7 (The inner city) -2.3~-4.7 (Korte Akkeren)	Recent anthropogenic layer, partly historical anthropogenic layer
	Lower	2.8~-7.4 0.7~-4.7 (The inner city) -2.3~-4.7 (Korte Akkeren)	2.8~-7.1 -1.6~-5.8 (the inner city) -3.1~-4.7 (Korte Akkeren)	Partly historical anthropogenic layer
Aquitard		2.8~-7.1 -1.6~-5.8 (the inner city) -3.1~-4.7 (Korte Akkeren)	-9.9~-17.2	Recent fluvial channel fill, Peat layer, Holocene floodplain
First Aquifer		-9.9~-17.2	-21.3~-22.3	Zuidplas channel belts, Pleistocene age deposits

3.2.4. Stresses

3.2.4.1. Surface water

When constructing the groundwater model, the surface water level in the canals is assumed to be constant. On the one hand, the groundwater level does not react fast to the fluctuation of the surface water level. On the other hand, though the surface water level does fluctuate, the deviation between the measured water level and the planned one is limited due to level control by the water board. For example, **Figure 23** shows the comparison between measurement of the surface water level in the inner city and the planned one; the fluctuation is only in centimeters. There is a rapid drop down and rise in surface water level on June 28th; it may be caused by the measuring error, which is negligible. As for the tidal river, de Hollandse IJssel, the river stage is also simulated as a constant value also because of the slow response of groundwater level to the fluctuation of the stage.

The conductance of the canal bed is highly dependent on the thickness of the bed sediment, the soil properties of the sediment and the permeability of the walls of the canals. Because the phreatic groundwater level in the inner city higher than the levels in the polders around, the groundwater is draining out from the inner city and the surface water in the inner city continues infiltrating to the

ground. Thus a smaller canal conductance in the inner city compared to that in other polders is expected. This conductance was subject to calibration.

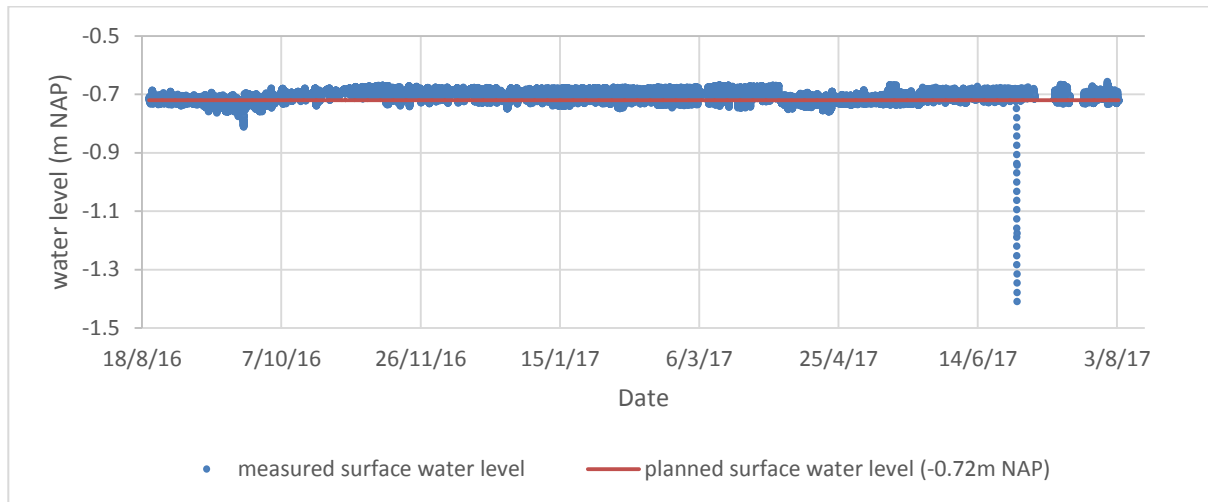


Figure 23 Comparison of measured surface water level and the planned one in the inner city (Source: http://rijnland.webgispublisher.nl/?map=Rijnland_viewer)

3.2.4.2. Sewerage system

In the groundwater model, the leaky back-stowed pipes can also be conceptualized as rivers: when the sewerage water level in the pipes is higher than the groundwater level, leakage from pipes to soil is expected, while when the groundwater level is higher than the water head in the pipes, water flux from soil to pipes will occur.

3.2.4.2.1. Infiltration transportation pipes (IT-Riool)

The infiltration transportation pipes are linked to the surface water in the polders and boezom, so the sewerage water levels in this kind of pipes equal to the water level in the canals. It is assumed that the surface water level is a constant due to the small deviation of the level and slow response of the groundwater level. The sewerage level in the infiltration transportation pipes is assumed to be the planned surface water level, too. What is more, because this kind of pipes is made to manage the phreatic water level, the conductance of the pipes should be a relatively large value.

3.2.4.2.2. Back-stowed pipes (Opgeboeid)

As mentioned in [Section 3.1.5](#), the reason for the leakage from the back-stowed pipes is the disjunction between the pipes and the cracks in the pipes. It is assumed that both the degrees of disconnection and the cracks are related to the ages of the pipes. It is because the disconnection is mainly caused by the uneven land subsidence. The older the pipes are, the higher degree of disjunction might occur. The extent of the cracks of the pipes is related to both the land subsidence and the pipe material. However, there the pipe material is also related to the age. In the very beginning, the sewerage pipes are made of bricks, which is easy to be cracked. Concrete sewerage pipes first occur in the middle 19th Century and start prevailing gradually. In early 20th Century, pipes made of cast iron and stoneware started to be used in the sewerage system. Then occur the plastic and fiberglass reinforced materials. Generally, the pipe material is becoming stronger and stronger with the change of time. As a result, the conductance of the pipes is assumed to be only related to its age. In this research, the pipes of the back-stowed system are divided into four groups according

to installation year, 1900 and earlier, 1900~1950, 1950~2000, after 2000, respectively. Different values of conductance are assigned to the pipes in different groups which need to be calibrated in the next stage.

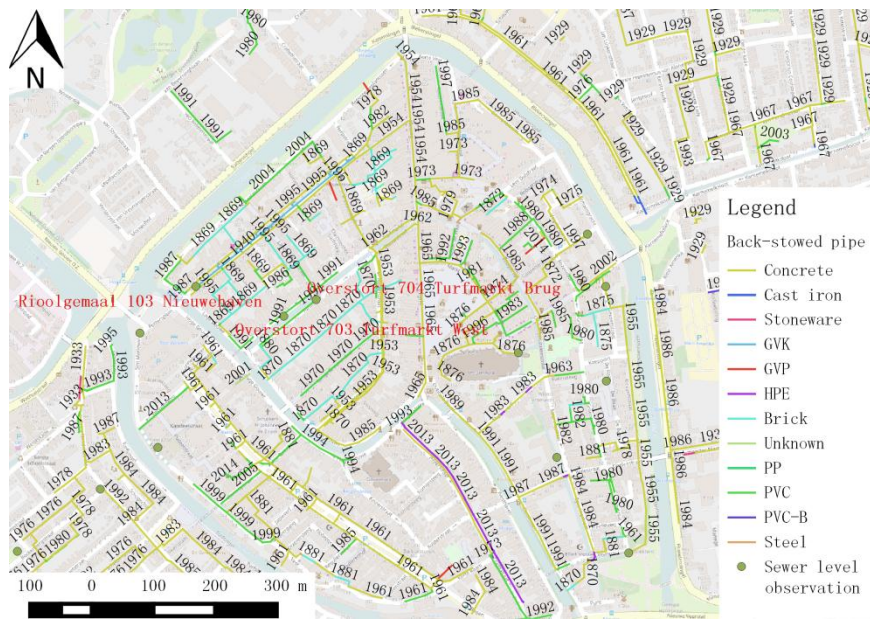


Figure 24 Back-stowed pipes and sewer level measurement point

As for the simulation of the opening and closing the weirs in the back-stowed system, it is represented by the changing sewerage water level in the model. Since the leaky pipes in the lower part of the inner city are relatively old and this area is also sensitive to the phreatic groundwater level, the filling and emptying of the leaky pipes are only simulated in the lower part of the inner city (Nieuwe Haven), and all the back-stowed pipes are assumed to be always filled. To simplify the simulation of the filling and emptying of the leaky pipes in the back-stowed system, the drainage schedule of the weir opening and closing is adopted. There are three kinds of status in the drainage schedule: 1. the pipes are filled; 2. the pipes are emptied; 3. situations in between. The municipality of Gouda holds the schedule of the opening and closing of the weirs, but they are not always correct. Alternatively, there are two ways to generate this schedule. Firstly, this schedule can be generated from sewer level monitoring data. I-Real is a company that have been measuring the sewerage level with a high frequency (every minute) in Gouda for a long time. It has three measuring spots around Nieuwe Haven (See [Figure 24](#)). Among these three points, the observation point Turfmarkt West and Turfmarkt Brug are measuring the sewerage level in the back-stowed pipes (See [Figure 25](#)). When the pipes in the back-stowed pipes are filled, the sewerage water levels at the measuring points are similar (approximately 10 cm lower than the planned surface water level). However, there is approximately 0.15 m difference between the observations at the two locations when the pipes are emptied. It is because that the measured sewerage water levels are the bottom level of the pipes when the pipes are emptied. The drainage schedule in this research is generated from the observation of these two monitoring locations. When the sewer level at most of the time is emptied, it is assumed that the back-stowed system is emptied on that day in the drainage schedule, and the water level of the sewer is assumed to equal to the bottom level of the pipes. When the sewer level at the most of the time is similar to the planned surface water at most of the time on that day, it is assumed that the pipes are filled in the drainage schedule, and the sewerage water level is simulated to be 10 cm lower than the planned surface water level. And when the pipes are emptied for only approximately half of the day, the sewerage level is assumed to be the average value of the

surface water level and the pipe bottom level. Developing the drainage schedule according to the sewerage level measurement can be seen as a direct method. A second approach is to develop the schedule indirectly based on groundwater level observation from Well 1-1.05. This observation well is closed to very leaky pipes, and it is very sensitive to the sewerage water level in the pipe (see [Figure 26](#)). As shown in the figure, the groundwater level only rises slightly or even drops rapidly during a heavy precipitation event. Usually, the leaky sewer pipes are filled with water, so when the groundwater level drops down rapidly, it means that the weir of the back-stowed system is opened and the pipes are emptied. In the meantime, a rapid rise of the groundwater level indicates the closing of the weir. The sewerage water level of the leaky pipes equals to the surface water level if the weir is closed. Moreover, the drainage schedule can be generated according to the duration of the emptying of filling the pipes on a particular day. In this research, the direct method is used to develop the drainage schedule of the back-stowed system. However, the indirect method is also applied here when the sewer level measurement data is missing.

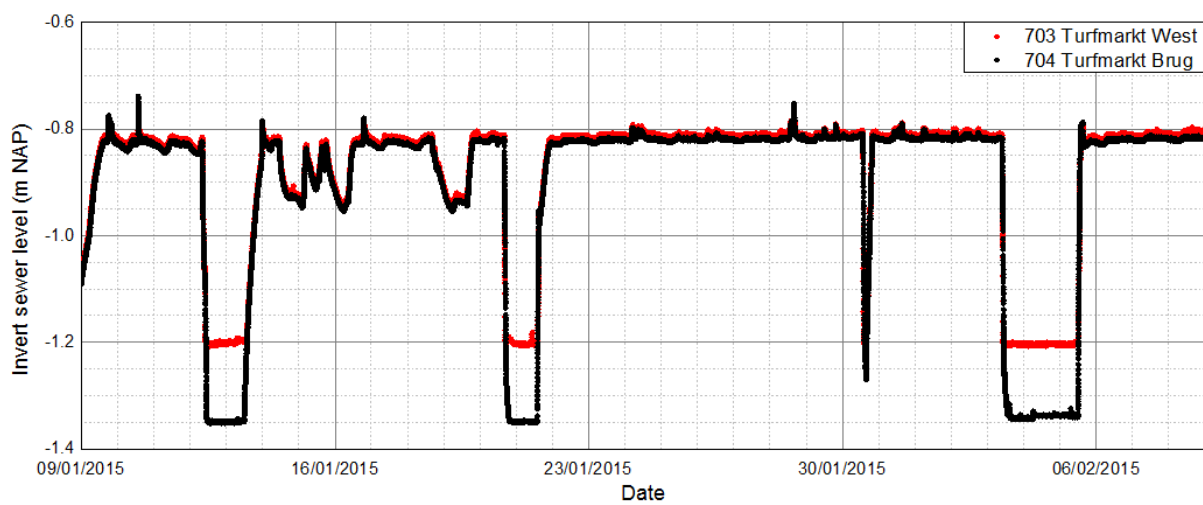


Figure 25 Sewerage level observations in the inner city.

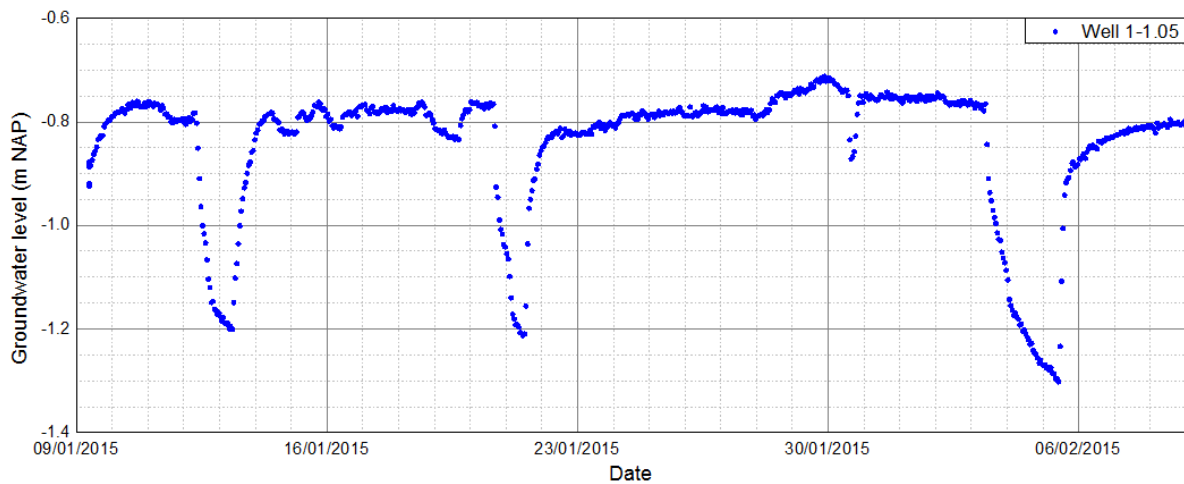


Figure 26 Groundwater level observations at Well 1-1.05

3.2.4.3. Recharge

In large parts of the model area, the unsaturated zone is extremely thin, often less than half a meter. Consequently, evapotranspiration is often at its potential rate. Moreover, recharge information is only available on a daily basis, as data on (potential) evapotranspiration are on a daily basis only. This is why it was decided to 'neglect' the hydrological processes in the unsaturated zone and feed the model with daily recharge values.

The recharge is the sum of the positive flux caused by precipitation and negative flux due to evapotranspiration. The value of daily recharge differs among all kinds of land cover. Aiming to indicate the spatial variance of daily recharge, in this research, the study area is divided into six kinds of land cover based on their hydrological behavior, impervious surface, pervious pavement, grassland, trees, backyards, water surfaces. The behavior of these kinds of land cover is conceptualized as follow:

- Impervious surface: This kind of land cover (for example, roofs and impervious pavements) has no positive or negative recharge flux.
- Pervious pavement: Part of the precipitation can infiltrate into the ground while there would not be any negative flux.
- Grassland/lawn: Both positive and negative flux through grassland can occur. However, since the root zone of grass is not deep, so the negative flux cannot reach the potential evapotranspiration when the groundwater table is low.
- Trees: Both positive and negative flux can occur. Since the root zone of the trees is thick enough to extract water under the groundwater table, so the negative flux equals to the potential evapotranspiration. In addition, because of the interception, the positive flux is always lower than the actual precipitation.
- Backyards: This type of land cover is a mixture of different kinds of land covers. The proportion and variety of the land cover differ from individual to individual. To simplify the simulation, it is assumed to be partly grassland and partly impervious pavement.
- Water surface: Same as impervious surface, neither positive nor negative flux can occur.

The land cover is assigned to every grid cells (size 2 m × 2 m) in the raster layer with the help of the GIS system. Then a series of recharge maps are produced according to the difference between the precipitation and potential evapotranspiration, called Z maps ($Z = P - E_p$, where P stands for the daily precipitation and E_p represents the potential evapotranspiration, the value z can be called as reference recharge):

- It is also assumed that if daily precipitation is less than potential evapotranspiration ($Z < 0$ m), all the precipitation will be evaporated on that day. The rest of evapotranspiration will be calculated based on the land cover.
- When the daily precipitation exceeds the potential evapotranspiration ($Z > 0$ m), the evapotranspiration is assumed to be the same as potential one. The infiltration is calculated according to the type of each land cover.
- Impervious surface: recharge R always equal to zero.
- Pervious pavement: when $Z \leq 0$ mm/day, recharge $R = 0$. When $Z > 0$ mm/day (precipitation exceeds potential evapotranspiration), recharge $R = Z \times (1 - C_{runoff})$, where C_{runoff} stands for the runoff coefficient of the pervious pavement. There are many factors influencing the value of the runoff coefficient, such as the material (permeability, clogging situation), joint width, precipitation

intensity (Korkealaakso, Kuosa, Niemeläinen, & Tikanmäki, 2014). In this research, the runoff generation processes in pervious pavement area are simulated focusing on the changing infiltration capacity caused by the precipitation. According to Green-Ampt Infiltration Model (David L. Freyberg, John W. Reeder, Joseph B. Franzini, & Remson, 2980), the infiltration capacity can be calculated with the equation:

$$f = K_0 \left[1 + \frac{(h_e + H)(\theta_s - \theta_i)}{F} \right]$$

where, f is the infiltration capacity at time t , K_0 is hydraulic conductivity, h_e is effective suction head, H is surface water depth, θ_s is volumetric soil moisture content, θ_i represents initial volumetric soil moisture content, and F is the net change in total soil moisture above the moving wetting front. This equation indicates that during a rainfall event, the infiltration capacity will decrease with the increase of the total net infiltration and finally reaches a final infiltration capacity. Moreover, if the rainfall intensity exceeds the infiltration capacity of the pervious material, then the exceeded part of the rainfall becomes the Hortonian overland flow. In the groundwater model, the runoff coefficient of the previous pavement is assumed to range from 0 to 0.8 according to the changing daily recharge (See [Figure 27](#)).

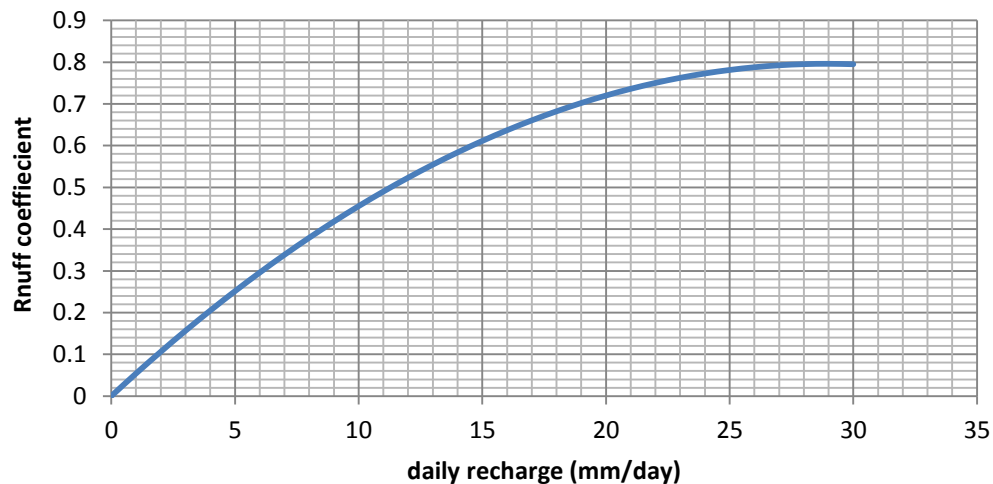


Figure 27 Changing runoff coefficient according to the changing daily recharge

- Grassland: when $Z > 0$, recharge $R = Z$. When $Z \leq 0$ mm/day, the crop coefficient is introduced to correct the evapotranspiration: $R = Z \times K_C$. The crop coefficient for grassland approximately ranges from 0.6 to 0.8 (Meyer, Gibeault, & Youngner, 1985). Because Gouda has a relatively high groundwater table, the crop coefficient could be large. The value 0.8 is used in this research.
- Backyards: In this research, the backyards are assumed to be partly grassland (75%) and partly impervious area (25%). Thus, the recharge through the backyards can be calculated as: $Z > 0, R = Z \times P_{grassland}$; $Z \leq 0, R = Z \times C \times P_{grassland}$.
- Water surface: recharge R always equal to zero.

The calculation of the recharge value under the trees is extracted from the Z maps because of its complexity caused by the interception progress: the effective precipitation (P_e) should be calculated first before comparing with the evapotranspiration. When the actual precipitation is smaller than or equals to the capacity of interception ($P \leq I$), there is no effective precipitation, recharge

$R = P_e - E_p = -E_p$. When the actual precipitation exceeds the interception capacity of the trees, recharge $R = P_e - E_p = P - I - E_p$.

An example of the recharge map is shown in **Figure 28**. This recharge map is used in groundwater model at steady state when the reference recharge is 0.87 mm/d. As shown in the figure, the very detailed recharge is estimated and assigned in the map. The amount of recharge flux in the grassland area is the largest one when compared with that in other areas, while the recharge in the brick pavement area the second highest one. The recharge in the backyards is a little bit less because it is assumed that there is 25% of the impermeable area. Same as the recharge in the surface water and roof areas, there is no recharge under the trees because of the effect of interception. **Figure 29** shows the cumulative frequency curve of Z values (reference recharge). The possibility of situations when the Z value is smaller than -6 mm or larger than 35 mm is considerably low. Therefore, the Z maps are generated from -6 mm to 35 mm. Then, these maps will be used in the transient groundwater model according to the daily meteorological data.

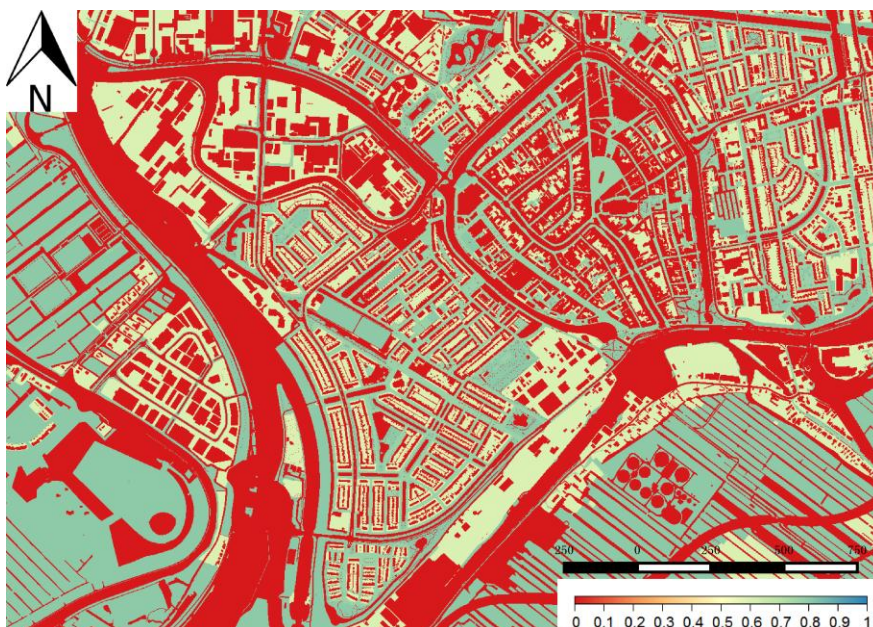


Figure 28 Map of recharge used in groundwater model at steady state (Unit: mm/d)

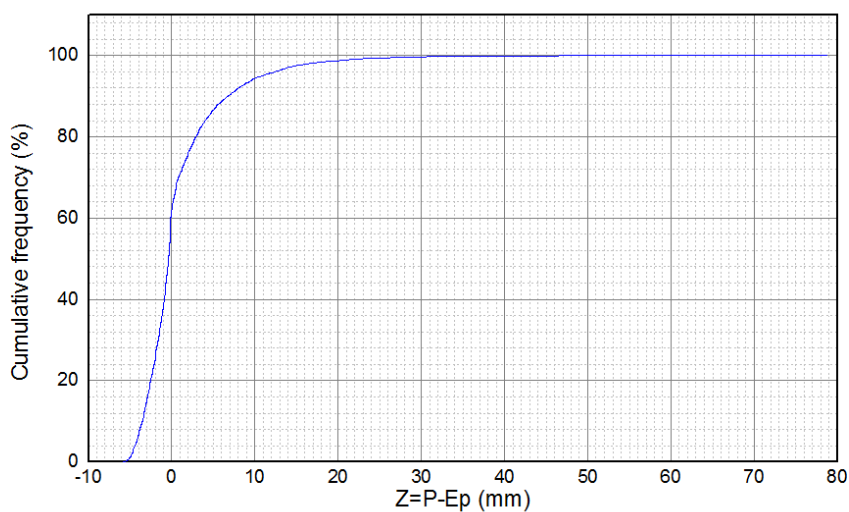


Figure 29 Cumulative frequency curve of Z value

3.2.4.4. Initial conditions

Initial conditions define the groundwater conditions at the start of the model simulation (Barnett et al., 2012). In practice, the initial conditions usually are defined with initial head in every grid cells for each aquifer. For a transient groundwater model, defining the initial condition is also a mathematical problem and may influence the results of the simulation (Barnett et al., 2012). Thus, it is important to define appropriate initial conditions. In this model, the groundwater level calculated at the steady state is used to be the initial condition of the transient model because the groundwater level calculated at steady state reasonably stays consistent with the boundary conditions and stresses in the model. However, errors also exist during the subsequent time steps, so allowing for a certain period to equilibrate the initial head is necessary. In this model, since the storage of the unsaturated zone in the phreatic aquifer is not included in the model and the data availability is limited, first three months of the model (from the beginning of November 2014 till the beginning of January 2015) is used to be the equilibration period. During the simulation, the groundwater level at the boundary of the model is assumed to be fixed to ensure a reasonable groundwater flow flux at the boundary. The fixed head used in this model is extracted from the result of the coarse regional model provided by Deltares at the steady state. Though the fixed head may not be accurate when compared to the actual observation level, it is still valid. It is because the sensitivity of the boundary head is tested when selecting the boundary of the model (see [Section 3.2.2](#)) to ensure that the groundwater level variation at the boundary has a very low impact on the groundwater level within the study area.

3.3. Calibration, validation and sensitivity analysis

As mentioned in [Section 3.1.6](#), the groundwater level in Gouda is observed hourly since January 2015 and some additional observation wells are added in May 2016. This two year period data is used here for model calibration and validation.

Before calibrating the model at transient state, the groundwater model is firstly calibrated at steady state. On the one hand, calibrating the groundwater level at steady state consumes less time, and it helps to get a general idea of the range of the parameters like hydraulic conductivity, vertical resistance, and river conductance. On the other hand, the calibrated groundwater level can be used as the initial state in the transient model. When calibrating the groundwater model at steady state, the modeled value is compared with the average groundwater level of all the observation wells. In the simulation of the steady state, the rate of infiltration and evapotranspiration is calculated using the average value of precipitation and potential evapotranspiration. The leaking sewer pipes are simulated to be backed up in the steady state.

After getting acceptable deviations between the modeled phreatic groundwater level and the average observation values, this model starts to be calibrated at transient state. In the calibration here, observed groundwater level data in 2015 ~ 2016 is used. Since the data in 64 observation wells are available, to simplify the calibration procedure, the data of the 8 wells used to correct the pattern of the modeled groundwater level, in the meanwhile, 3 indicators, the root mean squared error (RMSE), coefficient of determination (R^2), Nash-Sutcliffe efficiency, of the phreatic groundwater level simulation to make sure that the deviation in all the wells are acceptable. The root mean squared error evaluates the variance of the simulation errors, given by (Adamowski & Chan, 2011):

$$RMSE = \sqrt{\frac{1}{n} \sum_{i=1}^n (h_i - \hat{h}_i)^2} \quad (0.1)$$

where, h_i is the daily average value of the groundwater level observation on day i , while \hat{h}_i is the simulated groundwater level on day i . A perfect fit simulation can yield $RMSE=0$. The coefficient of determination (R^2) measures the degree of correlation among the observed and simulated values, which ranges from 0 (no statistical correlation) to 1 (perfect fit) (Adamowski & Chan, 2011). It is defined as (Daliakopoulos, Coulibaly, & Tsanis, 2005):

$$R^2 = 1 - \frac{\sum_{i=1}^n (h_i - \hat{h}_i)^2}{\sum_{i=1}^n h_i^2 - \frac{\sum_{i=1}^n \hat{h}_i^2}{n}} \quad (0.2)$$

The Nash-Sutcliffe efficiency is also used to quantitatively describe the accuracy of model simulation. It ranges from $-\infty$ to 1. A positive efficiency means that the model simulation predicts the groundwater level better than the mean groundwater level observation. The model reaches the perfect match of $E=1$. When $E=0$, the model simulation is as accurate as the mean value of the observation, while a negative efficiency indicates that the mean value of observation is a better predictor than the model. The efficiency is calculated as follow:

$$E = 1 - \frac{\sum_{i=1}^n (h_i - \hat{h}_i)^2}{\sum_{i=1}^n (h_i - \bar{h})^2} \quad (0.3)$$

where \bar{h} corresponds to the mean observed groundwater level. To correct the patterns of groundwater level, 4 observation wells in the inner city (Well 1-1.04, 1-1.08, 1-1.12, and 1-1.14) and 4 in Korte Akkeren (Well 2-1.07, 2-1.10, 2-1.14, and 2-1.19) are selected. These two groups of wells can both comprise a cross-section in the inner city and Korte Akkeren, respectively. There are two reasons why the monitoring data of Well 1-1.04 is selected for the calibration. Firstly, this observation well locates in near a back-stowed pipe, where the groundwater level is sensitive to the influence of the leakiness of the pipe. Secondly, this well lays at the lower part of the inner city, which is in a high vulnerability of both flooding and land subsidence. Then observation wells in the middle (Well 1-1.08) and in the higher part (Well 1-1.12 and 1-1.04) are also selected to calibrate the influence of the canals and Hollandse IJssel. Also, observation wells in the north (Well 2-1.07), middle (Well 2-1.10 and 2-1.14) and south (Well 2-1.19) part in Korte Akkeren are selected in the calibration to calibrate the influence of canals with different surface water level and Hollandse IJssel. Then, the model is validated with the groundwater level observation data in 2016 ~ 2017. Besides these wells selected in the calibration stage, more observation wells are selected this time, because there are some additional data in the lower part of the inner city since May 2016. Thus, the observation wells PB04, PB05, and PB08 are added to check the behavior of the groundwater model.

Then the sensitivity analysis is performed to measure the uncertainty of the model input parameters. In strict mathematical terms, a sensitivity measures how fast one quantity changes when another changes (Barnett et al., 2012). Here, the sensitivity stands for the derivative of a function. In groundwater modeling, after the trial-and-error calibration, sensitivity analysis involves changing a model parameter by a certain amount to establish how the model outputs are affected by that change. In the simulation of the groundwater system of Gouda, various parameters are involved, such as the conductance of the canals and sewerage pipe walls, the hydraulic conductivity and storage coefficient of aquifers as well as the vertical resistance of the aquitard. Their sensitivity is

tested by both adding and removing 50% to/from the calibrated value, re-running the model to obtain a new set of output in both the calibration and validation periods and observing the effect of the change. Though it does not give a real sensitivity (derivative), it also shows the sensitive effects of each parameter. In the meanwhile, when estimating the groundwater recharge, there are also many parameters involved, such as the changing runoff coefficient of the pervious pavement, the crop coefficient of the grassland, the interception amount of the trees and the percentage of the greens in the backyards. In this article, the sensitivity of these parameters is not calculated. However, the sensitivity of the groundwater recharge is calculated instead to show the importance of a precise estimation.

3.4. Scenarios

Once the groundwater model shows acceptable results during both calibration and verification stage, several alternative plans for urban (ground)water management can be applied to simulate its influence on the groundwater level in Gouda. The starting point of this simulation is at the end of the calibration period (December 31st, 2015). The meteorology data in 2016 ~ 2017 is also used in the scenario simulation. Results of the scenarios test will be analyzed by comparing the spatial influence via the mean value.

- **Scenario 0: Null**

In the null scenario, no change would happen. Since the starting point of this simulation is that at the end of 2015, the meteorology data in 2016~2015 is also used in the scenario simulation, the groundwater time series of model validation is used to compare with the results of other scenarios during analysis as the null scenario.

- **Scenario 1: Watertight sewerage pipes**

As mentioned in [Section 3.1.5](#), the back-stowed system can cause environmental problems because of the leakage of the sewerage water. To solve this problem, the municipality is trying to reconstruct its sewerage system. Up to now, some work has been done in Korte Akkeren. In this scenario, the groundwater level is simulated when all the back-stowed pipes are replaced by new watertight sewerage pipes. Thus, in this scenario simulation, the conductance for all the back-stowed pipes is replaced with zero, while the conductance of the infiltration transportation pipes remains the same.

- **Scenario 2: Lower surface water level in the inner city**

Since the land surface elevation in the northern part of the inner city is relatively low compared to that in the southern inner city, the northern area, especially Turfmarkt, is under a high vulnerability to flooding and inundation. Thus, it is assumed that the planned surface water level in the canals of the inner city is reduced by 20 cm in this scenario, aiming to observe its influence on the drop of the groundwater level.

- **Scenario 3: A new canal in Nieuwe Haven**

Besides, constructing a new canal in Nieuwe Haven is frequently brought forward in discussion in the future if the city with the municipality of Gouda. Thus its influence on groundwater level is tested with this groundwater model. In this scenario, the groundwater level of this canal also follows the

planned level of the inner city and the bottom of this canal is simulated to be -1.70 m NAP (in the upper anthropogenic layer with higher hydraulic conductivity).

- **Scenario 4: A new canal in Nieuwe Haven + Lower surface water level in the inner city**

Once the new canal in Nieuwe Haven is constructed, there would be more water infiltrated from the surface water system into the ground. This may help to prevent large drop of the groundwater level in the inner city when the surface water level is reduced by 20 cm. Thus, Scenario 2 and 3 are combined here.

- **Scenario 5: Infiltration Transportation pipes**

In this scenario, all the leaky sewerage pipes are replaced by the watertight pipes, while an infiltration transpiration pipes are installed near each back-stowed pipes. Thus, the infiltration of polluted water from the leaky sewers is stopped while the groundwater level can also be managed by these infiltration transpiration pipes.

4 Results

4.1. Model Calibration

4.1.1. Model parameters

There are two types of parameters need to be calibrated in the groundwater model, soil properties (hydraulic conductivity, vertical resistance, and storage coefficient) as well as the conductance of the water system (surface water and sewerage system). The model was first calibrated at the steady state to get estimation on the conductivity of the phreatic aquifers, the vertical resistance of the aquitard as well as the conductance of the water system. Moreover, the parameters are further calibrated at transient state while a new parameter, storage coefficient, is added in the model calibration. **Table 2** shows the calibrated soil properties in the model. The calibrated hydraulic conductivity of the upper phreatic aquifer layer is relatively higher than that of the lower layer, but it is acceptable when corresponding to a layer composed with sand and gravel. Wang (2016) did slug tests at 11 spots at the center of the inner city. According to her results, the conductance of the phreatic aquifer varies from 4 to 11 m/d. However, they are some local values, and whether this conductivity belongs to the upper phreatic layer or the historical one are unknown. Thus, the calibrated values of the hydraulic conductivities of the phreatic aquifers are still acceptable. As mentioned in **Section 3.2.2**, the peat layer in the study area is compressed because of the urban construction, and the influence of the groundwater level variation in the first aquifer on the groundwater level in the phreatic aquifer is very limited according to the study from Royal Haskoning DHV. Thus having such a high vertical resistance for the peat layer is reasonable. The calibrated values of the conductance of surface water and sewerage pipes are shown in **Figure 30** and **Figure 31**. The conductance of the canal bed is calibrated based on the groundwater observations. The conductance of the canals in the inner city is lower than that in other areas. It is because canal water in the inner city usually infiltrates into the ground, more deposition is expected in these canals resulting in lower permeable beds. The values conductance of the back stowed pipes is calibrated for four groups separated based on their ages. The older the pipes are, the higher conductance is assigned. The pipe conductance for each group is not only calibrated based on the groundwater level observation but also the field experiments and parameter analysis done by Wang (2016). According to her observation, the sewerage pipes built in the 19th Century by concrete or bricks can be identified most leaky pipes, the conductance of the pipe walls are suggested to be higher than 1.75 m²/d; the conductance of the sewerage pipes built by concrete in the first half of the 19th century is suggested to be 0.35~1.75 m²/d; Those plastic and fiberglass reinforced materials are much less permeable with a suggested conductance lower than 0.35 m²/d. The calibrated conductance of the pipes is shown in **Table 3**. The calibrated values are mostly within the suggested range of Wang's results.

Table 2 Calibrated value of soil parameter in the model

Model layer		Lithostratigraphy	Lithology	Calibrated value of soil parameter
Phreatic aquifer	Upper	Recent anthropogenic layer, partly historical anthropogenic layer	Sand, gravel and garden mould in recent anthropogenic layer, sandy clay and plenty debris of archeological admixture in historical anthropogenic layer	K= 30 m/d S= 0.8
	"Aquitard"	Imagined layer to divide two anthropogenic layers	N/A	C= 0.01 d
	Lower	Partly historical anthropogenic layer	sandy clay and plenty debris of archeological admixture	K= 15 m/d S= 0.0001
Aquitard		Recent fluvial channel fill, Peat layer, Holocene floodplain	Clay and peat	C= 5000 d (Korte Akkeren) C= 10000 d (The inner city)
First Aquifer		Zuidplas channel belts, Pleistocene age deposits	sand	K= 39 ~ 45 m/d

Table 3 Calibrated conductance of the pipes for 2 m × 2 m cell grid (Unit: m²/d)

Groups	Before 1900	1900~1950	1950~2000	After 2000	Infiltration-Transportation Pipes
Conductance	0.72~2	0.36	0.12	0	9.6



Figure 30 Conductance of surface water (Unit: m²/d)

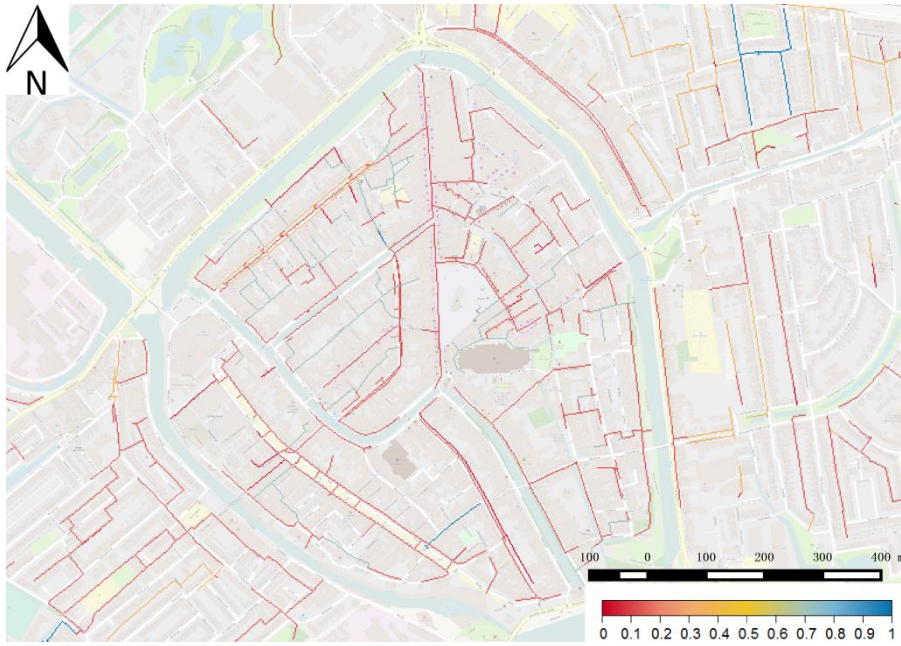


Figure 31 Conductance of sewerage pipes (Unit: m²/d)

4.1.2. Groundwater level at steady state

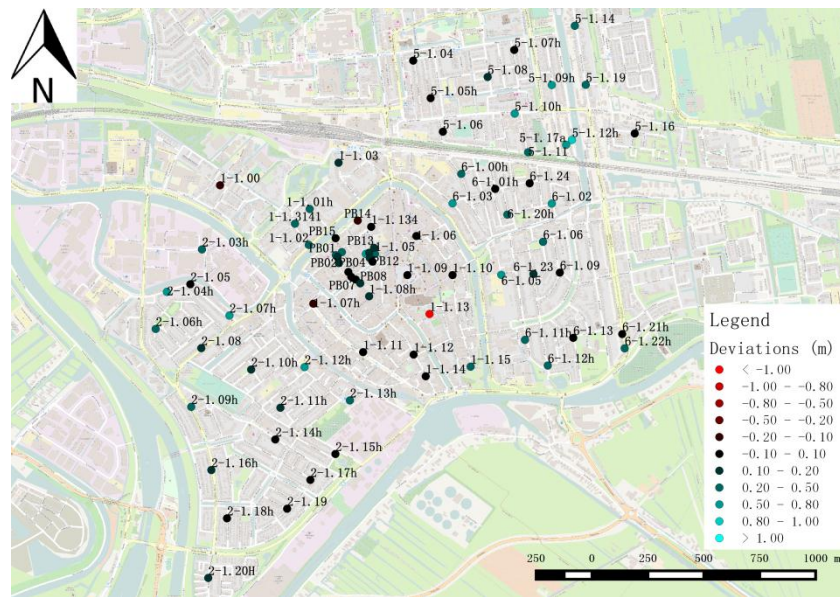


Figure 32 Deviations between the simulated groundwater levels at steady state and average observed sewerage level (Unit: m)

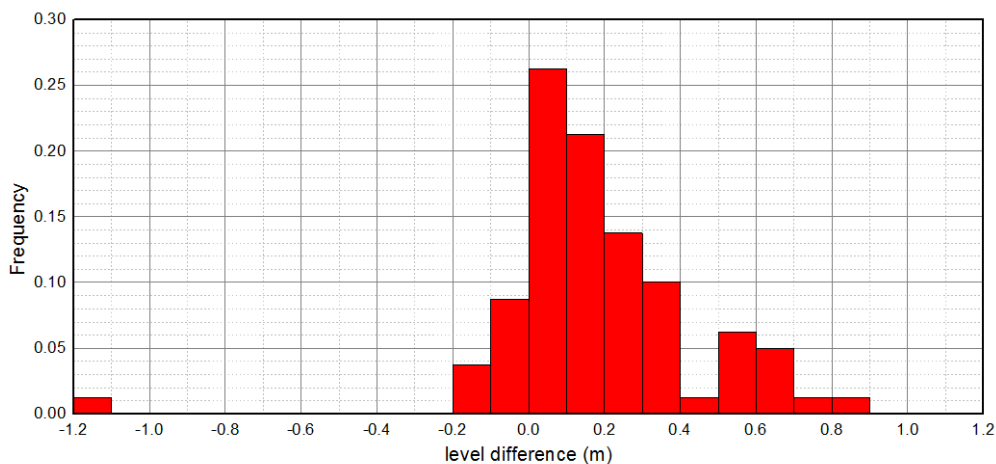


Figure 33 Histogram of the deviation between the simulated value and observed value

The groundwater model is firstly calibrated in the steady state to estimate the value of the hydraulic conductivity of the aquifer, the vertical resistance of the aquitard, and the conductance of the river and leaking pipes. The groundwater level simulated in the steady state is compared with the average phreatic groundwater level in all the observation wells. The difference between these two levels is shown in [Figure 32](#). And the histogram of these calculated differences is shown in [Figure 33](#). There are some locations where the simulated level has a relatively large positive deviation with the average observed value. They are mostly located on the border of the lower polders and close to the canal with a high surface water level. However, generally speaking, the differences between the simulated groundwater levels and the average observed levels are mostly distributed between -0.2 m to 0.2 m. The level deviation in the study area, the inner city and Korte Akkeren is considered acceptable. However, near the center of the inner city, there is a spot (Well 1-1.13) where the simulated groundwater table is more than 1 m lower than the observed value. Since the deviations at the observation wells nearby are much smaller, and there is no explanation for the high

groundwater table at this observation point found, this large deviation is ignored. The phreatic groundwater level distributions along two cross-sections are shown in **Figure 34**. These figures show apparent groundwater level differences among the different polders as expected. Thus, it can be concluded that the calibration in the steady state is feasible. According to the calculation of the water balance within the study area (See **Table 4**), nearly 80 % of the inflow flux comes from the surface water and leaking pipes, which indicates their significant influence on the groundwater level. In the meanwhile, the discharge flow out through the boundary of the inner city and Korte Akkeren contributes the most to the outflow fluxes. This is reasonable, since the surface elevations, as well as the groundwater levels in the polders nearby, are all lower than those in the inner city, and the lowest polder locates to the southwest of the study area, whose surface elevation and groundwater level are even lower than those in Korte Akkeren. The amount of the water fluxes flow out through the boundary of the model is larger than the inflow fluxes via the boundary. It is also reasonable because the polder inner city is the highest polder in the area around, the groundwater in the inner city is flowing to the polders nearby. Only a limited amount of groundwater in the phreatic aquifer flows into the first aquifer, because of the high resistance of the aquifer.

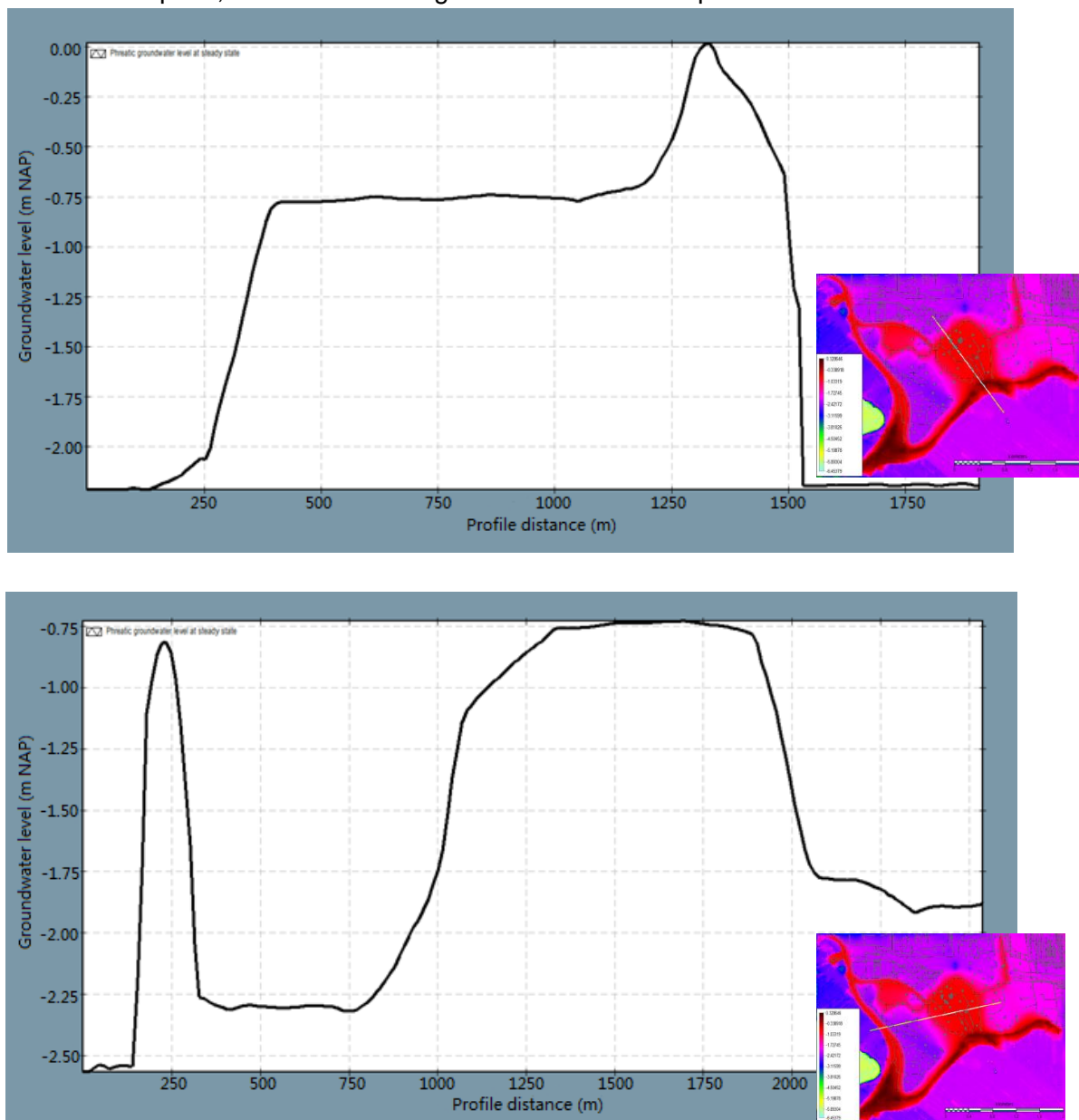


Figure 34 Groundwater levels along cross sections

Table 4 Water balance analysis at steady state

Flow fluxes	Inflow (%)	Outflow (%)
Surface water & leaking pipes	79.74	30.04
Recharge	9.60	0.00
Overland flow	0.00	15.37
Lower layer	0.00	9.19
Boundary	10.67	45.41

4.1.3. Time series at transient state

At this stage, the groundwater model is calibrated both according to the comparison of the time series of the simulated and measured groundwater level at the selected observation wells in the study area, as well as the root mean square error, R^2 , and Nash-Sutcliffe efficiency calculated with the simulated results and the daily average of observation at all the wells.

Two groups of the time series comparison between simulated groundwater level and the measurements in the inner city and Korte Akkeren are shown in [Figure 35 - 38](#) and [Figure 39 - 42](#), respectively. In the inner city, the groundwater model gives a reasonable estimation for the phreatic groundwater level at Well 1-1.04, which locates in northwestern of the inner city where it is under high vulnerability and near a leaking back-stowed pipe. And the patterns of the curve are similar to the observation. Well 1-1.08 is located in the center of the inner city. The groundwater level at this location is also influenced by the leaking pipes. Though the deviation between the simulated value and the observed value is larger, especially in summer, the model is still able to simulate the patterns. The estimation of the groundwater model at Well 1.14 is very accurate, while the estimation at Well 1-1.12 is continuously lower than the observed value. However, it is still acceptable since the simulation time series is almost in parallel with the observed time series and the deviation is only approximately 10 cm. The quality of the simulation in Korte Akkeren is not as good as that in the inner city, but with an acceptable deviation. As is shown in [Figure 30](#) and [Figure 42](#), at Well 2-1.10 and Well 2-1.19, the groundwater level in the wet season is obviously overestimated. As mentioned in [Section 3.2.4.2](#), the back-stowed system in Korte Akkeren is simulated to be always filled up. This may be the cause of the overestimation. However, the main objective of this modeling is focused on the extremely low groundwater level in the dry periods. Since the lower groundwater level is well estimated, the quality of this groundwater model is acceptable.

The RMSE, R^2 and Nash-Sutcliffe efficiency between the simulated groundwater level and the daily average of the observation are shown in [Figure 43 - 45](#), showing the goodness of fit. The RMSE in the study area are mostly distributed between 0 and 0.2 m, while the R^2 at most of the locations are above 0.90. These large RMSE values are mostly located at the boundary of lower polders and closed to a canal with a high water level, while the R^2 shows that the statistical correlation between groundwater level simulation and observation at Well 1-1.09 and Well1-1.15 is relatively low. The values of RMSE and R^2 at Well 1-1.13 show both a large simulation deviation and low statistical correlation between the model and reality. The Nash-Sutcliffe efficiency shows that, in general, the groundwater model predicts the groundwater level better in the inner city than that in Korte Akkeren. However, the value of the Nash-Sutcliffe efficiency is mostly negative. There are two main causes. Firstly, a negative efficiency can be yield when the simulated groundwater level has a constant

diviation with the observed values which is larger than the deviation of the observed values itself. For example, at Well 1-1.12 (see [Figure 37](#)), the diviation between the simulated values and the observed ones stays almost stable (approximately 8 cm). However, the calculated Nash-Sutcliffe efficiency at this well is negative (-1.38) because the deviations between the simulated values and observed values are always larger than the deviations between the observed values and the average observed value. Another cause of the negative values is that the observed values are more stable than it is simulated. It is the main cause of the negative efficiency in Korte Akkeren. Well 2-1.14 (see [Figure 41](#)) can be a typical example. The deviation between the simulation and observation of the groundwater level at Well 2-1.14 is around 4 cm, however, the Nash-Sutcliffe efficiency of the simulation is negative (-1.39) because the groundwater level is very stable along the time series even though the deviation of the simulation and reality is very small. In addition, since the observed groundwater level at this well is approximately 1 m higher than the observation at the wells nearby and doesn't have a same pattern, the deviation at Well 1-1.13 is ignored during calibration.

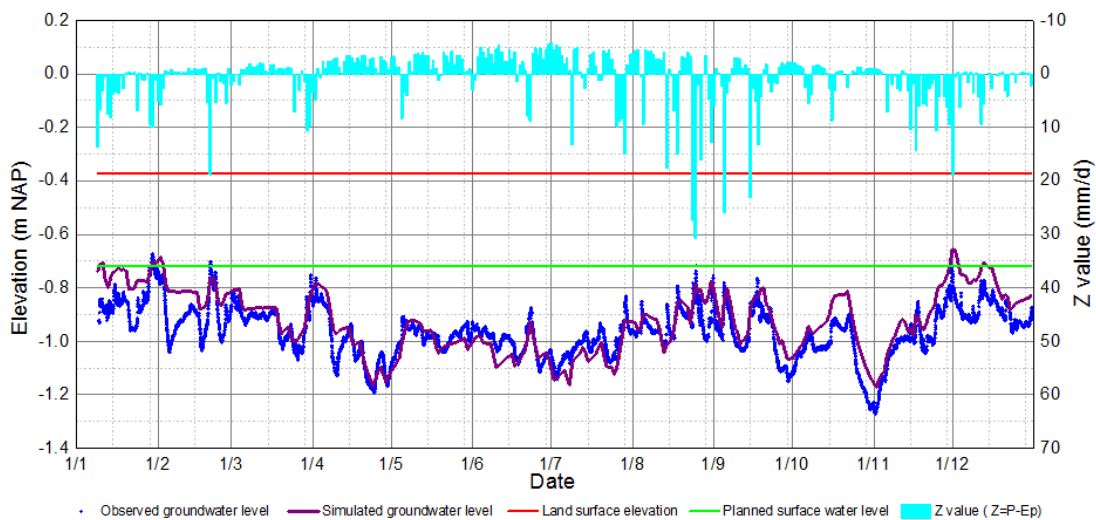


Figure 35 Calibration at Well 1-1.04 (RMSE = 0.05 m, $R^2 = 0.996$, $E = 0.68$)

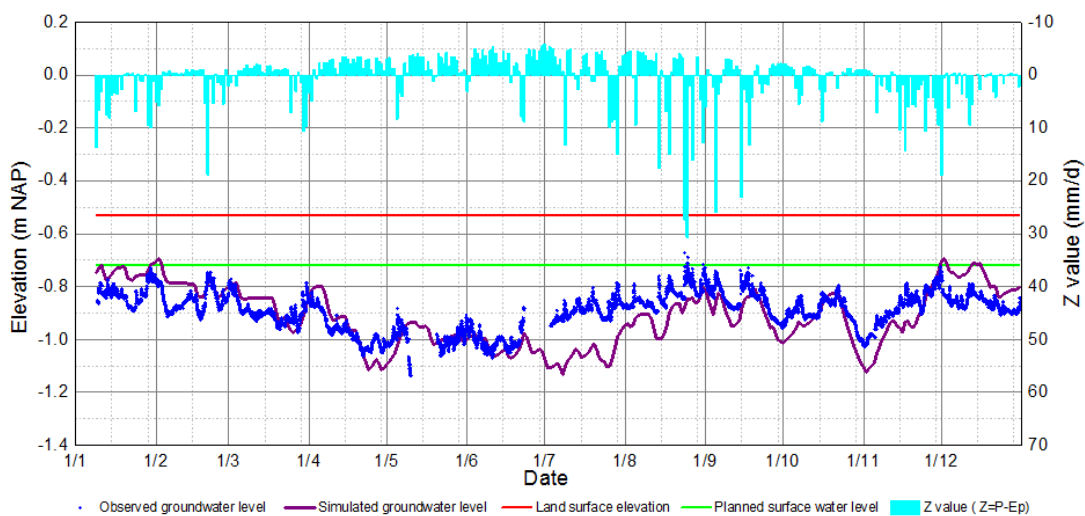


Figure 36 Calibration at Well 1-1.08 (RMSE = 0.09 m, $R^2 = 0.991$, $E = -0.66$)

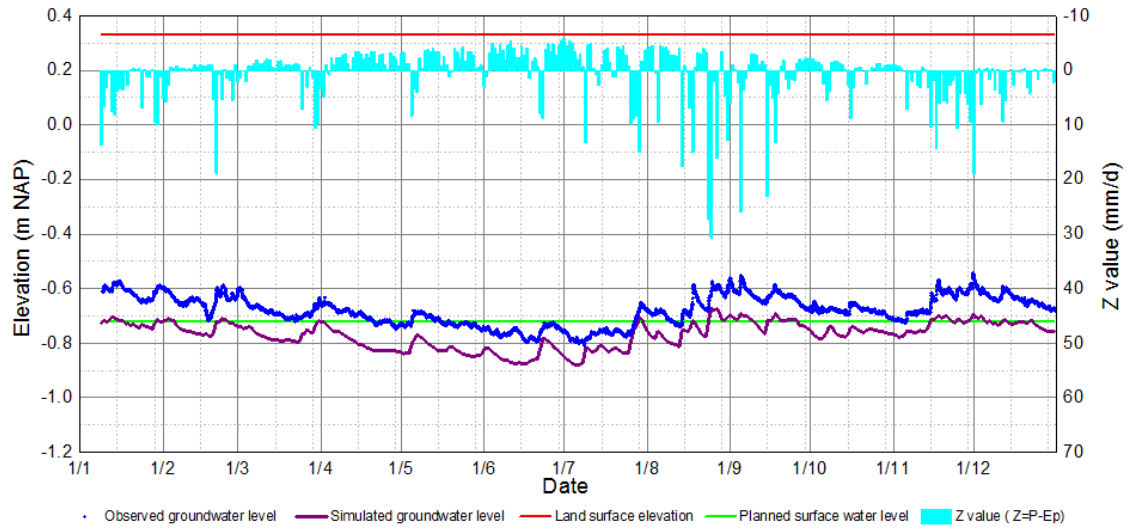


Figure 37 Calibration at Well 1-1.12 (RMSE = 0.08 m, $R^2 = 0.988$, E = -1.38)

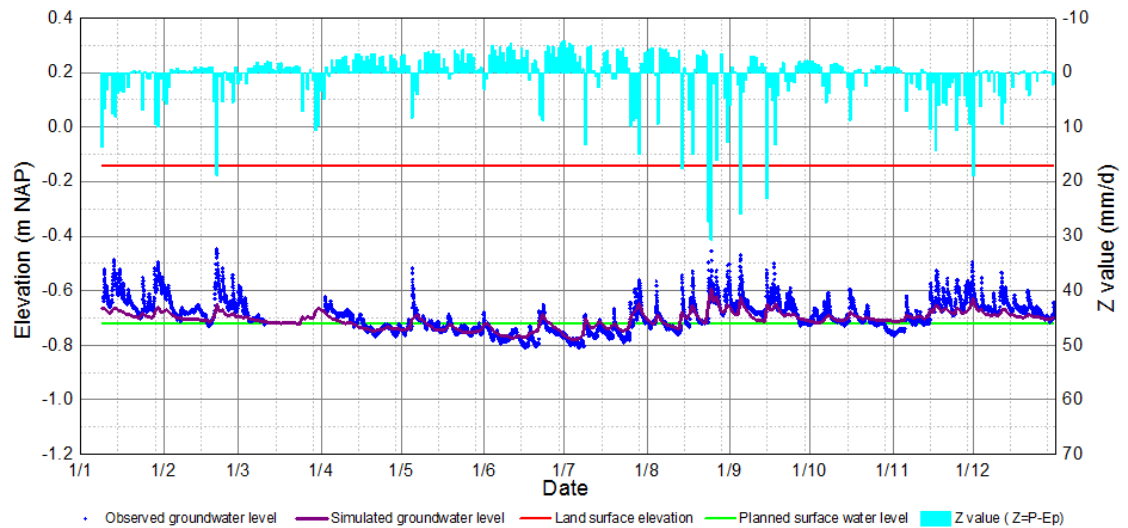


Figure 38 Calibration at Well 1-1.14 (RMSE = 0.04 m, $R^2 = 0.996$, E = 0.37)

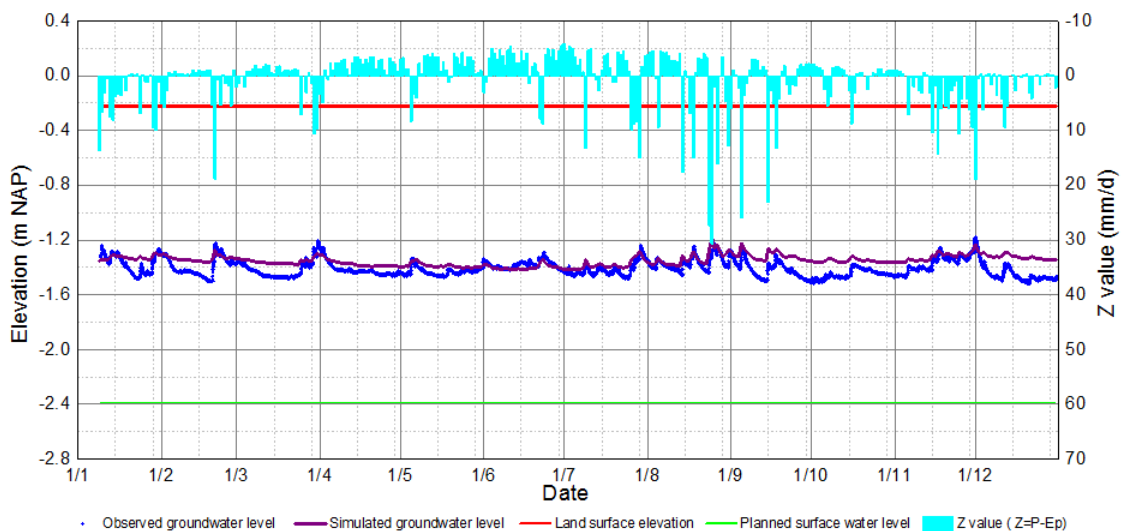


Figure 39 Calibration at Well 2-1.05 (RMSE = 0.06 m, $R^2 = 0.998$, E = -0.21)

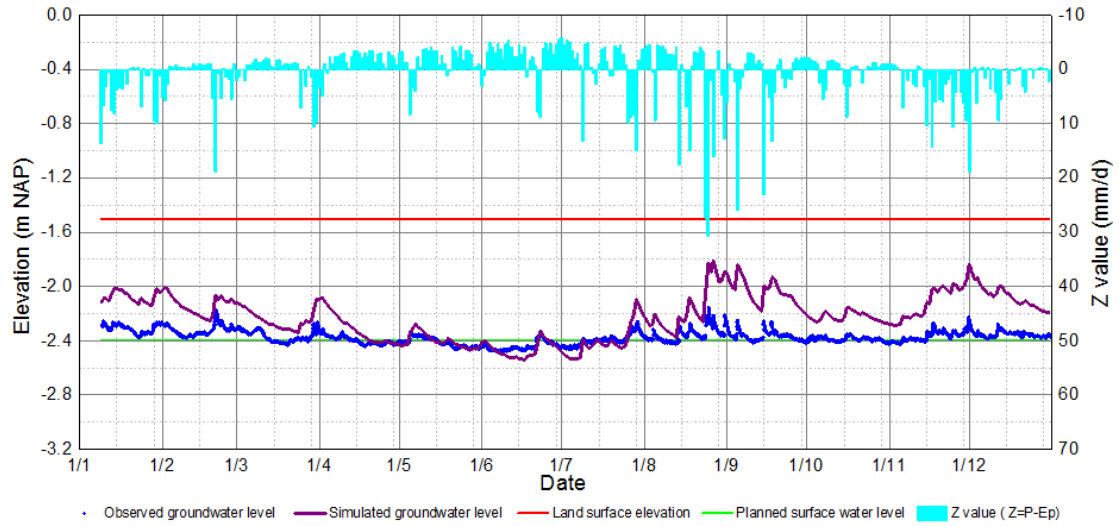


Figure 40 Calibration at Well 2-1.10 (RMSE = 0.20 m, $R^2 = 0.995$, $E = -9.96$)

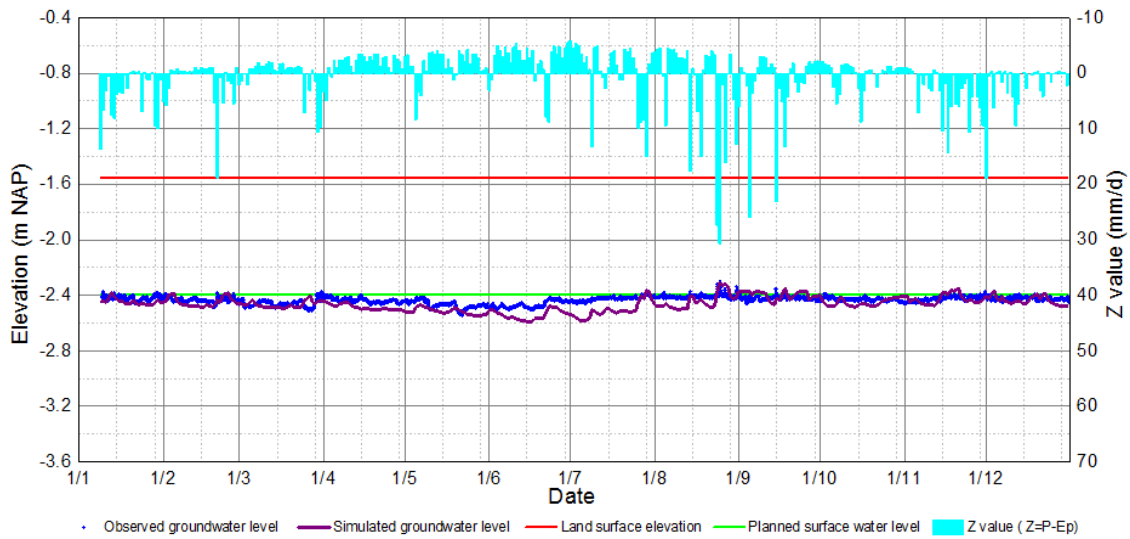


Figure 41 Calibration at Well 2-1.14 (RMSE = 0.04 m, $R^2 = 0.999$, $E = -1.39$)

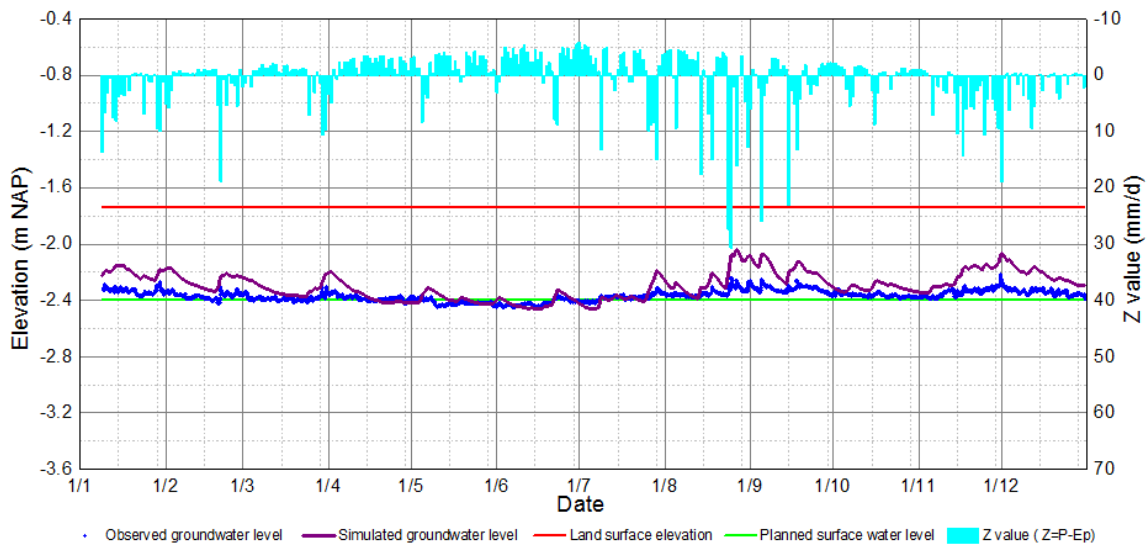


Figure 42 Calibration at Well 2-1.19 (RMSE = 0.10 m, $R^2 = 0.998$, $E = -6.91$)

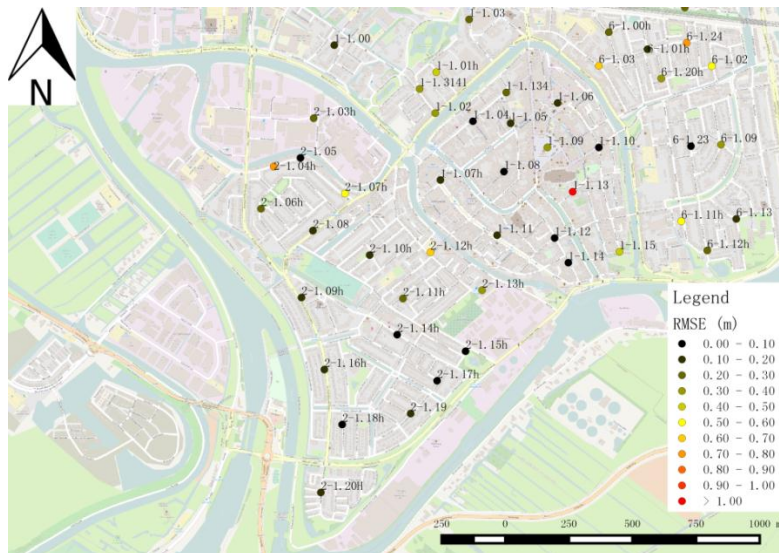


Figure 43 Root mean square error of the groundwater level simulation at observation wells at calibration state (2015-2016)

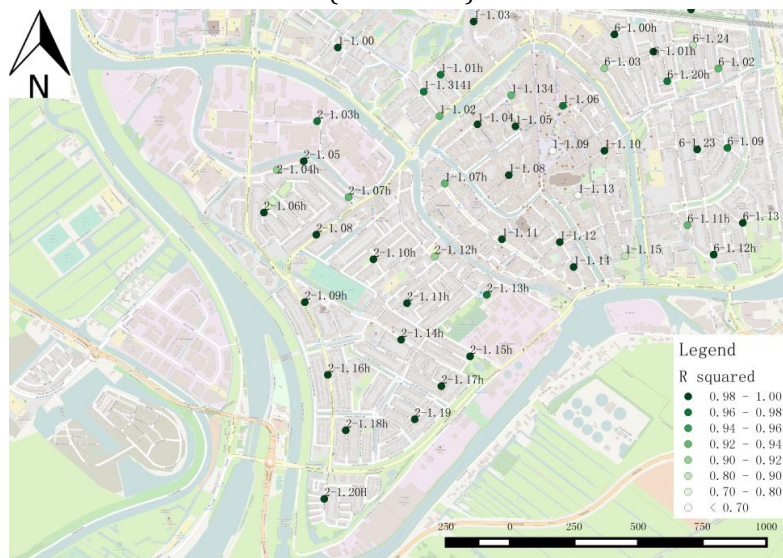


Figure 44 R² of the groundwater level simulation at observation wells at calibration state (2015-2016)

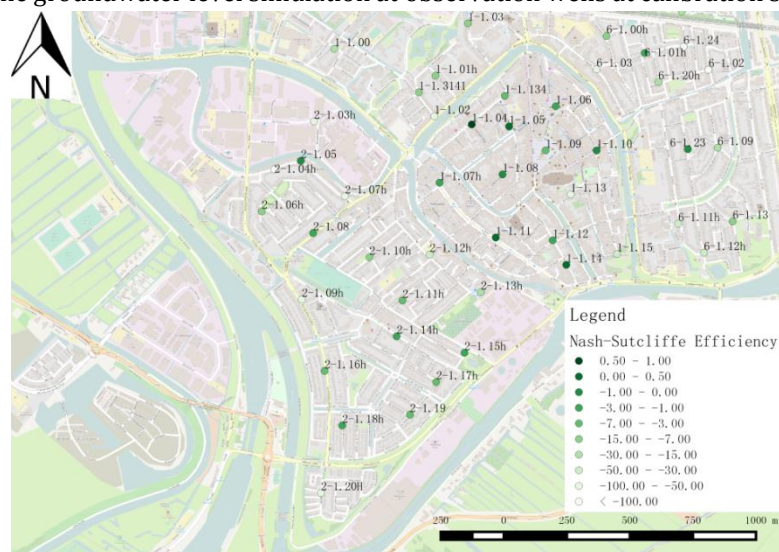


Figure 45 Nash-Sutcliffe efficiency of the groundwater level simulation at observation wells at calibration state (2015-2016)

4.2. Model verification

At the model validation stage, groundwater level observation data at more locations are available. The RMSE, R^2 and Nash-Sutcliff efficiency between the simulation and measurements at the observation wells are shown in **Figure 46 - 48**. Similar to the calibration results, generally speaking, the RMSE values at the observation wells in the study area are mostly within 0 ~ 0.2 m. The coefficients of determination (R^2) at the wells in the study area are mostly above 0.90. The larger RMSE and smaller R^2 values are mostly located at the boundary of the lower polders near a canal with the high surface water level, while low correlation between simulation and observation also can be found at Well 1-1.09 and 1-1.13. The Nash-Sutcliffe efficiencies at the observation wells show that the model can simulate the ground level in the inner city better than in Korte Akkeren. Though the efficiencies at several locations are negative, a negative value cannot indicate a bad simulation on groundwater level (discussed in **Section 4.1.2**). Then the time series of the groundwater level is compared at the observation wells. As shown in **Figure 49 - 59**, the estimation of groundwater level at Well 1-1.04, 1-1.14 is still accurate. Similar to the estimation quality at calibration stage, the groundwater level at Well 1-1.08 is underestimated in the summertime, while the simulated groundwater level at Well 1-1.12 is almost parallel to the observed time series with approximately 10 cm deviation. As for the fitness at the new observation wells in the inner city, the model is able to estimate the groundwater level at Well PB08 accurately, while underestimation of the groundwater level in the dry period also occurs at Well PB04 and PB05. However, the difference of the model performance between these two locations is that the level simulation at Well PB04 in the dry winter becomes well fitted again. Thus, the error of the model simulation at Well PB04 can be caused by the overestimation on evapotranspiration near the observation in summer, which can also be an explanation of the deviation between the simulation and reality at Well 1-1.08. The underestimation on pipe wall conductance nearby may be the reason of the deviation between the model simulation and observation at Well 1-1.05. The groundwater model is also able to give a good groundwater level simulation for the polder Korte Akkeren. The deviation between the simulated value and the observed value is acceptable, while the simulated groundwater level in the wet period at Well 2-1.10 is still overestimated. In general, the model is able to simulate the time series patterns while deviations between the simulation and observation is acceptable in the study area.

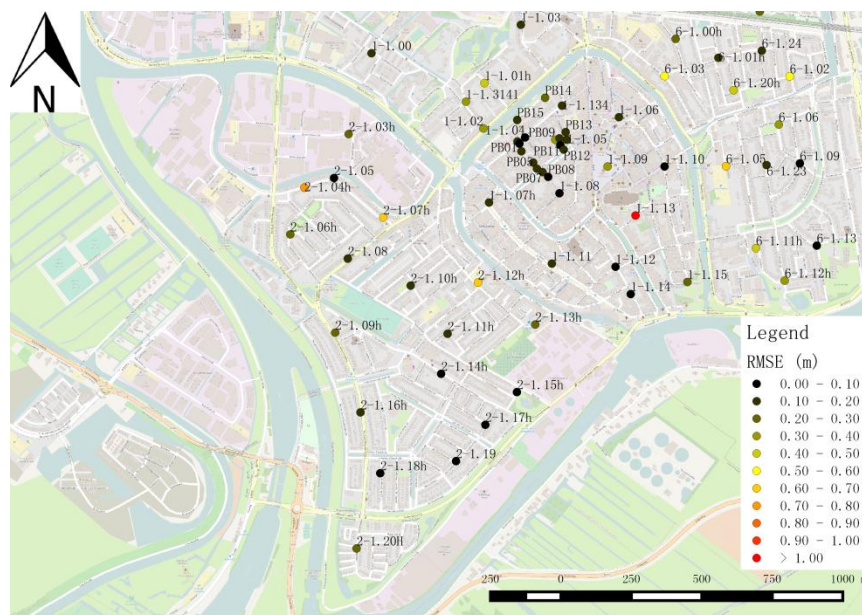


Figure 46 RMSE of the groundwater level simulation at observation wells at validation state (2016-2017)

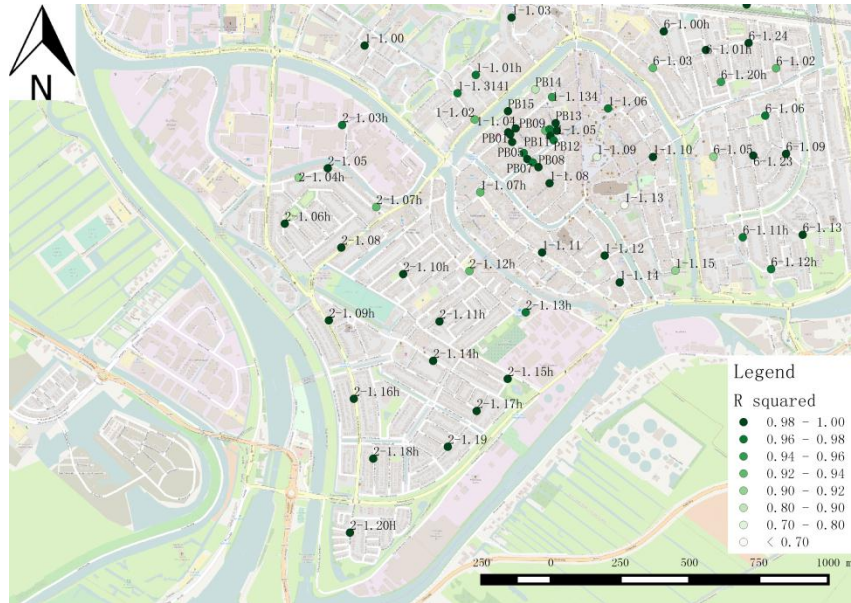


Figure 47 R² of the groundwater level simulation at observation wells at validation state (2016-2017)

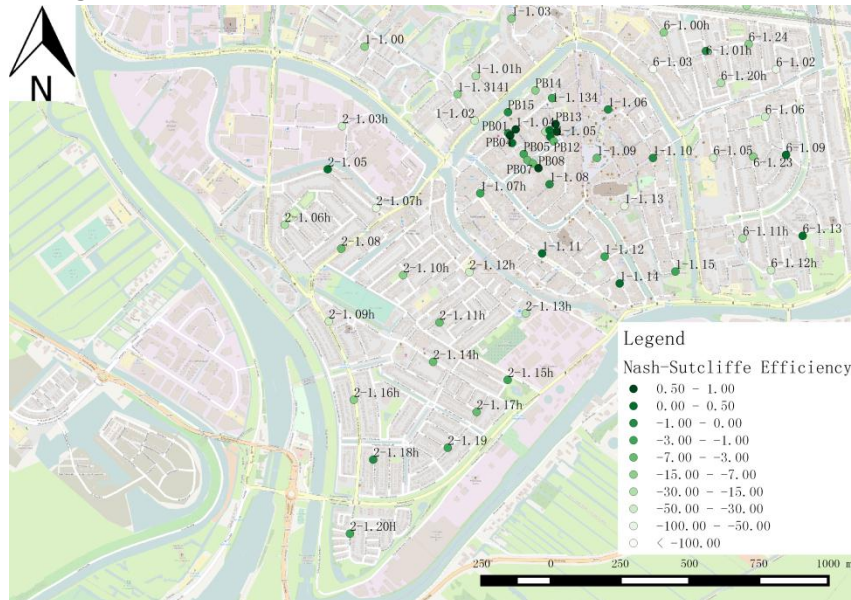


Figure 48 Nash-Sutcliffe efficiency of the groundwater level simulation at observation wells at validation state (2016-2017)

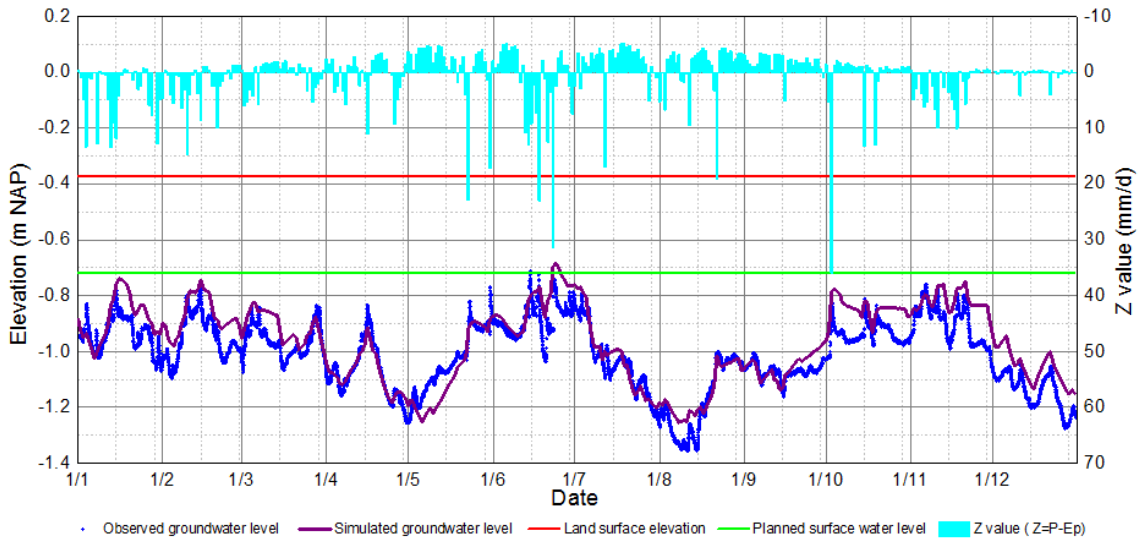


Figure 49 Validation at Well 1-1.04 (RMSE = 0.06 m, $R^2 = 0.996$, $E = 0.74$)

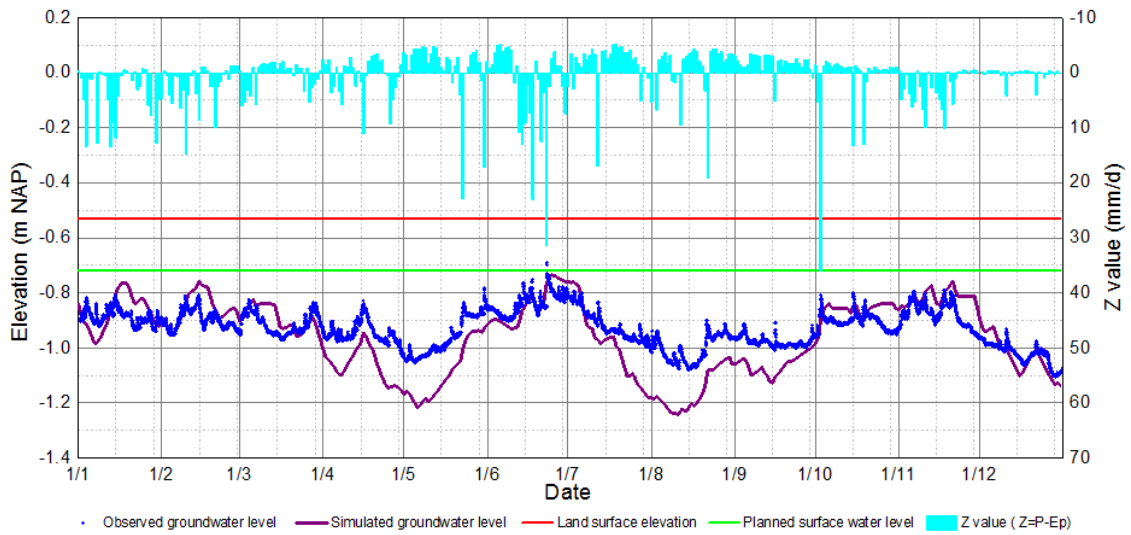


Figure 50 Validation at Well 1-1.08 (RMSE = 0.09 m, $R^2 = 0.992$, $E = -0.75$)

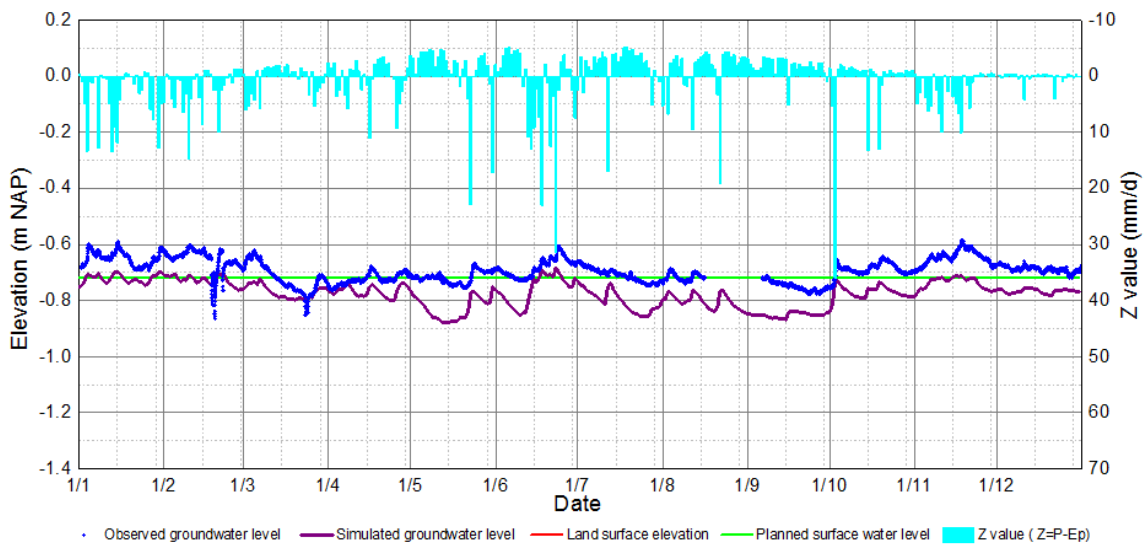


Figure 51 Validation at Well 1-1.12 (RMSE = 0.07 m, $R^2 = 0.993$, $E = -1.49$)

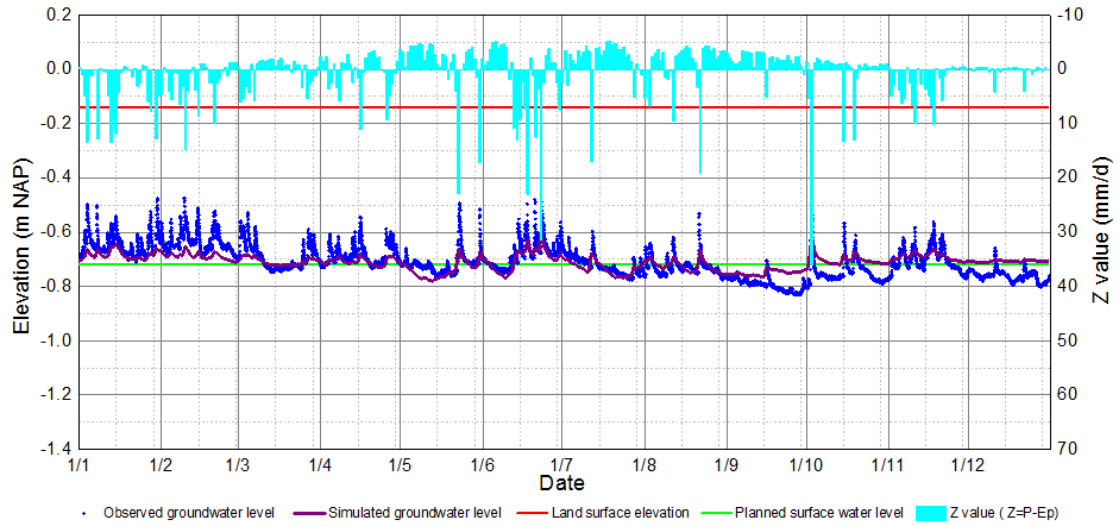


Figure 52 Validation at Well 1-1.14 (RMSE = 0.05 m, $R^2 = 0.995$, $E = 0.28$)

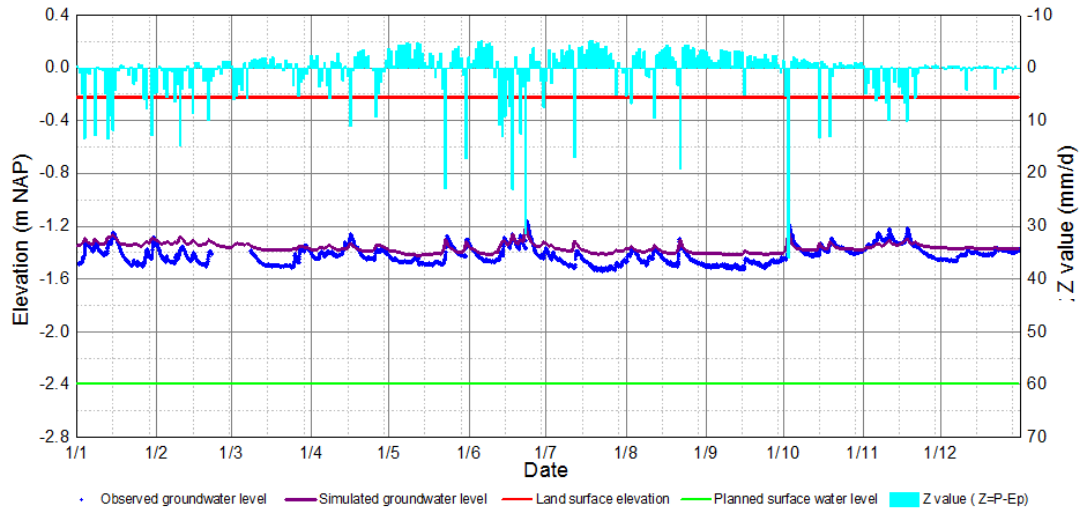


Figure 53 Validation at Well 2-1.05 (RMSE = 0.06m, $R^2 = 0.998$, $E = 0.09$)

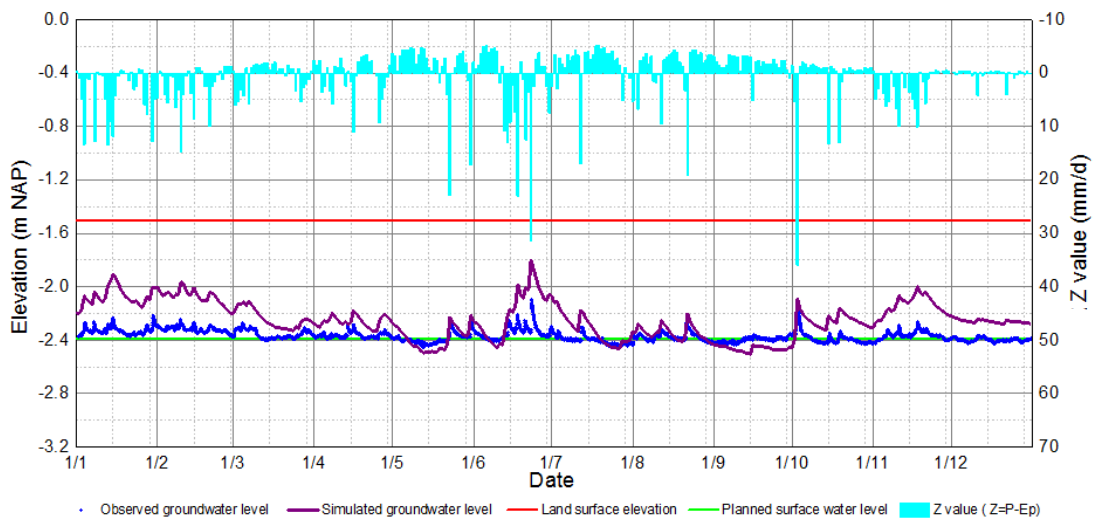


Figure 54 Validation at Well 2-1.10 (RMSE = 0.16 m, $R^2 = 0.995$, $E = -14.71$)

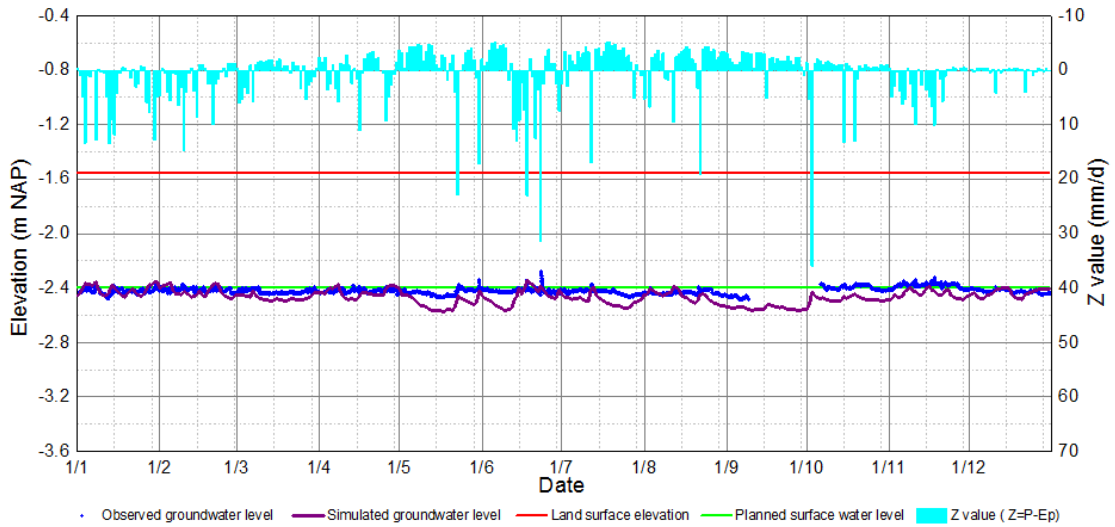


Figure 55 Validation at Well 2-1.14 (RMSE = 0.05 m, $R^2 = 0.999$, $E = -3.60$)

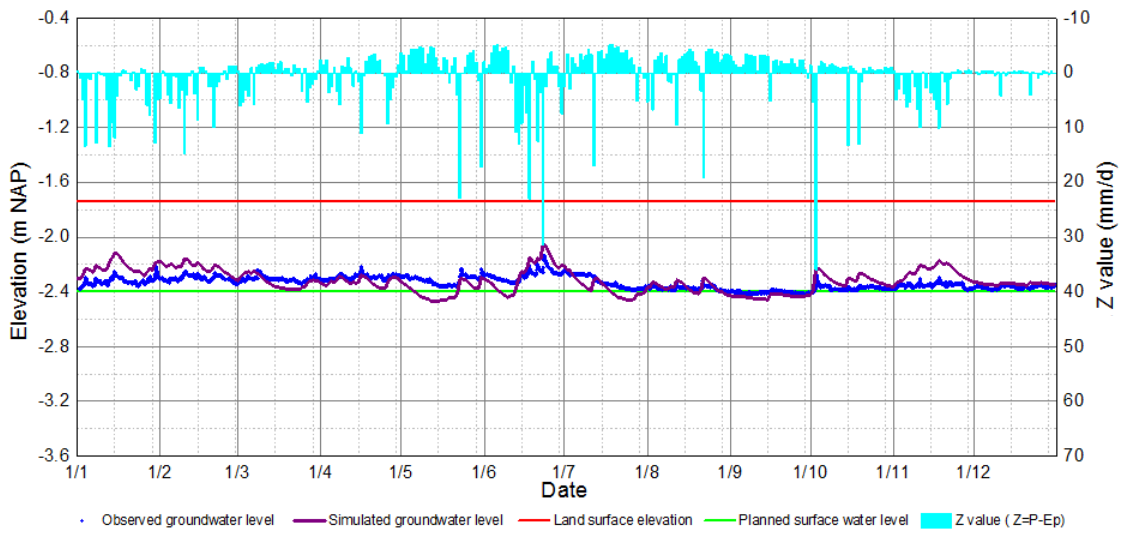


Figure 56 Validation at Well 2-1.19 (RMSE = 0.08 m, $R^2 = 0.999$, $E = -2.30$)

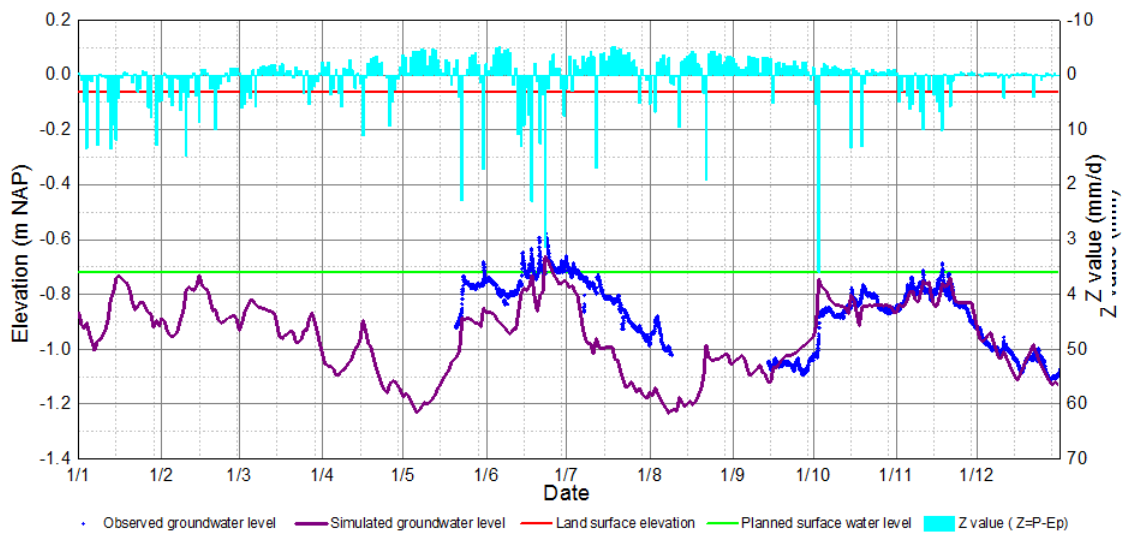


Figure 57 Validation at PB04 (RMSE = 0.11 m, $R^2 = 0.987$, $E = 0.21$)

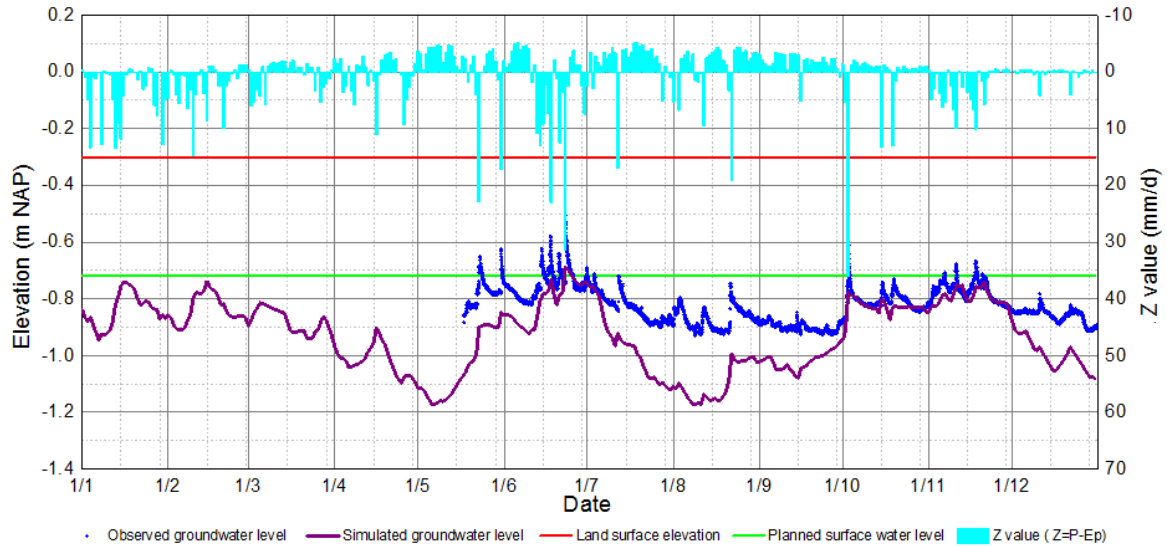


Figure 58 Validation at PB05 (RMSE = 0.12 m, $R^2 = 0.983$, E = -2.81)

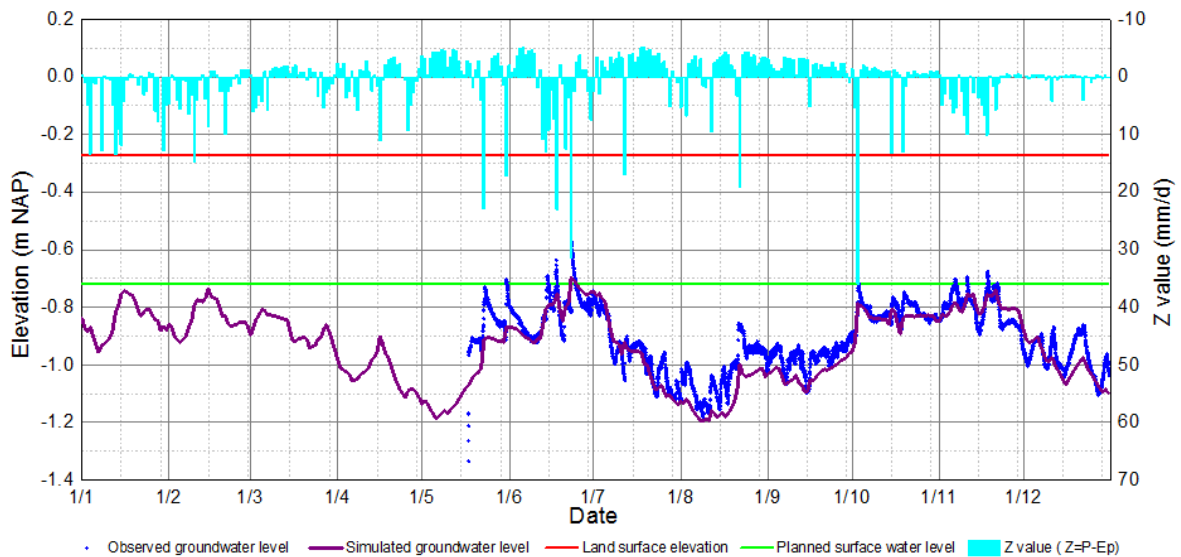


Figure 59 Validation at PB08 (RMSE = 0.05 m, $R^2 = 0.997$, E = 0.747)

4.3. Sensitivity Analysis

After model calibration and validation, the uncertainty of the model is measured by means of sensitivity analysis. The results of sensitivity analysis are presented in two dimensions, spatially and temporally. Two approaches are applied to present the spatial effects during the sensitivity test. Firstly, the mean value and the standard deviation of the level change after changing the input parameters are calculated at each groundwater monitoring wells (See [Appendix 1](#)). Calculating both the two values shows not only the average level change but also their extents of deviation. However, this only shows a discrete result. To get an idea on how the sensitivity acts continuously in the whole study area, the comparisons of the mean levels after changing the input parameters are also calculated. In the meanwhile, a groundwater observation well, PB 08 is chosen to show the temporal distribution of the deviations when the value of the input parameters is changed. There are two reasons for the choosing PB 08 as the representative. On the one hand, as shown in the

validation results, the groundwater estimation of this well is relatively good, which indicates a good estimation on the influence of the stresses; on the other hand, according to Wang (2016), PB 08 has been identified be sensitive to the precipitation, evapotranspiration, leakage of the sewerage pipes, while it also locates near a canal (around 30 m away), so that it is able to react to all the stress changes.

4.3.1. Conductance of canal bed

The effects on groundwater level in Gouda of adding and removing 50% to/from the calibrated canal conductance. The results are shown in **Figure 60 - 62**. It is indicated in the figures that the groundwater level in the north and west inner city is the most sensitive area to the change of canal conductance in the study area. When the canal conductance is reduced by 50%, the groundwater level in that area is reduced by approximately $10\text{ cm} \pm 4\text{ cm}$ on average, while the level change is increased by $4\text{ cm} \pm 2\text{ cm}$ on average when the conductance is increased by 50%. The groundwater level change after removing 50% from the calibrated canal conductance is more significant than that after adding 50% to the calibrated conductance. It is also can be observed from the graph that in the area where it is near the river or the boezem canal in Korte Akkeren and the south area of inner city next to the river, the groundwater level is increased slightly when the conductance of the canals is reduced and it also decreased a bit when the conductance is increased. According to the time series comparison at Well PB08, after changing the calibrated value of canal conductance, the deviation between the results are larger when the groundwater level is relatively lower, while the groundwater level change on high groundwater level occasion is very limited.

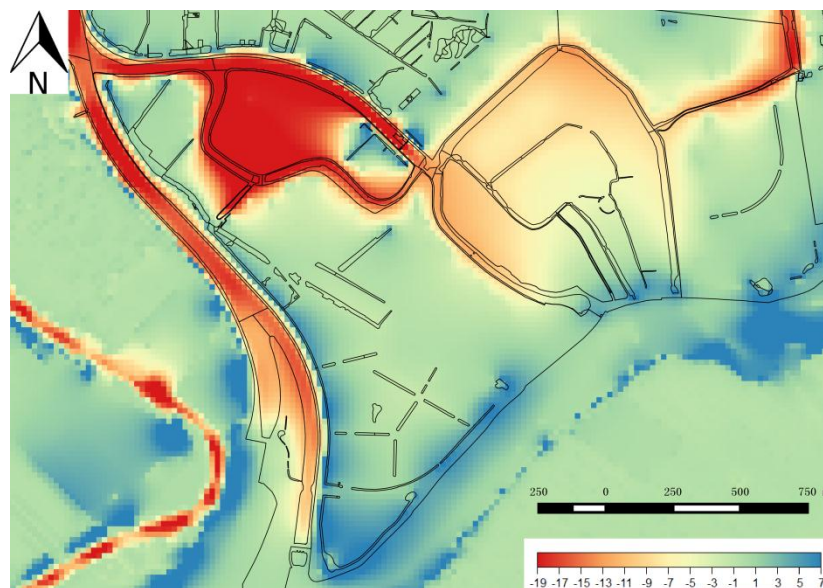


Figure 60 Change of mean groundwater level after removing 50% of amount from canal conductance (Unit: cm)

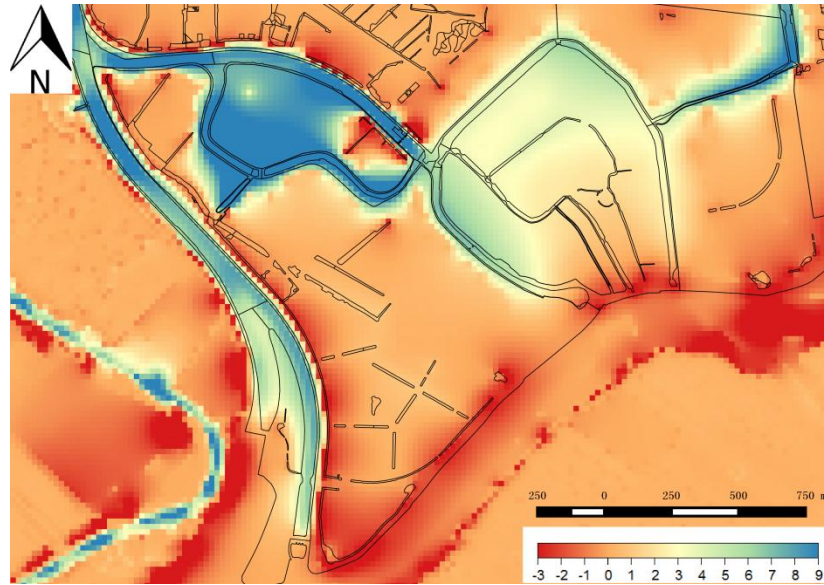


Figure 61 Change of mean groundwater level after adding 50% of amount to canal conductance (Unit: cm)

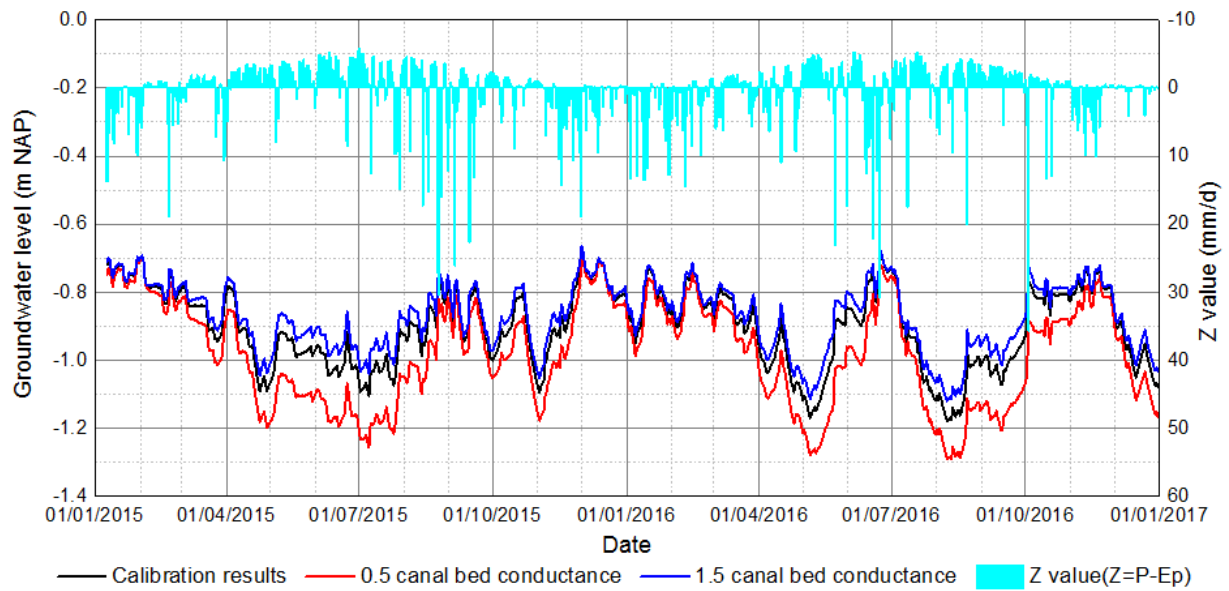


Figure 62 Time series of sensitivity test at Well PB08 (canal conductance)

4.3.2. Conductance of Sewerage pipe walls

The results of the sensitivity test of the conductance of sewerage pipes are shown in *Figure 63 - 65*. It is indicated by the figures that the groundwater level in the areas around the Turfmarkt in the inner city is very sensitive to the changes of the conductance of the sewerage pipe walls. When the conductance is reduced by 50%, there is on average about $9\text{ cm} \pm 5\text{ cm}$ increase on groundwater level in that area. When the conductance is increased by the same amount, the groundwater level in that area is raised by approximately $6\text{ cm} \pm 3\text{ cm}$. In the meanwhile, the groundwater level in the Korte Akkeren where the leaking pipes (both back stowed pipes and infiltration-transportation pipes) are located has a moderate change also when the conductance of the sewerage pipes are changed. As for the comparison of after changing the calibrated value of canal conductance, the deviation between the results is larger when the groundwater level is relatively lower, while the groundwater level change on high groundwater level occasion is very limited. As for the comparison of the time series, the deviation between the results is very obvious in dry periods, while it is smaller in the wet period.

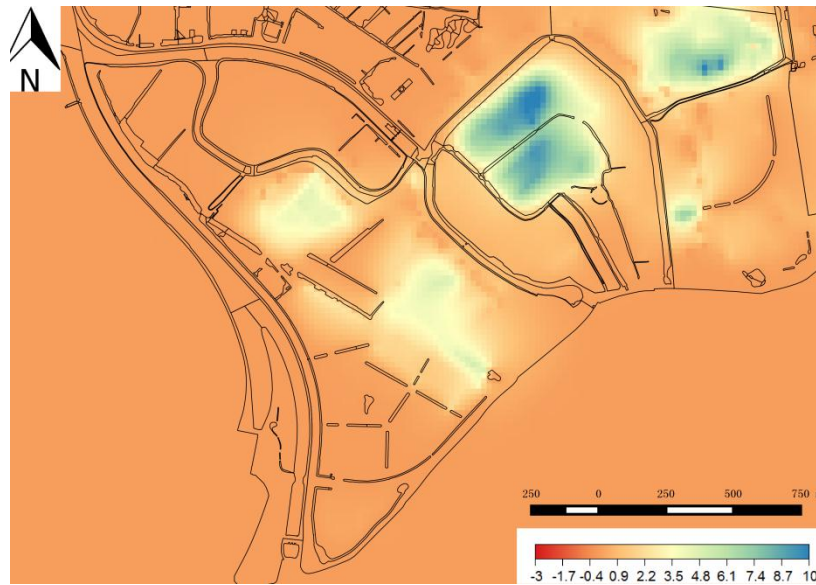


Figure 63 Change of mean groundwater level after removing 50% of amount from sewerage pipe conductance (Unit: cm)



Figure 64 Change of mean groundwater level after adding 50% of amount to sewerage pipe conductance (Unit: cm)

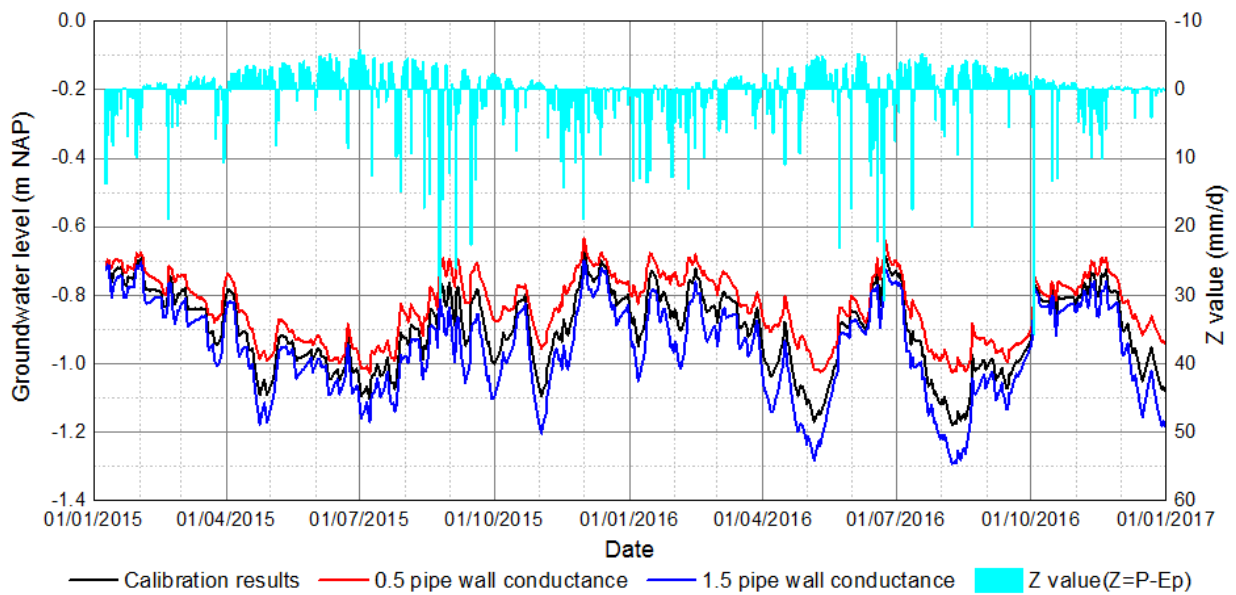


Figure 65 Time series of sensitivity test at Well PB08 (pipe wall conductance)

4.3.3. Hydrological conductivity of the upper phreatic aquifer layer

The groundwater level change on after adding and reducing 50 % of the hydrological conductivity of the upper phreatic aquifer is shown in [Figure 67 - 69](#). When the hydrological conductivity is reduced, the deviations of the groundwater level between the areas next to some boezem canals (whose bed locates in the upper phreatic aquifer) are enlarged. It indicates that when the hydrological conductivity of upper phreatic layer is altered, the effectiveness of the boezem canals has a more noticeable change. However, generally speaking, the groundwater level in most of the study area is decreased by 0~5 cm on average when the hydrological conductivity of the upper phreatic aquifer layer is reduced, while the level change is very limited when the hydrological conductivity is increased. There is no apparent temporal groundwater change deviation observed but the deviation is slightly larger in the dry period than that in the wet period when the hydrological conductivity of the upper phreatic aquifer layer is changed.

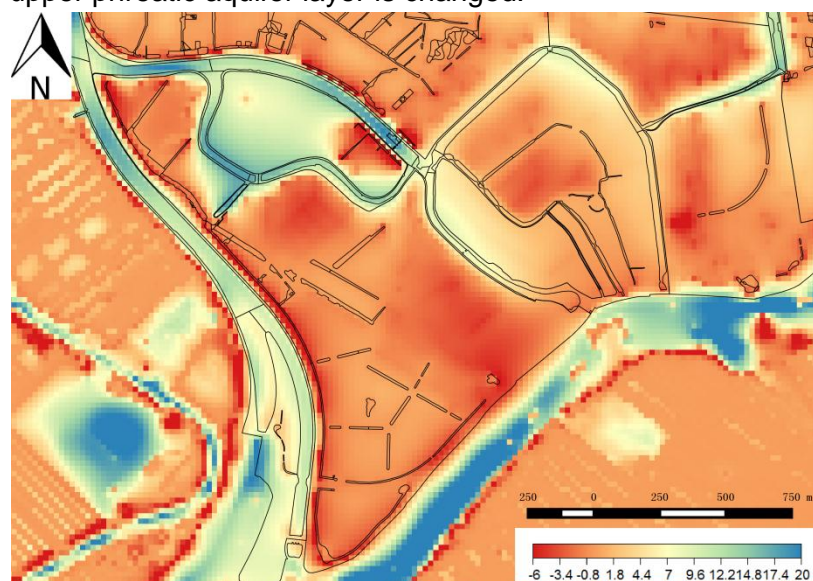


Figure 66 Change of mean groundwater level after removing 50% of amount from hydraulic conductivity of the upper phreatic aquifer layer (Unit: cm)

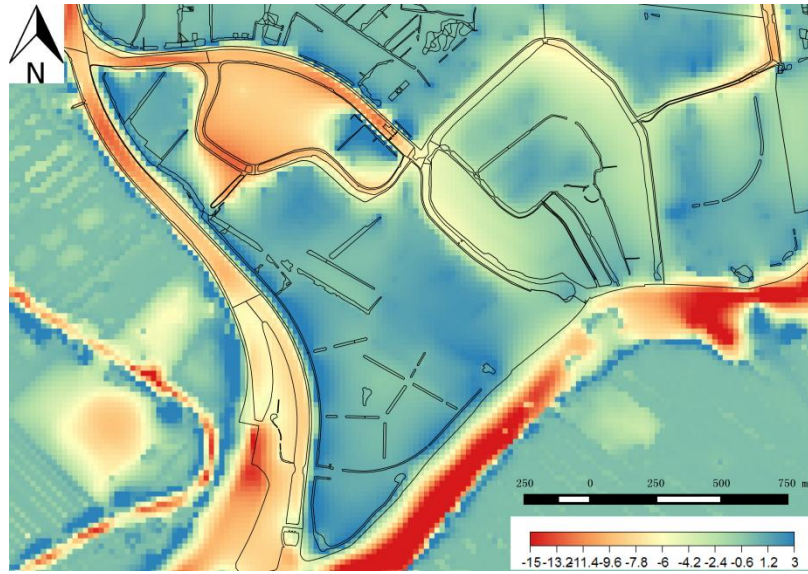


Figure 67 Change of mean groundwater level after adding 50% to hydraulic conductivity of the upper phreatic aquifer layer (Unit: cm)

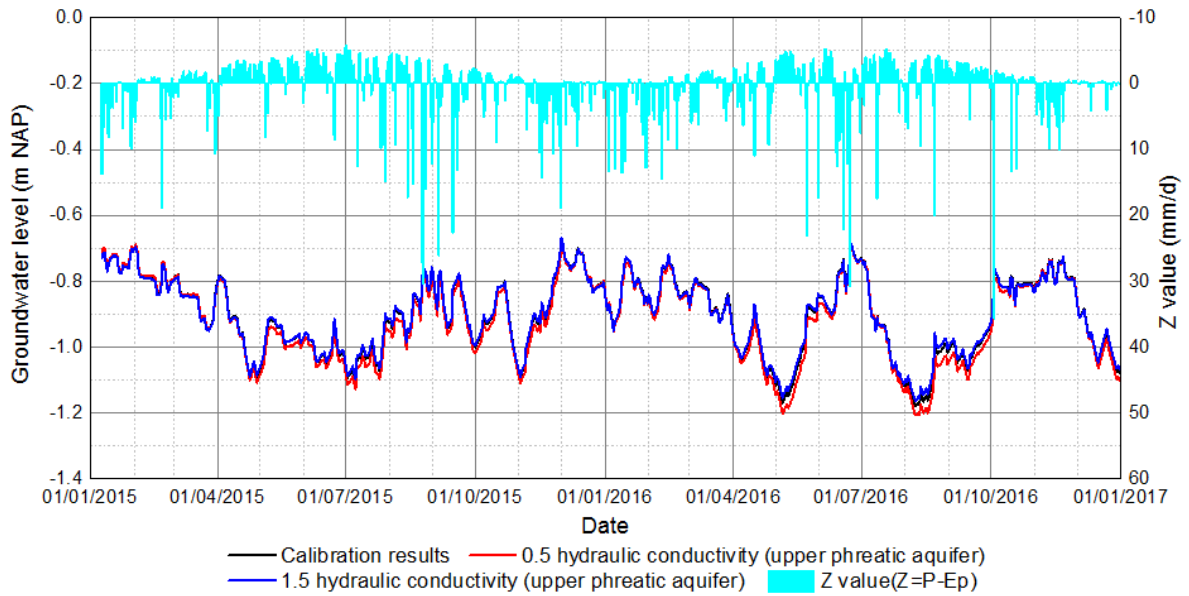


Figure 68 Time series of sensitivity test at Well PB08 (hydraulic conductivity at the upper phreatic aquifer)

4.3.4. Hydrological conductance of the lower phreatic aquifer layer

The effects on groundwater level in Gouda of adding and removing 50% to/from the calibrated hydrological conductance of the lower phreatic aquifer. **Figure 69 - 71** shows the results for the test. As shown in these figures, there is a relatively visible level change (2~4 cm decrease when the hydrological conductance is decreased by 50%, and 1~2 cm increase when the hydrological conductance is increased by the same amount) near the Turfmarkt, especially the Nieuwe Haven area. In the meanwhile, the groundwater level in the areas that near the boezem canal between the inner city and Korte Akkeren as well as the tidal river is more sensitive to the change of the hydrological conductance than other areas in general. The phreatic groundwater level in this area raised and dropped approximately 2 cm on average when the hydrological conductance is decreased and increased, respectively. Apart from the canals and the river, the level change near the leaky pipes, especially in the inner city is also relatively apparent. No obvious temporal groundwater change deviation is observed at Well PB08 but the deviation is slightly larger in the dry period than that in the wet period when the hydrological conductivity of the lower phreatic aquifer layer is changed.

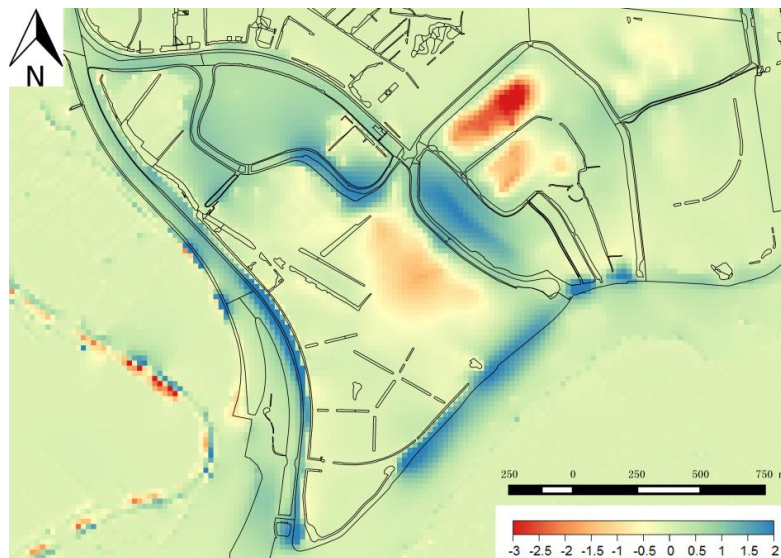


Figure 69 Change of mean groundwater level after removing 50% of amount from hydraulic conductivity of the lower phreatic aquifer layer (Unit: cm)

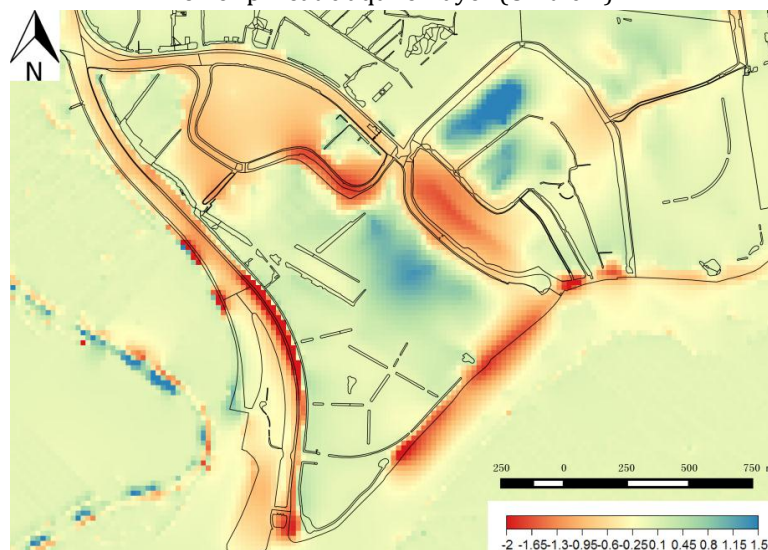


Figure 70 Change of mean groundwater level after adding 50% to hydraulic conductivity of the lower phreatic aquifer layer (Unit: cm)

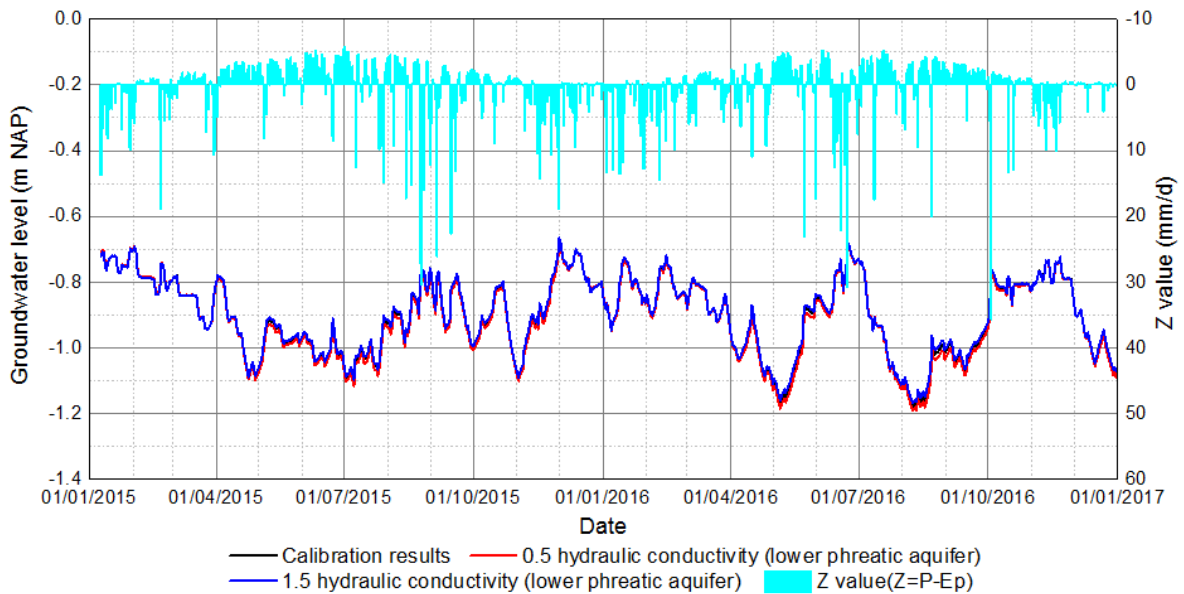


Figure 71 Time series of sensitivity test at Well PB08 (hydraulic conductivity of the lower phreatic aquifer)

4.3.5. Storage coefficient

The results of the sensitivity test of the storage coefficient in the upper phreatic layer are shown in **Figure 72 - 74**. It can be indicated from these figures that when increasing or reducing the storage coefficient in the upper phreatic layer by 50%, the groundwater level change in the study area is very limited, almost within 1cm, except the areas where the leaking pipes locate in Korte Akkeren. When the storage coefficient is reduced by 50%, there is approximately $1\text{ cm} \pm 4\text{ cm}$ decrease on groundwater level in the area where the infiltration-transportation pipes are installed, while the groundwater level is increased by $0.5\text{ cm} \pm 2.5\text{ cm}$ when the storage coefficient is increased by 50%. After changing the storage coefficient, the only noticeable change in the time series comparison is the changing fluctuation extent, while the average groundwater levels seldom have any deviation.

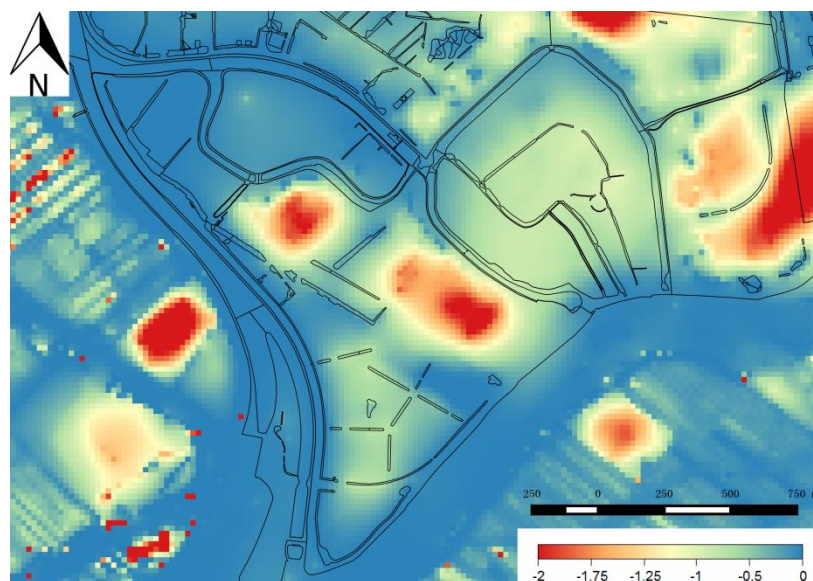


Figure 72 Change of mean groundwater level after removing 50% from storage coefficient (Unit: cm)

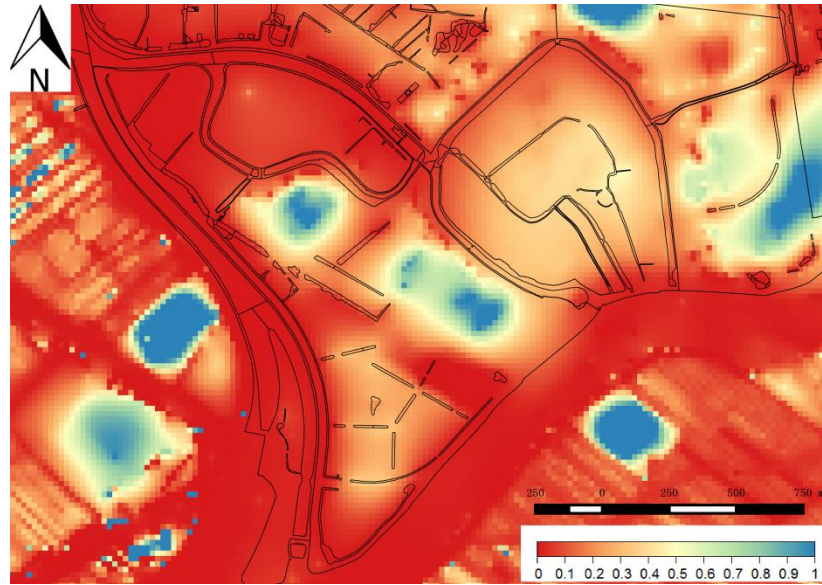


Figure 73 Change of mean groundwater level after adding 50% of amount to storage coefficient (Unit: cm)

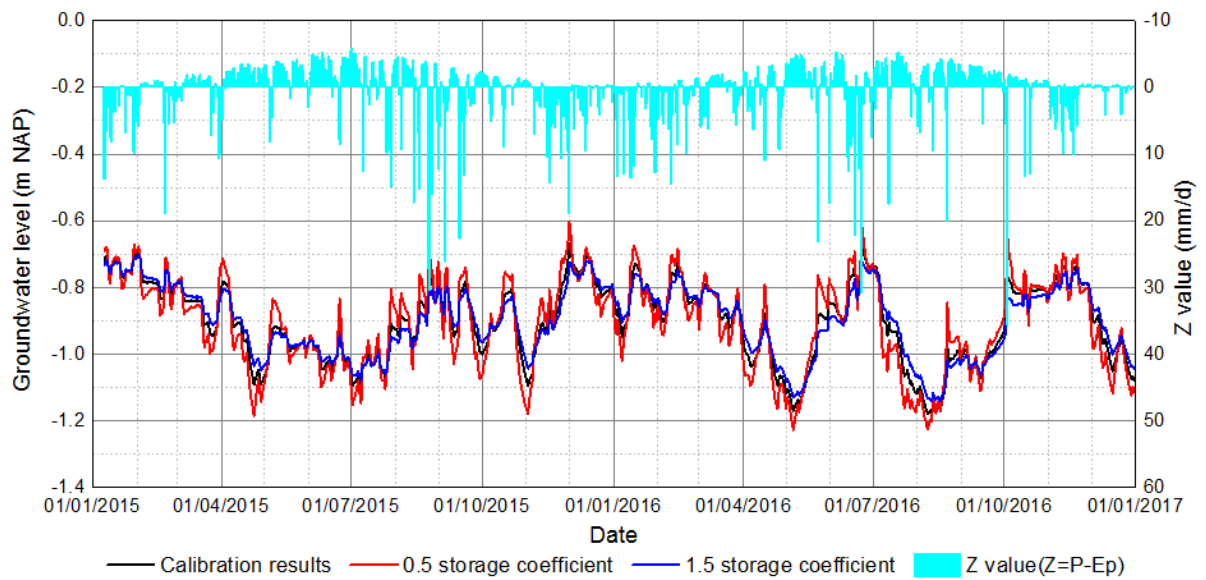


Figure 74 Time series of sensitivity test at Well PB08 (storage coefficient)

4.3.6. Vertical resistance

The results of the sensitivity test of the vertical resistance of the aquitard are shown in **Figure 75 - 77**. It can be indicated from the figures that the groundwater level change in the inner city is larger than that in the east part of the Korte Akkeren area is most sensitive to the change of vertical resistance. When the vertical resistance is reduced by 50%, the groundwater level in that area is reduced by approximately 8 cm on average, and the groundwater level is increased by around 2 cm. In the meanwhile, the deviation of the difference in that area is also larger than that in the other areas; they are 1 cm when the vertical resistance is set to be half of the calibrated value and 0.3 cm when the parameter is 1.5 time of the calibrated one. Since there is not much groundwater level change at PB08, the deviation of the groundwater level before and after changing the parameter is relatively even over time.

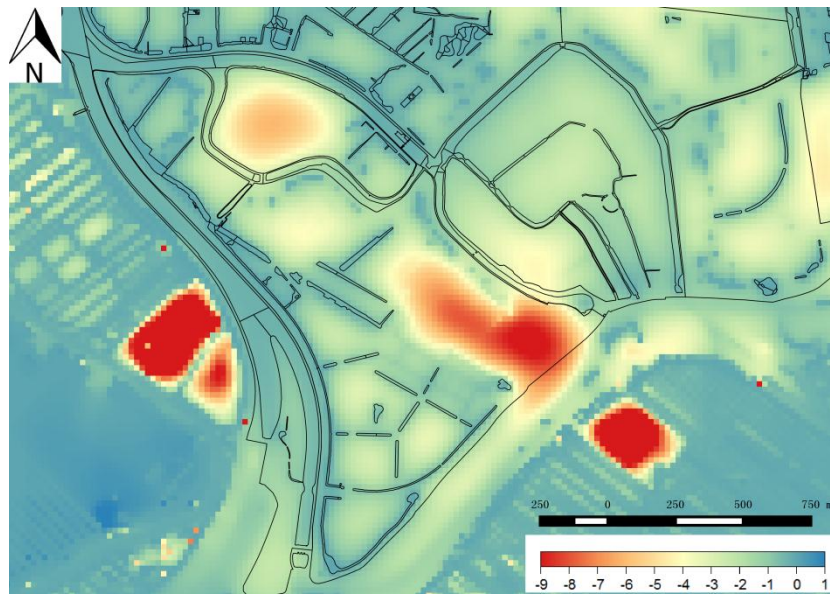


Figure 75 Change of mean groundwater level after removing 50% of value from vertical resistance (Unit: cm)

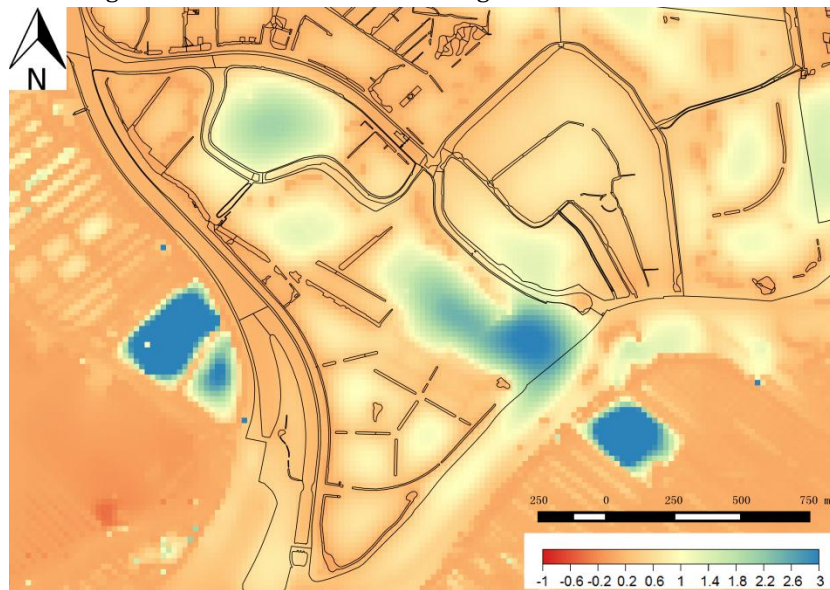


Figure 76 Change of mean groundwater level after adding 50% of value to vertical resistance (Unit: cm)

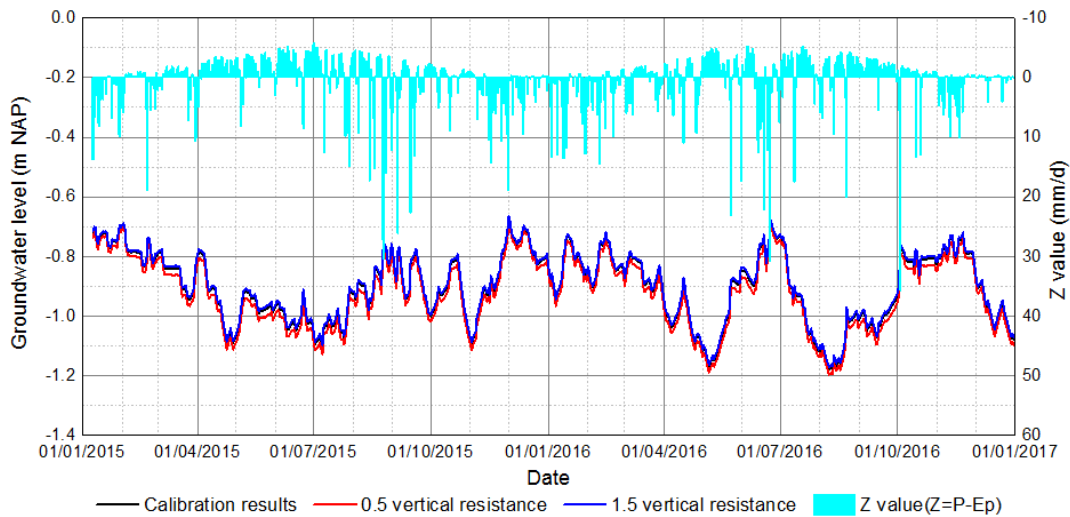


Figure 77 Time series of sensitivity test at Well PB08 (vertical resistance)

4.3.7. Groundwater Recharge

In this research, the groundwater recharge is calculated based on a series of assumptions and parameters, such as the crop coefficient of the grassland, the runoff coefficient of the pavement, the interception threshold of the trees, and the components of the backyards. In this article, the sensitivities of these parameters will not be tested. Instead, the sensitivity test of the groundwater recharge maps is performed. The results are shown in [Figure 78 - 80](#). When reduce the groundwater recharge by 50%, there is a slight groundwater level decrease, within 3 cm, happening in the study area. The groundwater level increase is approximately limited to 2 cm in the study area when the recharge value is increased by 50%. It also can be found from the figures that the closer a location is to the surface water, the less level change would be observed. According to the time series comparison, the groundwater level changes more in the wet period than that in the dry period. It may be because that the potential evaporation is limited to 5 mm/day, while the precipitation could be much larger. Thus, the influence of precipitation on high groundwater level should be more significant than the influence of evapotranspiration on low groundwater level in the sensitivity test.

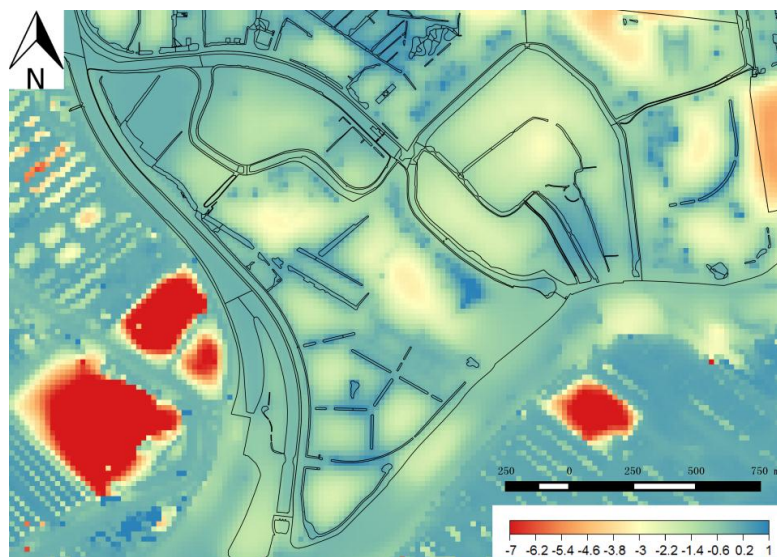


Figure 78 Change of mean groundwater level after removing 50% of calculated value from groundwater recharge (Unit: cm)

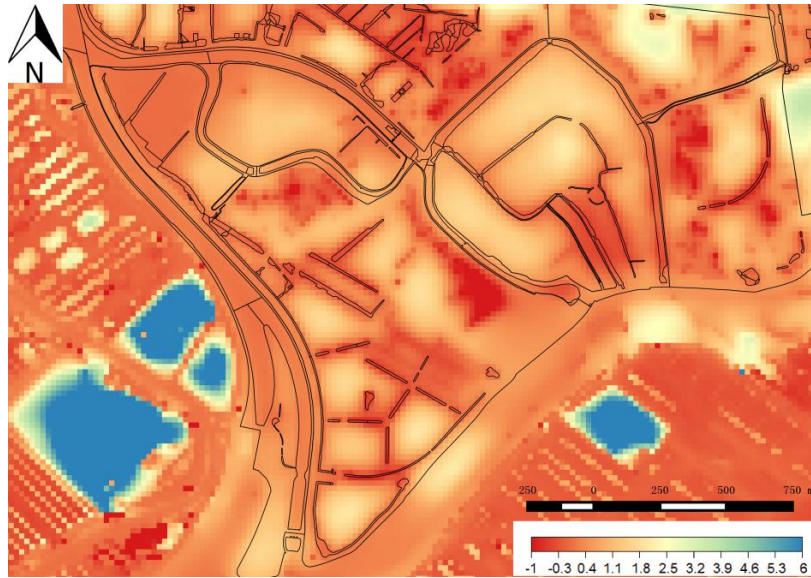


Figure 79 Change of mean groundwater level after adding 50% of calculated value to groundwater recharge (Unit: cm)

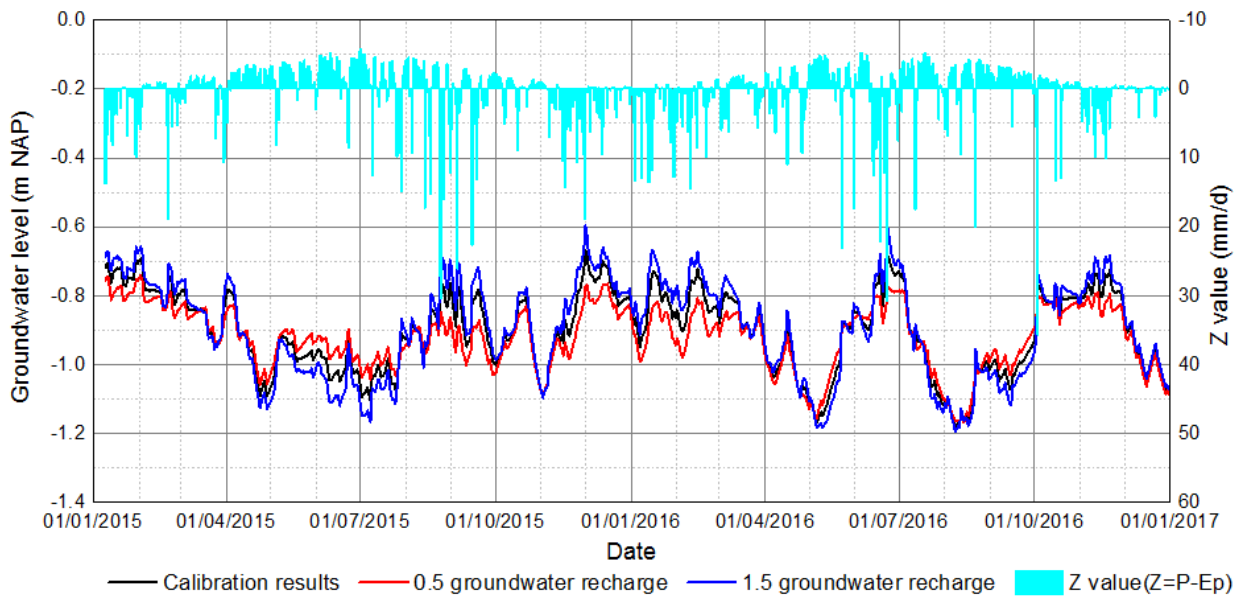


Figure 80 Time series of sensitivity test at Well PB08 (groundwater recharge)

4.4. Scenario Analysis

Now that the simulation quality of the model is considered to be acceptable, four urban water management scenarios are studied to estimate their influence on groundwater level in Gouda. Here, their influence is also presented in two ways, the mean value together with the standard deviation of the level change is compared with the result in null scenario (See [Appendix 2](#)), and the comparison of the mean level between various scenarios and the null scenario is calculated. Similar to the sensitivity test, an observation well is chosen for each scenario to compare the temporal distribution of the groundwater level changes. For Scenario 1, 2, and 5, the observation well PB08 is chosen because the groundwater level at this location is sensitive to all the stresses, while Well 1-1.04 is chosen for Scenario 3 and 4 since it should be relatively sensitive to the new canal that located nearby.

4.4.1. Scenario 1: Water tight sewerage pipes

The influence of the replacing all the back-stowed pipes into new watertight sewerage pipes are shown in [Figure 81](#). As shown in the figure, replacing the pipes would have a significant influence in the groundwater level in the inner city. The groundwater level would rise on average by approximately 20 ± 10 cm in the northern part of the inner city, which could bring higher vulnerability to flooding and inundation. However, replacing the pipes would not have large influence on the level in the Korte Akkeren and southern part of the inner city. The groundwater level will rise thereby approximately from 0 to 7 ± 0 to 3 cm, which is much smaller than that in the inner city. The rising extent of the groundwater level at this scenario is also relative to the leakiness of the old back-stowed system. The reason why the groundwater level in the northern inner city has a largest rise is that both the density and the age of the back-stowed systems are large when compared with those in other areas, while only simulating the emptying and refilling processes in the leaky sewerage pipes in the north part of the inner city can also contribute to the large spatial deviation of groundwater increase. As shown in [Figure 82](#), the groundwater level in the dry period has a considerably rise when compared to that in the wet period.

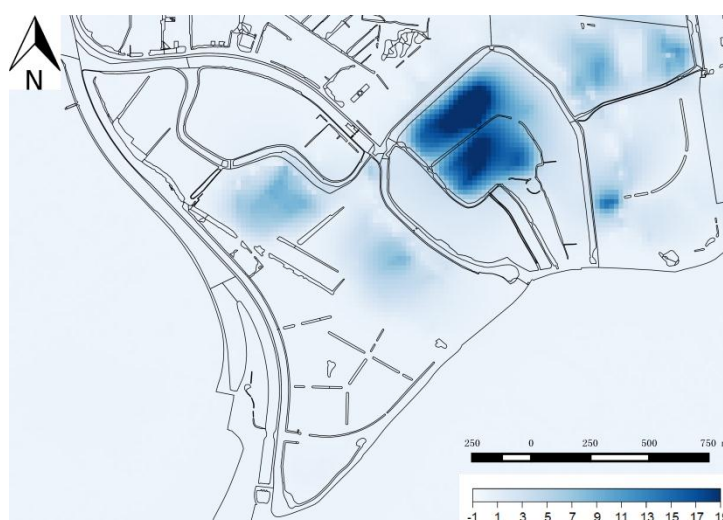


Figure 81 difference of mean groundwater level between Scenario 1 and null scenario (Unit: cm)

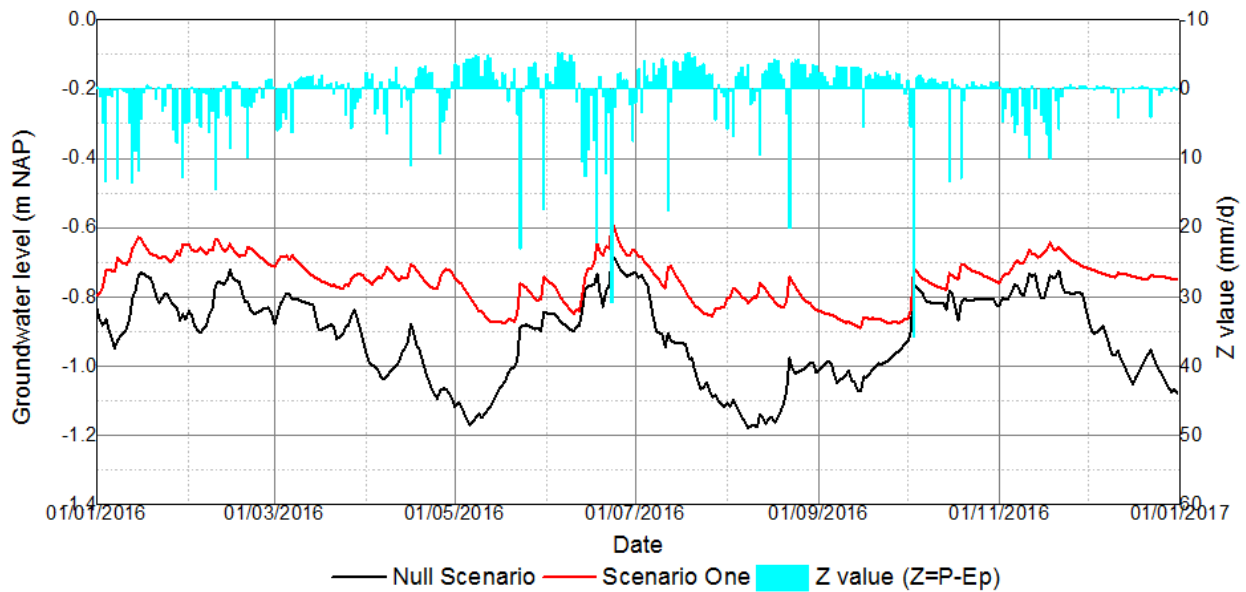


Figure 82 Time series of scenario test at Well PB08 (Scenario 1)

4.4.2. Scenario 2: Lower surface water level in the inner city

In this scenario, the surface water level of the canals in the inner city is reduced by 20 cm. The average spatial change of the groundwater level is shown in [Figure 83](#). As shown in the figure, the surface water decreasing would have a large influence on the inner city. The average groundwater level drop ranges from 13 cm to 19 cm with a deviation within 2.5 cm. Its influence on the groundwater level in the southeastern part of the inner city is the largest. The groundwater level decreases more when it is closer to the canals. This change of the groundwater level may accelerate land subsidence and increase the risk of the damage to the wooden piles of some historical buildings in the inner city. According to the time series at PB08 ([Figure 84](#)), the level drop is almost even along the year.

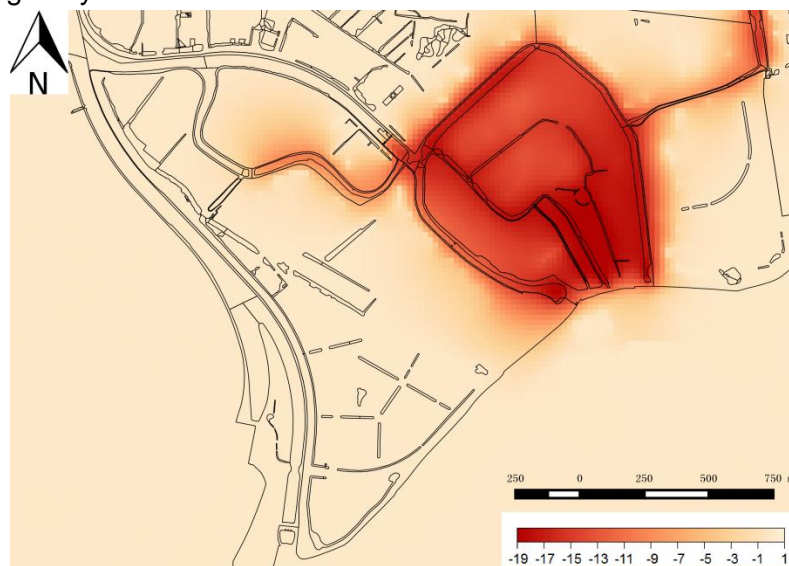


Figure 83 Difference of mean groundwater level between Scenario 2 and null scenario (Unit: cm)

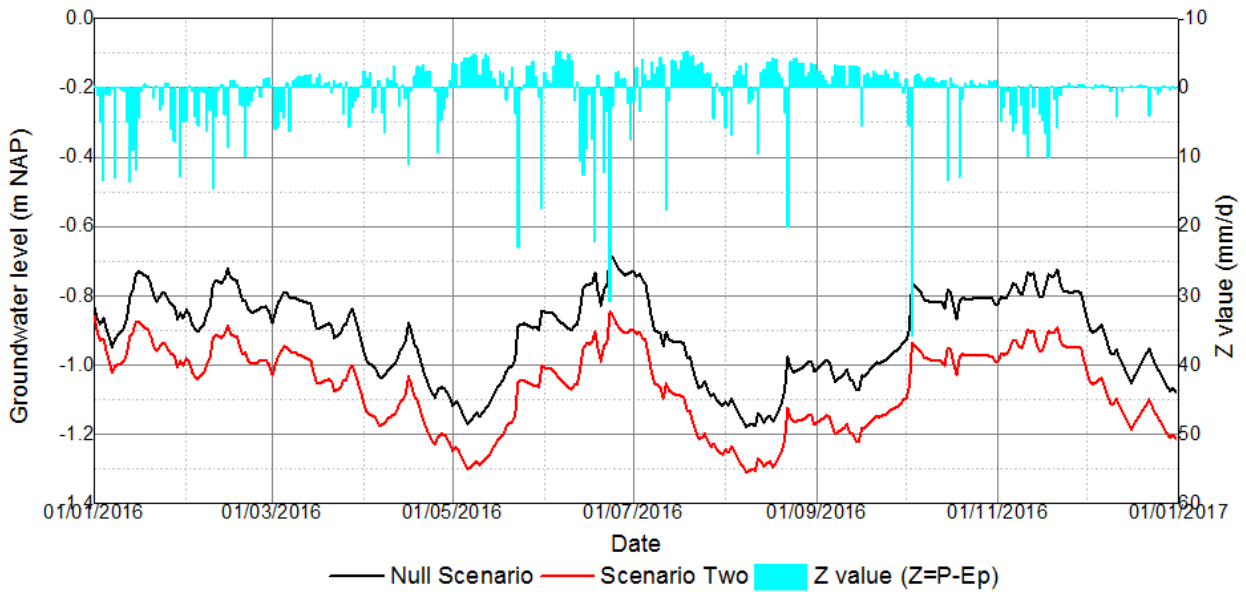


Figure 84 Time series of scenario test at Well PB08 (Scenario 2)

4.4.3. Scenario 3: A new canal in Nieuwe Haven

In this scenario, a new canal is simulated to be constructed in Nieuwe Haven with a bottom level of -1.7m NAP. Its influence on the average water level nearby is shown in *Figure 85*. As shown in the figure, the influence of the new canal on the groundwater level in the inner city is very limited. It only influences the groundwater level nearby and the groundwater level would only be raised by centimeters. There is approximately 2 to 8 cm rise in groundwater level in the northern part of the inner city with a deviation of 0 to 5 cm. According to the time series shown in *Figure 86*, the apparent level rise in the dry period can be observed while the level rise in the wet period is very limited.

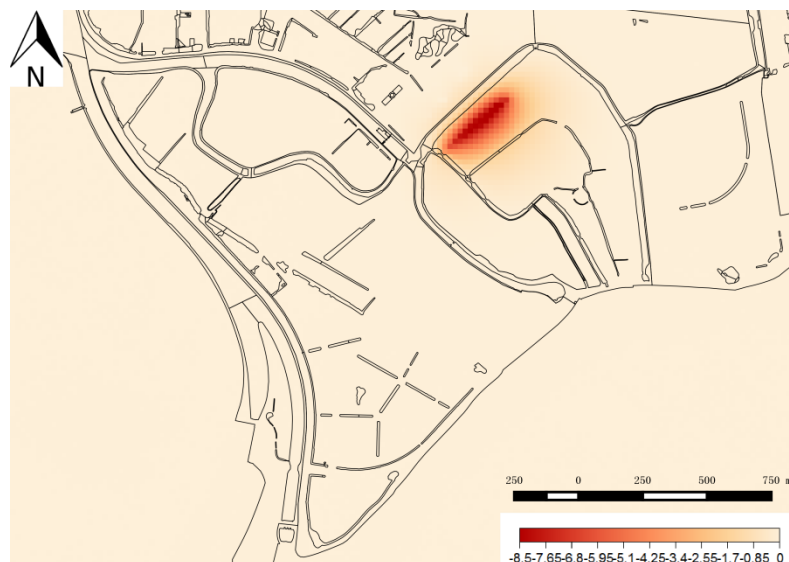


Figure 85 Difference of mean groundwater level between Scenario 3 and null scenario (Unit: cm)

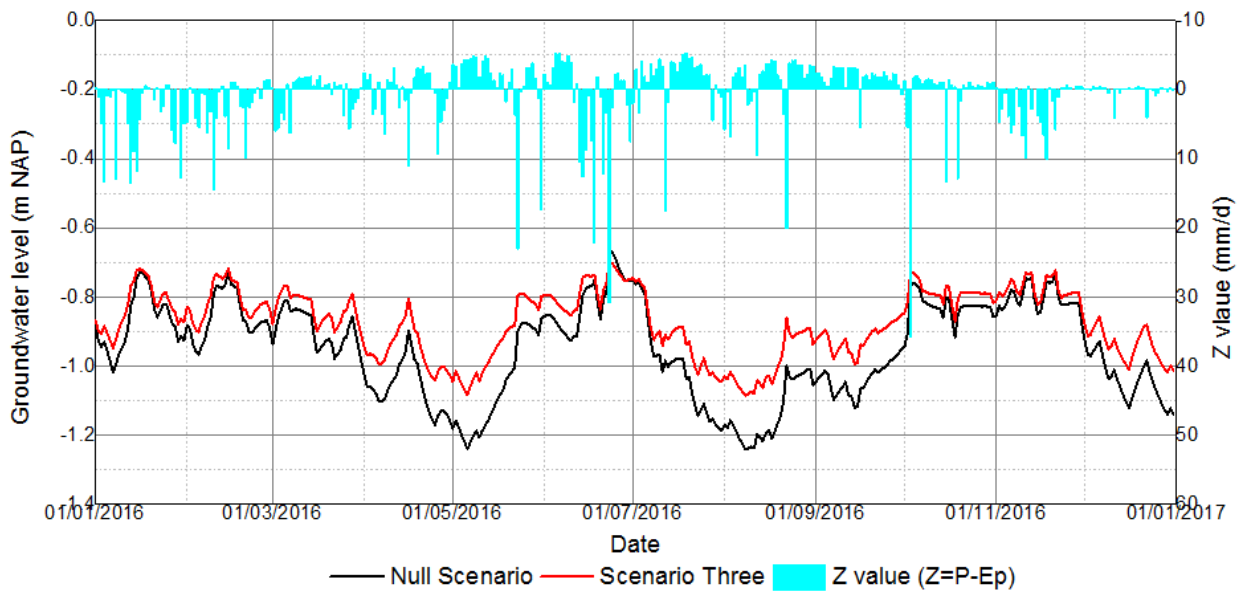


Figure 86 Time series of scenario test at Well PB04 (Scenario 3)

4.4.4. Scenario 4: A new canal in Nieuwe Haven + lower surface water level in the inner city

After the construction of a new canal, more infiltration could be expected in the area nearby. In this scenario, the influence of the new canal on the groundwater level after reducing the surface water level of the canals in the inner city is simulated. The result is shown in [Figure 87](#). As shown in the figure, the canal has a noticeable influence on the maintaining the groundwater level since the level change ($7\sim 10\text{ cm} \pm 1\sim 5\text{ cm}$) is obviously reduced in the area nearby when compare to Scenario 2 from ($13\sim 17\text{ cm} \pm 1.5\sim 2.5\text{ cm}$). However, its effective area is very limited, only groundwater level in the area near the canal is influenced. The groundwater level at PB 04 has a relatively large drop down in wet period, while there is almost no change in extremely low groundwater level (see [Figure 88](#)). Thus, though lowering the surface water level in the inner city causes the groundwater level drop, the water infiltration from the new canal helps to limit the groundwater decrease in the dry period, which is useful for reducing the hazard of flood and land subsidence in the area nearby.

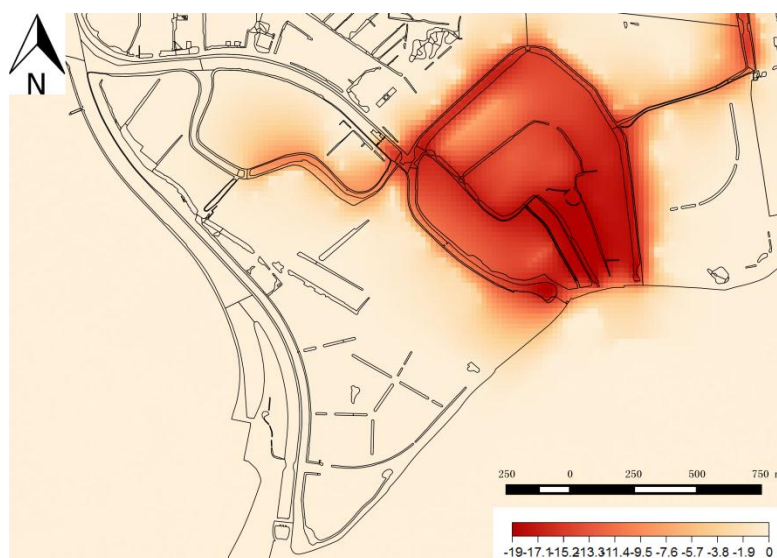


Figure 87 Difference of mean groundwater level between Scenario 4 and null scenario (Unit: cm)

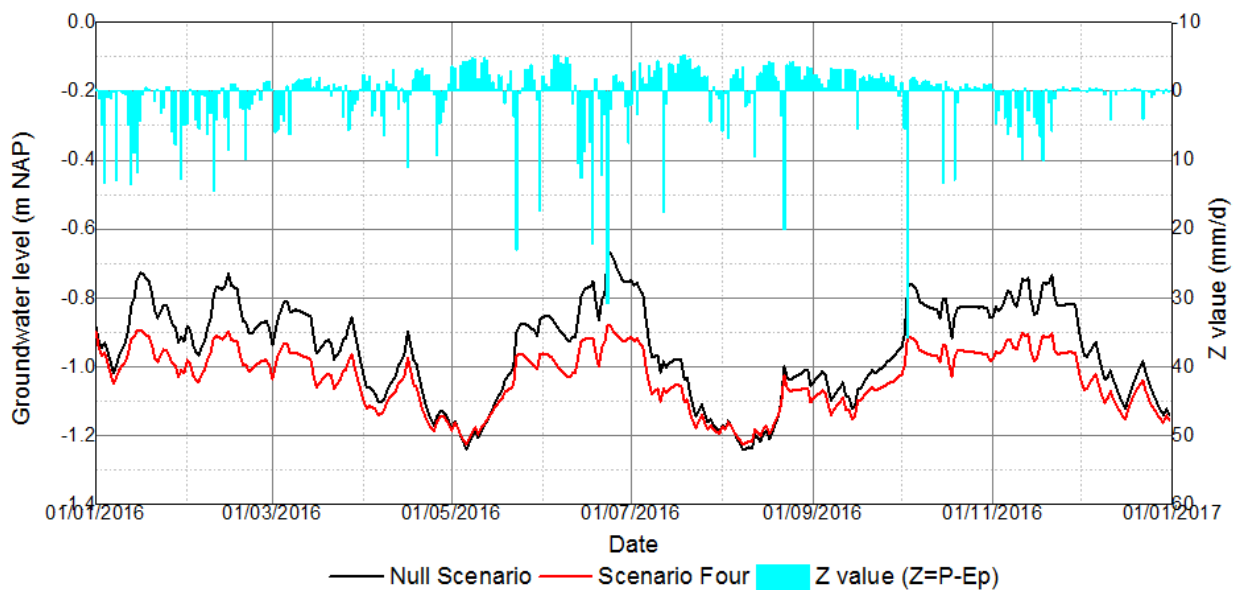


Figure 88 Time series of scenario test at Well PB04 (Scenario 4)

4.4.5. Scenario 5: Infiltration Transportation pipes

In this scenario, it is assumed that all the leaky back-stowed pipes are replaced with watertight pipes, and an infiltration transportation pipe is also installed next to these pipes. The result of the simulation is shown in [Figure 89](#). The result shows a considerable groundwater level decrease (up to around 60 cm) at the boundary of the inner city, indicating a steeper groundwater level slope because of the increased pipe wall conductance. An obvious level increase (20 to 30 meters on average) in the north part of the inner city can also be observed, while there is seldom any groundwater level change in other areas. The comparison of the groundwater level time series simulation at PB08 is shown in [Figure 90](#). After installing the infiltration transportation pipes, there is only a little bit rises on the groundwater level at this well in the wet period while the groundwater level increased a lot in dry periods. Because that the groundwater level in the dry period is similar to the surface water level in the study area, having pipes with a larger conductance only increases the groundwater level by a limited extent. In dry periods, the interaction between groundwater and leaky sewerage water becomes the dominant process. Thus, after the installation of the infiltration transportation pipes, the groundwater level has a dramatic rise, which is even more than that in Scenario 1 because of the water supply from these pipes. There are mainly two reasons for the dramatic spatial variance of the groundwater level change in the inner city. Firstly, the back-stowed pipes in the north part of the inner city are generally older than those in the south part, indicating a larger pipe wall conductance and groundwater level drop down during the emptying the pipes. Secondly, the pipe emptying and refilling processes are simulated in that area. Thus, the interaction between the leaky pipes and groundwater might be underestimated in the south part of the inner city.

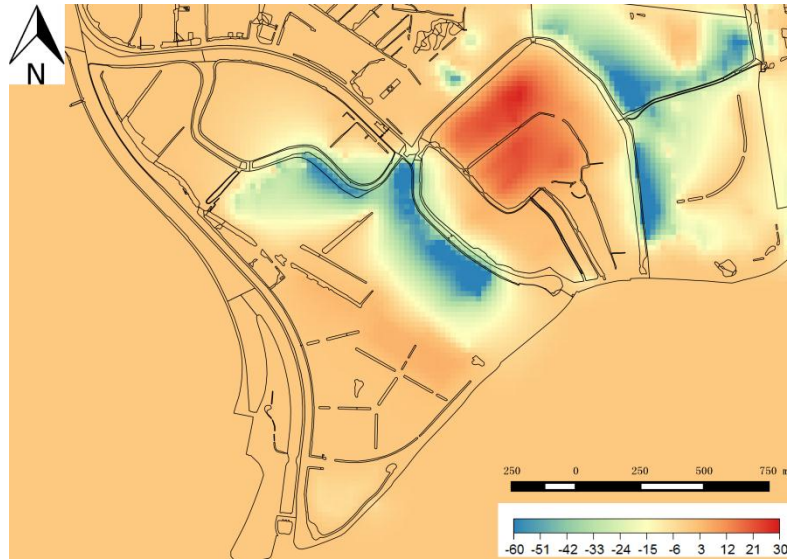


Figure 89 Difference of mean groundwater level between Scenario 5 and null scenario (Unit: cm)

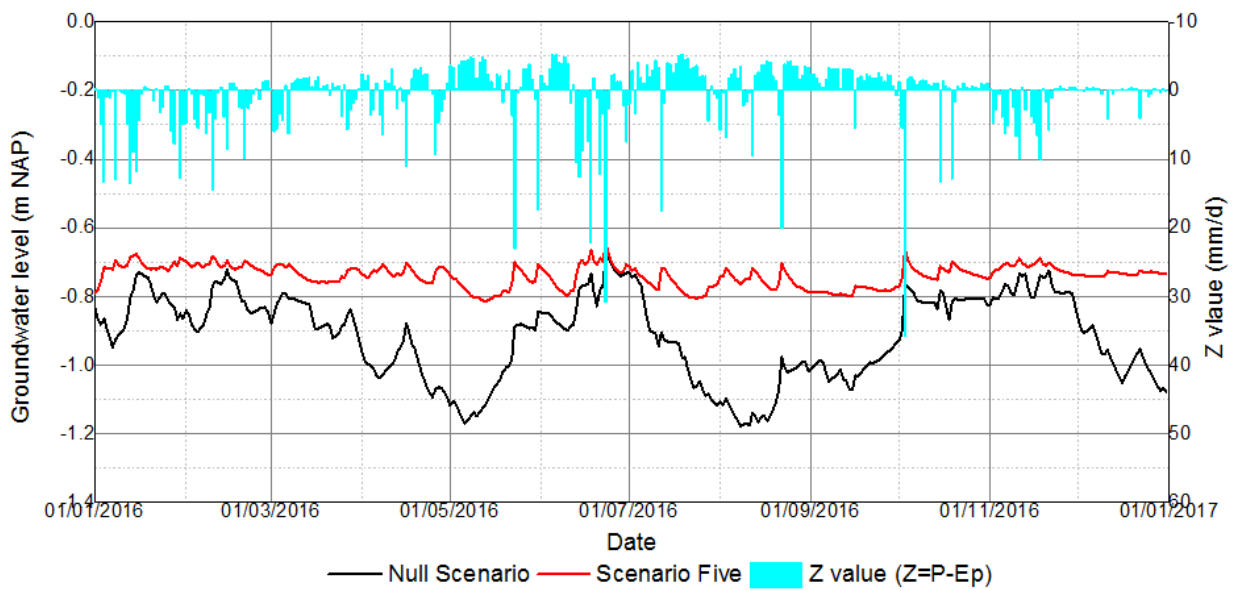


Figure 90 Time series of scenario test at Well PB08 (Scenario 5)

5 Discussion

In this research, a high-resolution groundwater model is established for Gouda. A most important part in the modeling procedure is efficiently describing the most effective elements in details in the groundwater system. Though the calibration and validation results show acceptable estimations on groundwater level in the study area, the uncertainties of the model should not be neglected. These uncertainties come from the assumptions made to deal with the problem of high spatial heterogeneity and simplify the simulation during model construction. Here are some examples. Firstly, when estimating the groundwater recharge based on different forms of urban land use, simplification is applied by neglecting the hydrological processes in the unsaturated zone. Instead, a constant crop coefficient is estimated to simulate the evapotranspiration amount for grassland. Secondly, fixed percentages of impermeable surfaces and grassed area are applied for all the backyards in the study area. This assumption succeeds to distinguish the groundwater recharge in the backyards with those of other land cover types but causes certain deviations with the reality. What's more, the changing runoff coefficient is applied according to the daily precipitation rather than soil moisture or infiltration capacity. All these assumptions can produce errors in the simulation of the reality. Giving precise estimation of the groundwater recharge values at local details surely improves the estimation of groundwater level, especially in Korte Akkeren where the percentage of the pervious surfaces is larger than that in the inner city. However, the uncertainty of the groundwater recharge is not a dominant one in this groundwater model, according to the sensitivity test performed in [Section 4.3](#). Instead, the groundwater level in the study area is more sensitive to the components like leaking sewerage pipes and canals. It is because there are a large percentage of impervious and semi-impervious land surfaces in the urban area of Gouda, which limited the groundwater recharge. In the meanwhile, the network of the canals and leaking sewerage pipes are dense in the study area, which makes them relatively more effective stresses than groundwater recharge in the groundwater system. Thus, having a relatively precise way to describe the interaction between groundwater and leaking pipes as well as canals becomes more important. However, besides the uncertainties of the calibrated parameter, the errors caused by the assumptions made when simulating these stresses are remained to be discussed. For instance, when simulating the leakage between the sewerage water and groundwater, fixed conductance is assigned to each group of back-stowed pipes according to their age. Though there is some relationship between the leakiness and the sewerage pipes according to Wang (2016), their relationship is indirect. The leakiness of the sewerage pipes is directly related to the uneven land subsidence as well as the material of the pipes (discussed in [Section 3.2.4.2](#)). During the groundwater simulation at transient state, there are only three states of the sewerage water level defined. The deviation between this simplified simulation of the sewerage water level and the real one can result in deviations between the groundwater simulation results and the reality. In addition, the surface water level is simulated to be fixed. In the scenario test, when the surface water level in the inner city drops 20 cm, the average groundwater level decreases from 13 cm to 19 cm. This indicates that the groundwater level is pretty sensitive to the level change in the canals. Thus, the ignorance of the level fluctuation in the canals also contributes to the errors in the model simulation. What's more, uncertainties of this model also come from the limitation of the information. The construction of the subsurface structure can be an example. In this research, the elevations of the top and bottom of the shallow subsurface are interpolated on the basis of the lithological borehole

logs. The limitation of the subsurface observation and information also causes the deviation between the model and the reality – in view of the enormous spatial heterogeneity of complex subsurface structure in the city. These uncertainties and simplification of the model concluded above could be the reason for the deviation between the groundwater level simulation and observation.

When calibrating and validating the model, the Nash-Sutcliffe efficiency is calculated to indicate the quality of the model simulation. However, the Nash-Sutcliffe efficiencies at several locations are negative. There are two main causes. Firstly, a negative efficiency can be yield when the simulated groundwater level has a constant deviation with the observed values which is larger than the deviation of the observed value even though they has a very similar pattern. When the deviations between the simulated values and observed values during the time series are almost constant and larger than the deviations between the observed values, $\sum (h_i - \hat{h}_i)^2$ would exceeds $\sum (\hat{h}_i - \bar{h})^2$, leading to a negative Nash-Sutcliffe efficiency. Another cause of the negative values is that the observed values are more stable than it is simulated. It is the main cause of the negative efficiency in Korte Akkeren. For example, a negative efficiency is calculated at Well 2-1.14 even when the deviation between the simulation and the observation is only around 4 cm because the observed groundwater level is very stable generating a very small $\sum (\hat{h}_i - \bar{h})^2$. Thus, having a negative Nash-Sutcliffe efficiency doesn't really indicate a bad groundwater simulation. This efficiency is not a best option for the indication of quality of the simulation for this model.

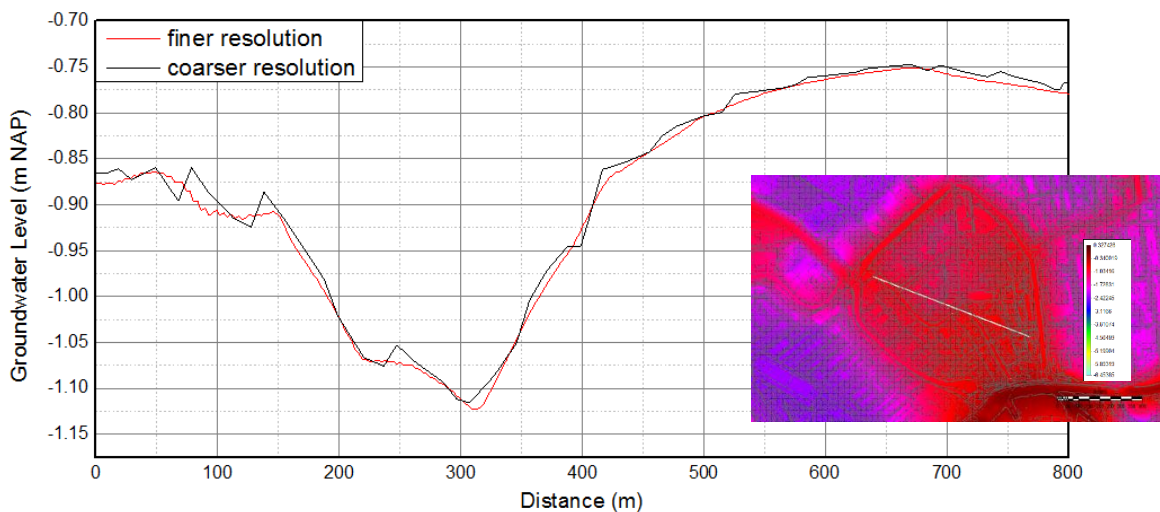


Figure 91 Simulated groundwater level along a cross-section on December 31, 2016 from 2 m × 2 m and 20 m × 20 m spatial resolution models

Another point worth discussing is the resolution of the model. A very fine spatial resolution (2 m × 2 m) is chosen when constructing the model so that more local details are able to be included in the models to solve the problem of the spatial heterogeneity of the model. For example, fine resolution input layers are able to show the relatively precise and detailed location information of stresses such as the surface water, leaking pipes. Then a detailed groundwater level distribution can be calculated, which also shows a larger spatial heterogeneity. A comparison is shown in [Figure 91](#). This figure shows the comparison of the simulated groundwater level along a cross-section on a random date (December 31, 2016) from different spatial resolution models, 2 m × 2 m and 20 m × 20 m, respectively. The groundwater level along the cross-section of the finer resolution model is

smoother than that of the coarser one, while the result of the coarser model misses some details when compared with that of the finer resolution. This detailed output of a fine resolution model is appropriate to study the small scaled influence of the groundwater, such as its effects on uneven land subsidence and the protection of wooden piles of houses. However, a higher spatial resolution also increases the uncertainties of the model calibration. Besides, in this research, the model only included some main effective stresses in the model. Other stresses or disturbances, such as some household pumps, are neglected, which may affect the accuracy of the groundwater distribution at a small scale.

6 Conclusion

This research studies the methods for constructing a high-resolution dynamic model for parts of Gouda. This model should be able to simulate the groundwater level at local details over time. Then several water management strategies can be tested in this model to observe their effects on the phreatic groundwater levels. What's more, this model should be sufficient to link to a land subsidence model for further study on land subsidence in Gouda.

To achieve this aim, the relevant hydrological processes are investigated. According to the investigation, a high-resolution groundwater model is built including high spatial heterogeneity in the urban area. Then the model was calibrated and validated using the input data from the end of 2014 until the end of 2016. After getting a sufficient set of the input parameters, their sensitivities are analyzed to estimate the uncertainties of the model. Then some examples of scenario analysis are performed to observe their effects on the phreatic groundwater level.

6.1. Relevant hydrological processes

To simulate the behavior of the groundwater system for Gouda, investigating the groundwater related processes is a vital step. A dense groundwater monitoring network had been installed in the historical inner city in Gouda to measure the groundwater level in a high frequency since 2015. In the mid-2016, another 15 observation wells are installed in the inner city at more representative locations to observe the influential factors on groundwater. Wang (2016) looked into these observations and found that the infiltration from pervious areas, evapotranspiration from various vegetated areas, leakage from the sewerage system, and surface water are identified to be the most influencing elements on groundwater system. Wang addressed the influence of spatial variation of infiltration and evapotranspiration caused by land cover or even vegetation types on the heterogeneity of groundwater level: A faster reaction on intense rainfall event are detected in observation wells near the vegetated area, while the groundwater level descending trend near the trees are more obvious than that near grassed area. Gouda has witnessed the history of the evolution of materials used in sewerage pipes: From brick to concrete in 1869, then cast iron and stoneware pipes come to the stage in 20th Century till plastic and fiberglass reinforced materials prevailing nowadays. The materials used to produce sewerage pipes are fragile at the beginning and become stronger and stronger in the later stage. The fragile historical sewerage pipes are leaky because of cracking and disjunction caused by uneven land subsidence. As the pipe materials become stronger nowadays, situations like pipe cracking and disjunction are less and less likely to happen, indicating a decreasing trend on the pipe wall conductance. The municipality of Gouda is also replacing the leaky pipes with water-tight ones, and the infiltration-transpiration pipes with high wall conductance are installed to maintain the groundwater level in the city. As for the interaction between the groundwater and surface water, generally speaking, the groundwater level in the inner city is lower than the surface water level, while the groundwater tables are higher than the surface water table in Korte Akkeren. Thus, the surface water is infiltrating from the canals into the ground, while seepage into the canals is expected in Korte Akkeren. This also indicates a higher bed resistance for the canals in the inner city than those in Korte Akkeren. Apart from these stresses,

leakage between the groundwater in different aquifers may also influence the phreatic layers. However, according to Johan Boleij's research (2013), the influence of the groundwater level change in the first aquifer on the groundwater in the phreatic aquifer is very limited, demonstrating a high resistance aquitard in between. The groundwater level change in the first aquifer can be regarded as a disturbance in this model.

6.2. Conceptualization and Construction of Groundwater model

In this research, the high-resolution groundwater model (2 m × 2 m) is constructed on the basis of a coarser regional model with a 100 m × 100 m with iModFlow as the modeling tool. The temporal resolution is decided to be one day because both groundwater level change and land subsidence are slow progress. A sensitivity test is performed for the spatial (both horizontal and vertical) boundary decision making. Once the spatial boundary is chosen, the original model is clipped for further finer model construction. The groundwater level at the boundary of this clipped model is kept fixed to ensure a reasonable groundwater flow flux at the boundary. It consists of the phreatic aquifer, first aquifer and the aquitard in between, while the groundwater level in the first aquifer is fixed. The subsurface structure in approximately first 15 m of the model is modified according to the lithological log of the groundwater observation wells and research done by Van Laarhoven (2017). The shallow subsurface (approximately first 15 m) is divided into three layers: the upper phreatic aquifer, the lower phreatic aquifer, and aquitard. The upper phreatic aquifer consists of clean marine sand and gravels in the recent anthropogenic layer, while the lower phreatic aquifer layer in the model contains part of the recent anthropogenic layer and the silty historical anthropogenic layer. Part of the recent anthropogenic layer is defined as the lower phreatic layer to make sure that the groundwater in the top aquifer will not be dried in the model simulation. The peaty and clayey layer lying beneath is simulated as the aquitard.

Then the most influential stresses are conceptualized and estimated for the model simulation. When simulating the spatial heterogeneity of the groundwater recharge (infiltration and evapotranspiration) in Gouda, the land surface is divided into seven types, impervious surface, pervious pavement, Grassland/lawn, Trees, Backyards, and water surface. For every land cover type, the estimation of the daily groundwater recharge is estimated based on their surface permeability, vegetation type and the daily reference recharge value (z). Then these daily recharge values are assigned to each grid cell within the model boundary according to a land use map. When calculating the daily transpiration in the vegetated area, it is assumed to be at the potential level because the unsaturated zone is very shallow. To simulate the leakiness of the leaky historical sewerage pipes, four different values of pipe wall conductance are assigned to four groups of leaky historical sewerage pipes divided according to their age as recommended by Wang (2016). Three states of sewerage water level (the backed up system, the emptied system, and the situation in between) are defined for model simulation. Finally, the surface water level in the study area is assumed to be constant in the simulation, since the groundwater level change is a slow progress and the water level fluctuation in the canal is limited due to the level control by the water board.

In this research, the groundwater level calculated at the steady state is used to be the initial condition of the transient model. Due to the limited data availability and the ignorant of the saturated

zone storage, the data between the beginning of November 2015 and the beginning of January 2015 is used for equilibrating the initial head before transient state calibration. During the whole simulation, the fixed head at the boundary is defined to be equal to the head at the steady state of the coarser regional model.

6.3. Groundwater model calibration and validation

Firstly, the groundwater model is calibrated at steady state to estimate the range of the parameters like hydraulic conductivity of each aquifer, vertical resistance, and river conductance. Then the calibrated groundwater level at the steady state is used as the initial state of the transient model. Because of the limitation of the data availability, this model is calibrated using the groundwater observation in period 2015~2016, and validated with the data in period 2016~2017. The groundwater level observations of 8 wells (Well 1-1.04, 1-1.08, 1-1.12, 1-1.14 in the inner city and Well 2-1.07, 2-1.10, 2-1.14, 2-1.19 in Korte Akkeren) are used to calibrate the patterns of the simulated groundwater level, while the root mean squared error, coefficient of determination (R^2), and Nash-Sutcliffe efficiency between the simulated phreatic groundwater level and the daily average value of the measurements at every observation wells are calculated to make sure that the deviation in all the wells are acceptable. Same strategies are used in the model verification stage to validate the performance of the model, but the observations at three more observation wells (PB04, PB05, and PB08) are added to show the fitting quality over time since more observation wells are added in the inner city in 2016.

When calibrating the groundwater model, the data from Van Laarhoven and Wang's field work, like subsurface stratigraphy, slug tests and estimation on the conductance of sewerage pipes, are also regarded as a reference. Generally speaking, this groundwater model is able to give an acceptable estimation of the study area according to the results of the calibration and validation. The RMSE of the calculated groundwater level as compared to the observed ones was smaller than 0.35 m (0.24 m within the study area) in 80% of the observation wells used for validation, while the R^2 of the simulation is larger than 0.926 in 80% of the observation wells. Relatively larger deviation and smaller statistical correlation between the simulated value and observed value were found at some locations in Korte Akkeren near a canal with a higher surface water level, while relatively low correlation between simulation and observation also can be found at Well 1-1.09, 1-1.13 and 1.15. When looking at the time series of groundwater level, the model is able to give a reasonable estimation on the groundwater level at most of the observation wells while the groundwater level in dry season at Well 1-1.08 is always underestimated and the groundwater level in the wet period at Well 2-1.10 is always overestimated. Though the model uncertainty caused by simplifying the reality produces the deviation between the simulated groundwater level and the observed value, this model is able to simulate the different groundwater levels in different polders, and the pattern of the time series are also similar to the observed one. Since the model Thus this groundwater model is feasible for the simulation of the groundwater level in Gouda and linked to the land subsidence model.

6.4. Sensitivity analysis

After model calibration and validation, a sensitivity test is performed to test the model sensitivity to some input parameters, the conductance of the canal bed and sewerage pipes, hydraulic conductivity of the upper and lower phreatic aquifer, storage coefficient, vertical resistance, and groundwater recharge. Their sensitivity is tested by both adding and removing 50% to/from the calibrated value, re-running the model to obtain a new set of output in both the calibration and validation periods and observing the effect of the change.

In this research, the sensitivity of the model is represented in two dimensions, spatial and temporal. To present the spatial effects during the sensitivity test, the average groundwater level change in the study area is calculated. The time series at observation well PB 08 is chosen to compare the temporal distribution if the level change. According to the results, it can be found that this model is more sensitive to the pipe wall conductance and canal bed, while the groundwater level is less sensitive to the hydraulic conductivity and vertical resistance. The storage coefficient only changes the fluctuation extent while there is almost no change in the average level. When changing the groundwater recharge in the study area, the groundwater level in the wet period rises more than the groundwater drops in the dry period.

6.5. Scenario analysis

Since the groundwater model seems applicable for the level simulation in the study area, this model is used for the simulation of the water management scenarios. In this research, 4 scenarios are simulated: 1. replacing all the back-stowed pipes with new watertight pipes; 2. reducing the surface water level by 20 cm in the inner city; 3. constructing a new canal in Nieuwe Haven; 4. constructing a new canal in Nieuwe Haven and reducing the surface water level by 20 cm in the inner city. Among these scenarios, the groundwater level changes in the inner city are all larger than those Korte Akkeren.

● Scenario 1: watertight pipes

Replacing the leaking pipes could raise the groundwater level both in the inner city and Korte Akkeren. The level change in Korte Akkeren is mild (approximately 0~7 cm). However, the groundwater level in the inner city would increase from 0 to 25 cm. This is because that the ages of the sewerage pipes in the inner city, generally speaking, are relatively older than those in Korte Akkeren. Thus larger pipe conductance values in the inner city are expected. Thus the rise of the groundwater level in the inner city is relatively more significant when compared with that in Korte Akkeren. This rise could increase the risk of flooding in that area. As for the temporal distribution, after replacing the watertight pipes, the level increase in the dry period is more evident than that in the wet period. However, since this area is already under a high vulnerability because of the limited freeboard at the canals and high groundwater level, drainage pipes could be installed in this area for the drainage of the groundwater surplus in that area while minimizing groundwater flooding.

● Scenario 2: Lower surface water level in the inner city

In this scenario, the surface water level in the canals in the inner city is decreased by 20 cm. According to the results, the groundwater level at the inner city is very sensitive to this change, the

level change in the inner city ranges from approximately 12 to 19 cm. This result also shows a high impact of the surface water on the groundwater level. And the groundwater level drop is almost even in both the dry period and wet period. The apparent groundwater level change has a high risk of accelerating the land subsidence and bringing damage to the wooden piles of the historical houses.

- **Scenario 3: A new canal in Nieuwe Haven**

When constructing a new canal in Nieuwe Haven, only a very limited area would be influenced by the infiltration from the canal. Moreover, their change of the groundwater level is mild: there is around 8 cm rise in groundwater level near Nieuwe Haven while the increase of the groundwater level near Turfmarkt is only 3 cm. The groundwater rise in wet period is not obvious. As a result, though constructing the new canals could raise the groundwater level in the northern part of the inner city, the raised hazard is very limited.

- **Scenario 4: A new canal in Nieuwe Haven + lower surface water level in the inner city**

While the surface water level is reduced by 20 cm, the drop of the groundwater level near the canal is limited to approximately 8 cm from 13 cm (if there is no canal in Nieuwe Haven), which is an undeniable influence, and these level drop in the wet period contribute most of the average groundwater level change. As a result, though lowering the surface water level in the inner city causes the groundwater level drop, the water infiltration from the new canal helps to limit the groundwater decrease in the dry period, which is suitable for reducing the hazard of flood and land subsidence in the area nearby.

- **Scenario 5: Infiltration Transportation pipes**

In this scenario, the groundwater level at the boundary of the inner city decreases apparently because of the increased pipe wall conductance, while it has a relatively significant increase in the north part of the inner city. In the inner city the groundwater level increase mostly happens in the dry periods, because the interaction between groundwater and leaky sewerage water is the dominant processes at that time, while the groundwater level increase in the wet season is relatively mild than that in the Scenario 1, when the leaky pipes are only replaced by watertight ones.

7 Recommendation

This research describes the construction method on a high-resolution groundwater model for a small region of urban area in Gouda, the Netherlands. Though a series of assumptions is made to simplify the hydrological processes and the simulation of the large spatial heterogeneity of the land surface and subsurface, the performance of this groundwater level is feasible to simulate the pattern and the different groundwater levels in different polders, indicating that the groundwater model included a sufficient identification and estimation on the major influential factors in the geohydrological cycle.

However, the uncertainties of the model should also be well recognized. These uncertainties come from the simplification of the geohydrological processes in the model simulation and spatial heterogeneity due to the limitation of data availability. Thus, several aspects can work on to improve this groundwater model. Firstly, more information on spatial heterogeneity such as lithostratigraphic information for a larger area can be studied to support the groundwater model. Van Laarhoven (2017) only did his fieldwork in and constructed his 3D geological model for the inner city and a large part of Korte Akkeren, which is only a part of the groundwater model. If the lithostratigraphic information for a larger area is studied, the simulation of the spatial heterogeneity of the subsurface structure can be improved. Secondly, the water filling and emptying of the leaky back-stowed system was only simulated in the center area of the inner city with three states of the sewerage water level. According to the sensitivity analysis and the scenario analysis, the influence of the sewerage pipes is large on groundwater level. However, only three states of the sewerage water level are defined in the simulation, which brings errors to the model. Thus, to improve this model, it is suggested that a hydrodynamic model simulating the water level in the sewerage system would also help. Also, the recharge map is generated from the land cover types while simplifying the hydrological processes in the unsaturated zone with a correction factor for evapotranspiration, assigning a specific runoff coefficient to the pervious pavement, and assuming the composition of the backyards. The accuracy and uncertainty of the groundwater recharge simulation as well as whether there are any alternative ways to estimate groundwater recharge for different forms of urban land use are remained to be discussed. What is more, the groundwater level at Well 1-1.13 is approximately 1m higher than the observation from other wells nearby, which fails to be simulated in the groundwater model. Thus, there might be some other effective hydrological processes happening at that location. It still needs further investigation.

Another point worth discussing is the model resolution and efficiency. Since the groundwater model is built in a very high spatial resolution, this quasi-groundwater model contains $2400 \times 2094 \times 3$ grid cells. This massive amount of grid cells also indicates that this model needs a relatively large period for running (about 10 hours for one-year data) and a large space to save the output (approximately 160 GB for one year data). This could be a large limitation for the storage as well as processing the data in the later stage. At the later stage, whether using such a high resolution or whether the boundary of the model could be discussed according to the aim of later research. Though the model results with coarser resolution miss some groundwater level details and are not as smooth as the results of a finer resolution, the groundwater level differences between them is relatively small. Thus,

having a fine resolution in the study area but coarser resolution in the other areas could be a good solution for reducing the running time and output size.

Last but not least, this high-resolution groundwater model has already included very detailed information of urban land surfaces and underground structures. Thus, this model can also be used to be a groundwater assessment tool for urban water management. In this research, four urban (ground)water management scenarios are analyzed using this model, but the impact of climate change is still not included in this model. In the further research, more urban water management scenarios (For example, the effect of a designed drainage-infiltration-transportation sewer system in the inner city) and climate change scenarios can be applied to test their influence on groundwater regime for land subsidence estimation study.

Bibliography

- Adamowski, J., & Chan, H. F. (2011). A wavelet neural network conjunction model for groundwater level forecasting. *Journal of Hydrology*, 407(1-4), 28-40. doi:10.1016/j.jhydrol.2011.06.013
- Arkansas Geological Survey. (2015). Land subsidence. Retrieved from <https://www.geology.ar.gov/geohazards/landsubsidence.html>
- Barnett, B., Townley, L. R., Post, V., Evans, R. E., Hunt, R. J., Peeters, L., . . . Boronkay, A. (2012). *Australian groundwater modelling guidelines*: National Water Commission, Canberra.
- Beretta, G. P., Avanzini, M., & Pagotto, A. (2004). Managing groundwater rise: Experimental results and modelling of water pumping from a quarry lake in Milan urban area (Italy). *Environmental Geology*, 45(5), 600-608. doi:10.1007/s00254-003-0918-7
- Bierkens, M. F. (1996). Modeling hydraulic conductivity of a complex confining layer at various spatial scales. *Water Resources Research*, 32(8), 2396-2382. doi:10.1029/96WR01465
- Boersma, C. (2015). Land subsidence in peat areas. Retrieved from <https://www.deltares.nl/app/uploads/2015/02/Dossier-Subsidence-Delta-Life-3.pdf>
- Boleij, J. (2013). *Grondwaterwinning Croda Onderzoek primaire- en omgevingseffecten stopzetten grondwaterwinning*.
- Carneiro, J., & Carvalho, J. M. (2010). Groundwater modelling as an urban planning tool: issues raised by a small-scale model. *Quarterly Journal of Engineering Geology and Hydrogeology*, 43(2), 157-170. doi:10.1144/1470-9236/08-028
- Chu, S. T. (1978). Infiltration during an unsteady rain. *Water Resources Research*, 14(3), 461-466. doi:10.1029/WR014i003p00461
- Coalitie: 'Stevige stad op slappe bodem'. (2015a). *Bodemdaling: kwetsbaarheden van de binnenstad van Gouda*. Retrieved from <https://stevigestadoplappedodem.files.wordpress.com/2015/11/knelpunten-en-eerste-analyse-zakkende-binnenstad.pdf>
- Coalitie: 'Stevige stad op slappe bodem'. (2015b). De Geschiedenis. *Bodemdaling en Gouda*. Retrieved from <https://stevigestad.net/de-geschiedenis/>
- Cuenca, M. C., & Hanssen, R. (2007). SUBSIDENCE DUE TO PEAT DECOMPOSITION IN THE NETHERLANDS, KINEMATIC OBSERVATIONS FROM RADAR INTERFEROMETRY. In *Proc. of FRINGE 2007 Workshop* (pp. 1-6). Frascati, Italy.
- Daliakopoulos, I. N., Coulibaly, P., & Tsanis, I. K. (2005). Groundwater level forecasting using artificial neural networks. *Journal of Hydrology*, 309(1-4), 229-240. doi:10.1016/j.jhydrol.2004.12.001
- Dams, J., Woldeamlak, S. T., & Batelaan, O. (2008). Predicting land-use change and its impact on the groundwater system of the Kleine Nete catchment, Belgium. *Hydrology and Earth System Sciences*, 12(6), 1369-1385. doi:10.5194/hess-12-1369-2008
- David L. Freyberg, John W. Reeder, Joseph B. Franzini, & Remson, I. (1980). Application of the Green-Ampt Model to infiltration under time-dependent surface water depths. *Water Resources Research*, 16(3), 517-528. doi:10.1029/WR016i003p00517
- Deverel, S. J., & Leighton, D. A. (2010). Historic, Recent, and Future Subsidence, Sacramento-San Joaquin Delta, California, USA. *San Francisco Estuary and Watershed Science*, 8(2).
- Elfeki, A., & Dekking, M. (2001). A Markov Chain Model for Subsurface Characterization: Theory and Applications. *Mathematical Geology*, 33(5), 569-589. doi:10.1023/a:1011044812133
- Epting, J., Huggenberger, P., & Rauber, M. (2008). Integrated methods and scenario development for urban groundwater management and protection during tunnel road construction: a case

- study of urban hydrogeology in the city of Basel, Switzerland. *Hydrogeology Journal*, 16(3), 575-591. doi:10.1007/s10040-007-0242-5
- Fletcher, T. D., Andrieu, H., & Hamel, P. (2013). Understanding, management and modelling of urban hydrology and its consequences for receiving waters: A state of the art. *Advances in Water Resources*, 51, 261-279. doi:10.1016/j.advwatres.2012.09.001
- Hoogheemraadschap van Rijnland. (2014). Living Lab. Retrieved from <https://www.bewustlevenmetwater.nl/klimaatverandering/living-lab/>
- IPCC. (2014). Climate Change 2014: Impacts, Adaptation, and Vulnerability. Part A: Global and Sectoral Aspects. In C. B. Field, V. R. Barros, D. J. Dokken, K. J. Mach, M. D. Mastrandrea, T. E. Bilir, M. Chatterjee, K. L. Ebi, Y. O. Estrada, R. C. Genova, B. Girma, E. S. Kissel, A. N. Levy, S. MacCracken, P. R. Mastrandrea, & L. L. White (Eds.): Cambridge University Press, Cambridge, United Kingdom and New York, NY, USA.
- Jacobs, A. F. G., & De Bruin, H. A. R. (1998). Makkink's equation for evapotranspiration applied to unstressed maize. *Hydrological Processes*, 12(7), 1063-1066. doi:10.1002/(SICI)1099-1085(19980615)12:7<1063::AID-HYP640>3.0.CO;2-2
- Korkealaakso, J., Kuosa, H., Niemeläinen, E., & Tikanmäki, M. (2014). *Review of pervious pavement dimensioning, hydrological models and their parameter needs. State-of-the-Art (VTT-R-08227-13)*. Retrieved from http://www.vtt.fi/files/sites/class/CLASS_WP4_SOTA_Dimensioning_and_Models.pdf
- Koster, K., Erkens, G., & Zwanenburg, C. (2016). A new soil mechanics approach to quantify and predict land subsidence by peat compression. *Geophysical Research Letters*, 43(20), 10792-10799. doi:10.1002/2016GL071116
- Lerner, D. N. (2002). Identifying and quantifying urban recharge: a review. *Hydrogeology Journal*, 10(1), 143-152. doi:10.1007/s10040-001-0177-1
- Levins, R. (1993). A Response to Orzack and Sober: Formal Analysis and the Fluidity of Science. *The Quarterly Review of Biology*, 68(4), 547-555. doi:10.1086/418302
- McGinty, W. A., Smeins, F. E., & Merrill, L. B. (1979). Influence of Soil, Vegetation, and Grazing Management on Infiltration Rate and Sediment Production of Edwards Plateau Rangeland. *Journal of Range Management*, 32(1), 33-37. doi:10.2307/3897380
- McMahon, T. A., Malano, H. M., & Schultz, B. (2015). Comment on the Reference to Makkink Potential Evaporation Equation. *Journal of Irrigation and Drainage Engineering*, 141(1), 02514001. doi:doi:10.1061/(ASCE)IR.1943-4774.0000845
- Meliefste, M. C. (2014). *Verbreed basisrioleringsplan Korte Akkeren Capaciteit en emissieberekeningen*.
- Meyer, J. L., Gibeault, V. A., & Youngner, V. B. (1985). Irrigation of turfgrass below replacement of evapotranspiration as a means of water conservation: determining crop coefficient of turfgrasses. In 5. *International Turfgrass Research Conference, Avignon (France), 1-5 Jul 1985 (Vol. INRA)*.
- Miles, B., Kalbacher, T., Kolditz, O., Chen, C., Gronewold, J., Wang, W., & Peter, A. (2007). Development and parameterisation of a complex hydrogeological model based on high-resolution direct-push data. *Environmental Geology*, 52(7), 1399-1412. doi:10.1007/s00254-006-0582-9
- Miracapillo, C., & Howard, K. W. F. (2007). Groundwater modelling to evaluate the risk of aquifer depletion due to a construction site in an urban area in Basel, Switzerland. In *Urban Groundwater, Meeting the Challenge: Selected Papers from the 32nd International Geological Congress (IGC), Florence, Italy, August 2004 (pp. 259-270)*.

- Nas, B., & Berktaş, A. (2010). Groundwater quality mapping in urban groundwater using GIS. *Environmental Monitoring and Assessment*, 160(1), 215-227. doi:10.1007/s10661-008-0689-4
- Nienhuis, P. H. (2010). *Environmental history of the Rhine-Meuse Delta: an ecological story on evolving human-environmental relations coping with climate change and sea-level rise*: Springer.
- Penman, H. L. (1950). THE DEPENDENCE OF TRANSPIRATION ON WEATHER AND SOIL CONDITIONS. *European Journal of Soil Science*, 1(1), 74-89. doi:10.1111/j.1365-2389.1950.tb00720.x
- Querner, E. P., Jansen, P. C., & Kwakernaak, C. (2008). Effects of water level strategies in Dutch peatlands: a scenario study for the polder Zegveld. In *Proceedings of the 13th International Peat Congress: After Wise Use-The future of Peatlands, Tullamore, Ireland, 8-13 June, 2008* (pp. 620-623).
- Rawson, H. M., Begg, J. E., & Woodward, R. G. (1977). The effect of atmospheric humidity on photosynthesis, transpiration and water use efficiency of leaves of several plant species. *Planta*, 134(1), 5-10. doi:10.1007/bf00390086
- Rosenberg, M. (2018, 11 January, 2018). Polders and Dikes of the Netherlands: The Reclamation of Land in the Netherlands Through Dikes and Polders. Retrieved from <https://www.thoughtco.com/polders-and-dikes-of-the-netherlands-1435535>
- Schirmer, M., Leschik, S., & Musolff, A. (2013). Current research in urban hydrogeology—a review. *Advances in Water Resources*, 51, 280-291. doi:10.1016/j.advwatres.2012.06.015
- Shot, E. (2011). *Binnenstad Gouda Verbreed basistioleringsplan*.
- Stafleu, J., Maljers, D., Gunnink, J. L., Menkovic, A., & Busschers, F. S. (2011). 3D modelling of the shallow subsurface of Zeeland, the Netherlands. *Netherlands Journal of Geosciences*, 90(4), 293-310. doi:10.1017/S0016774600000597
- Stanley, D. J. (1988). Subsidence in the Northeastern Nile Delta: Rapid Rates, Possible Causes, and Consequences. *Science*, 240(4851), 497-500.
- Taylor, R. G., Cronin, A. A., Lerner, D. N., Tellam, J. H., Bottrell, S. H., Rueedi, J., & Barrett, M. H. (2006). Hydrochemical evidence of the depth of penetration of anthropogenic recharge in sandstone aquifers underlying two mature cities in the UK. *Applied Geochemistry*, 21(9), 1570-1592. doi:10.1016/j.apgeochem.2006.06.015
- Thrash, I. (1997). Infiltration rate of soil around drinking troughs in the Kruger National Park, South Africa. *Journal of arid environments*, 35(4), 617-625. doi:10.1006/jare.1996.0227
- Törnqvist, T. E., Wallace, D. J., Storms, J. E. A., Wallinga, J., Van Dam, R. L., Blaauw, M., . . . Snijders, E. M. A. (2008). Mississippi Delta subsidence primarily caused by compaction of Holocene strata. *Nature Geoscience*, 1(3), 173-176. doi:10.1038/ngeo129
- USGS. (2016). Land Subsidence. Retrieved from <https://water.usgs.gov/ogw/subsidence.html>
- Van den Akker, J. J. H., Kuikman, P. J., De Vries, F., Hoving, I., Pleijter, M., Hendriks, P. F. A., . . . Kwakernaak, C. (2010). Emission of CO₂ from agricultural peat soils in the Netherlands and ways to limit this emission. In *Proceedings of the 13th International Peat Congress After Wise Use--The Future of Peatlands, Vol. 1 Oral Presentations, Tullamore, Ireland, 8--13 June 2008* (Vol. 1, pp. 645-648).
- Van den Born, G. J. (2016). *Subsiding soils, rising costs. Possible measures against peatland subsidence in rural and urban areas*. Retrieved from http://www.pbl.nl/sites/default/files/cms/publicaties/Subsiding%20soils,%20rising%20costs_Findings.pdf

- Van Laarhoven, S. (2017). *Influence of loading history on subsurface architecture and subsidence potential for the historical city of Gouda, The Netherlands*. (Master Degree Thesis), Utrecht University.
- Van Schoubroeck, F. (2010). *The remarkable history of polder systems in The Netherlands*. Paper presented at the Agricultural Heritage Systems of the 21st Century, Chennai, India. http://www.fao.org/fileadmin/templates/giahs/PDF/Dutch-Polder-System_2010.pdf
- Vázquez-Suñé, E., & Sanchez-Vila, X. (1999). Groundwater modelling in urban areas as a tool for local authority management: Barcelona case study (Spain). *IAHS PUBLICATION*, 65-72.
- Vázquez-Suñé, E., Sánchez-Vila, X., & Carrera, J. (2005). Introductory review of specific factors influencing urban groundwater, an emerging branch of hydrogeology, with reference to Barcelona, Spain. *Hydrogeology Journal*, 13(3), 522-533. doi:10.1007/s10040-004-0360-2
- Vermeulen, P. T. M., Burgering, L. M. T., & Minnema, B. (2016). *iMOD user manual. version: 3.3*. Utrecht, the Netherlands: Deltares.
- Wang, H. (2016). *Controlling urban groundwater in delta areas: A case study at Turfmarkt, Gouda, the Netherlands*. (Master Degree Thesis), Delft University of Technology, Delft. (7d2fc0cd-a80d-49c6-a4fa-8c967e8ea63f)
- Wikipedia. (2017). Korte Akkeren. Retrieved from https://nl.wikipedia.org/wiki/Korte_Akkeren
- Zhang, L., & Kennedy, C. (2006). Determination of Sustainable Yield in Urban Groundwater Systems: Beijing, China. *Journal of Hydrologic Engineering*, 11(1), 21-28. doi:10.1061/(ASCE)1084-0699(2006)11:1(21)
- Zhou, X., Chen, M., & Liang, C. (2003). Optimal schemes of groundwater exploitation for prevention of seawater intrusion in the Leizhou Peninsula in southern China. *Environmental Geology*, 43(8), 978-985. doi:10.1007/s00254-002-0722-9

Appendix 1: the mean value and the standard deviation of the level change in sensitivity test

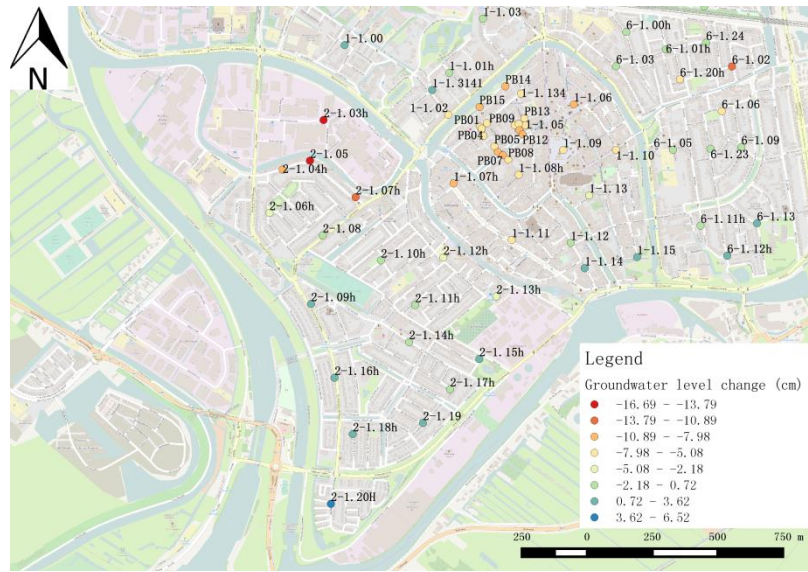


Figure 92 Average value of groundwater level change after removing 50% of amount from canal conductance

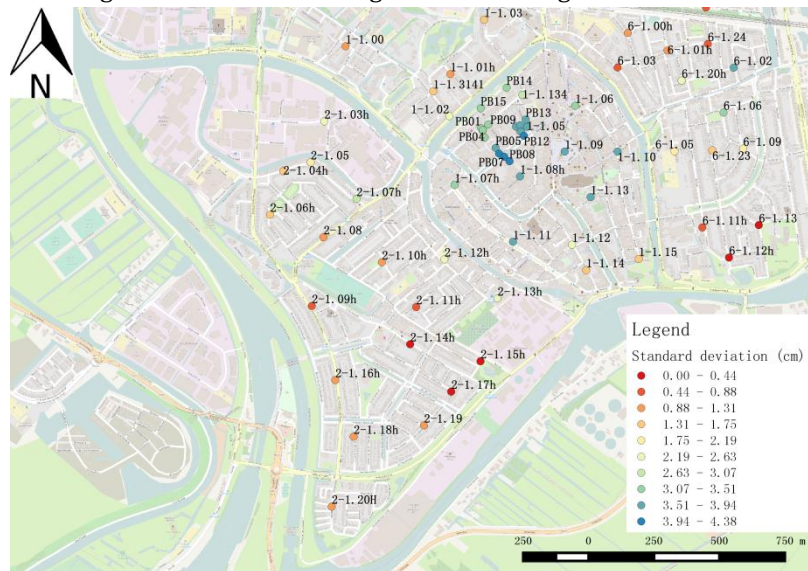


Figure 93 Standard Deviation of groundwater level change after removing 50% of amount from canal conductance

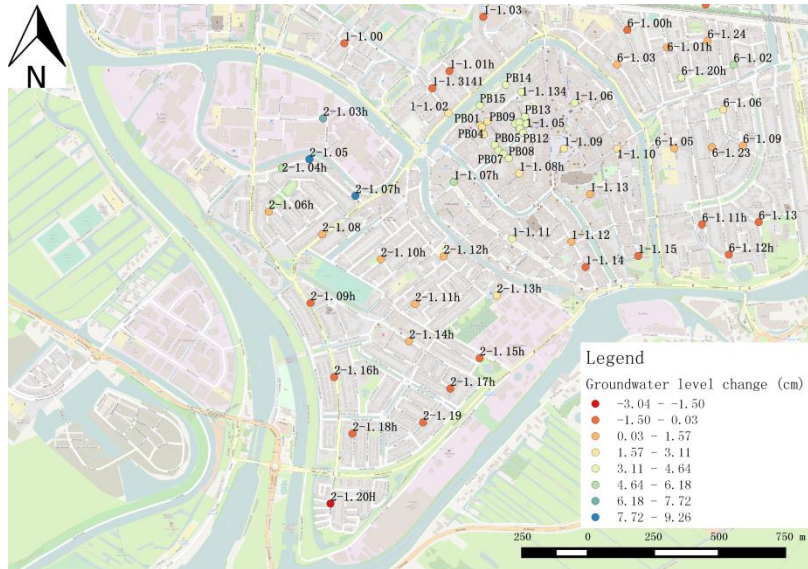


Figure 94 Average value of groundwater level change after adding 50% of amount to canal conductance

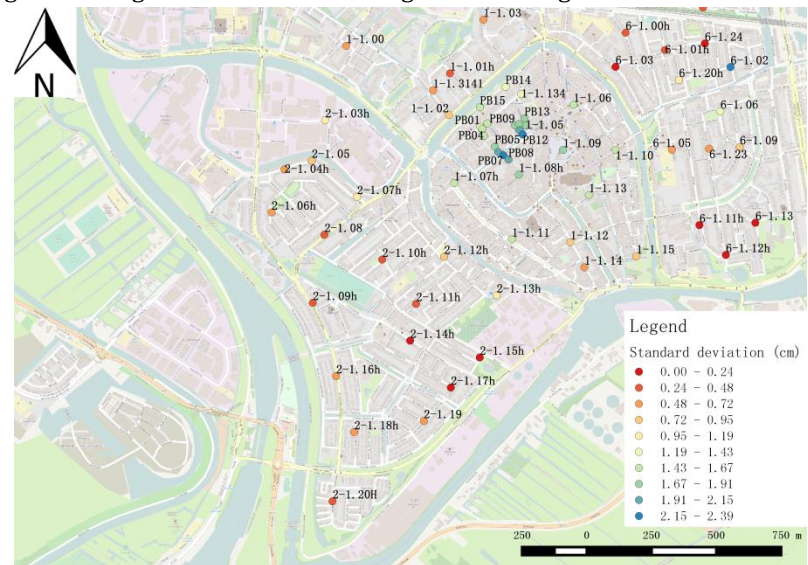


Figure 95 Standard Deviation of groundwater level change after adding 50% of amount to canal conductance

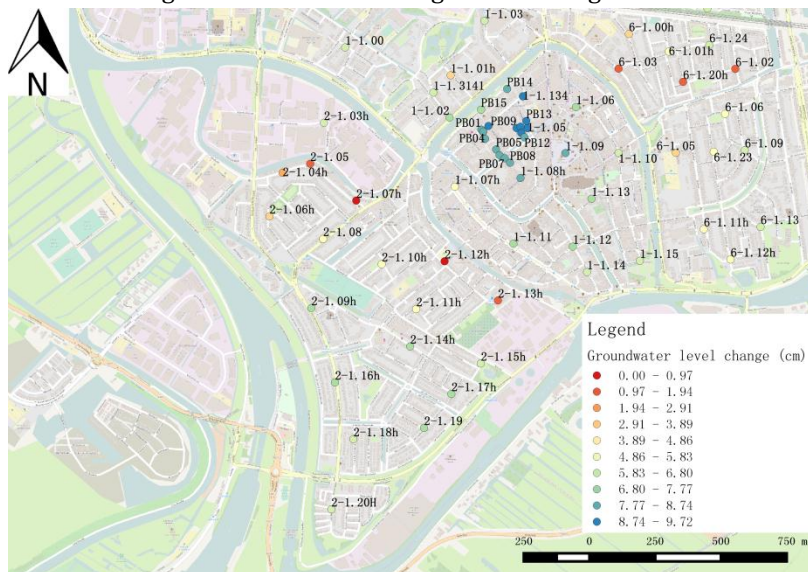


Figure 96 Average value of groundwater level change after removing 50% of amount from sewerage pipe conductance

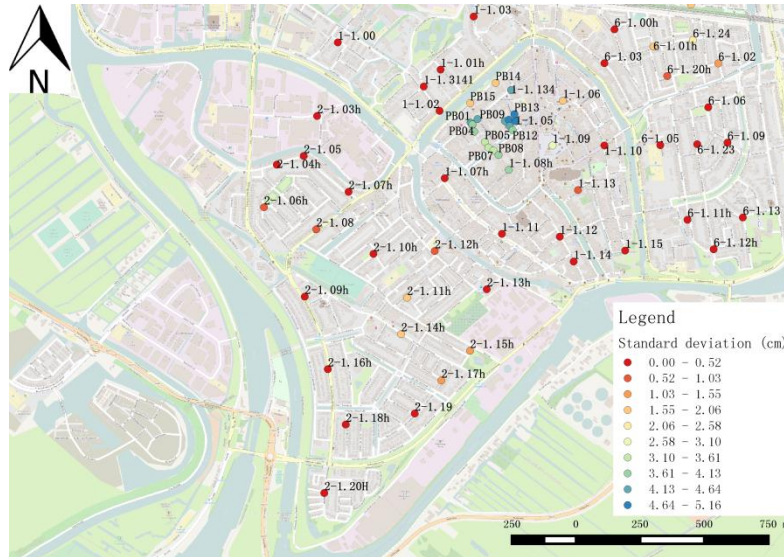


Figure 97 Standard Deviation of groundwater level change after removing 50% of amount from pipe conductance

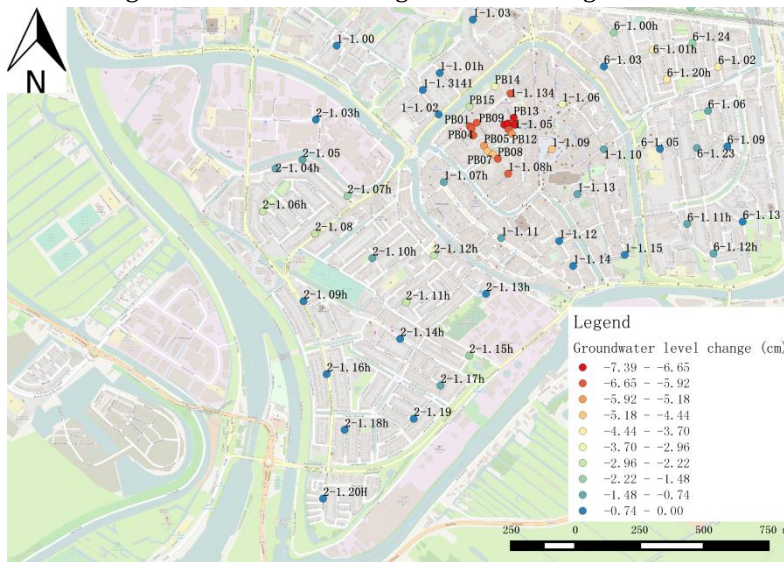


Figure 98 Average value of groundwater level change after adding 50% of amount to sewerage pipe conductance

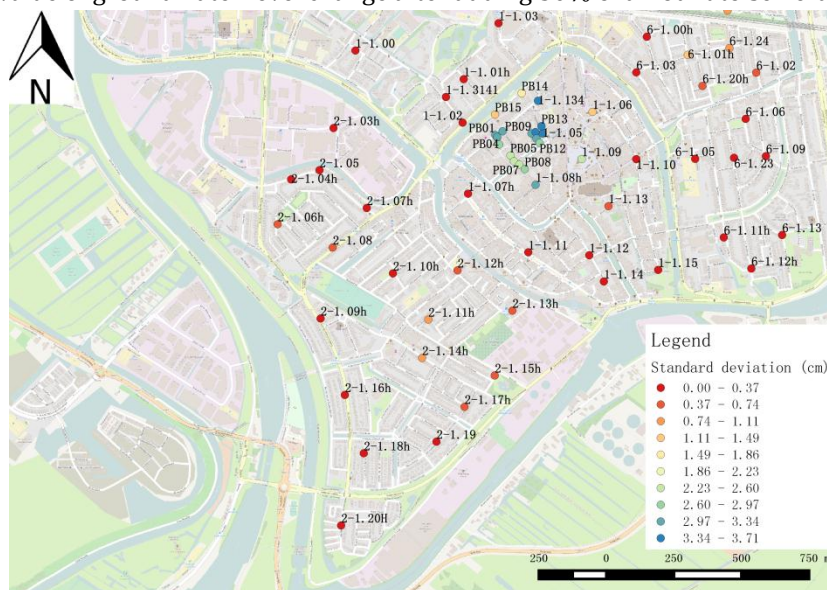


Figure 99 Standard Deviation of groundwater level change after adding 50% of amount to sewerage pipe conductance

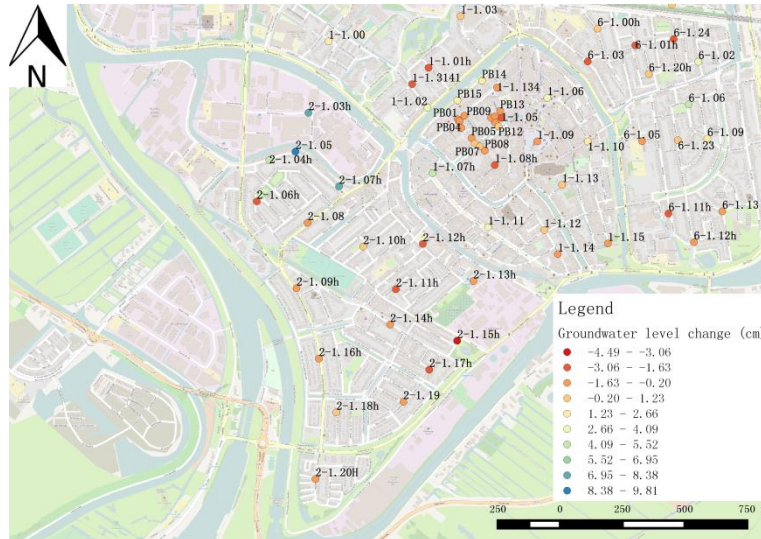


Figure 100 Average value of groundwater level change after removing 50% of amount from hydraulic conductivity of the upper phreatic aquifer layer

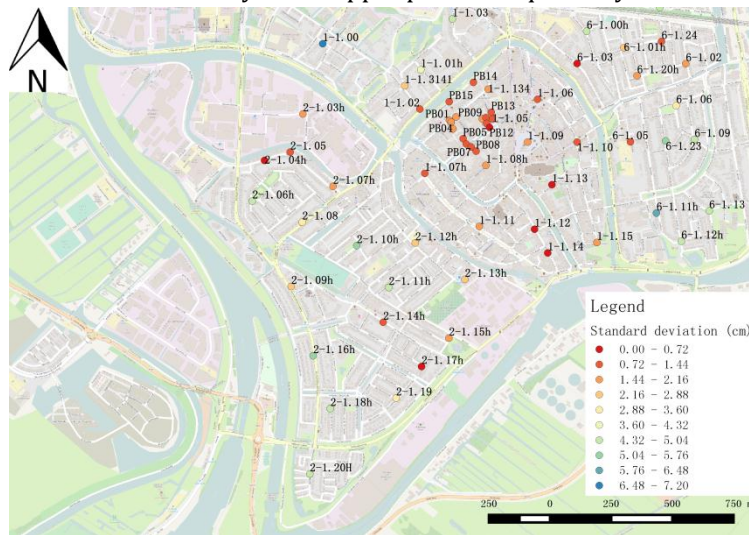


Figure 101 Standard Deviation of groundwater level change after removing 50% of amount from hydraulic conductivity of the upper phreatic aquifer layer

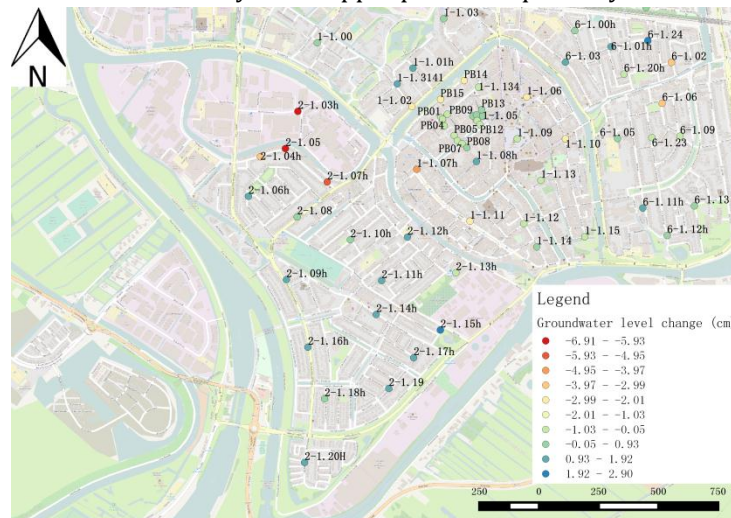


Figure 102 Average value of groundwater level change after adding 50% to hydraulic conductivity of the upper phreatic aquifer layer

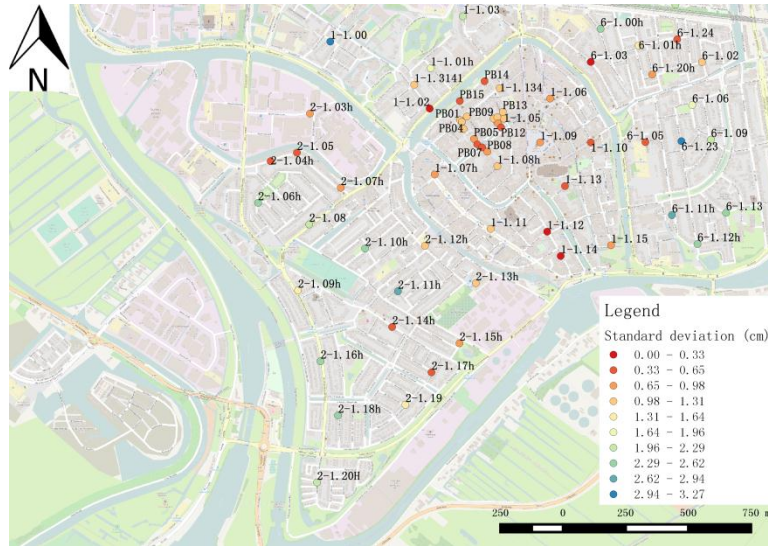


Figure 103 Standard Deviation of groundwater level change after adding 50% to hydraulic conductivity of the upper phreatic aquifer layer

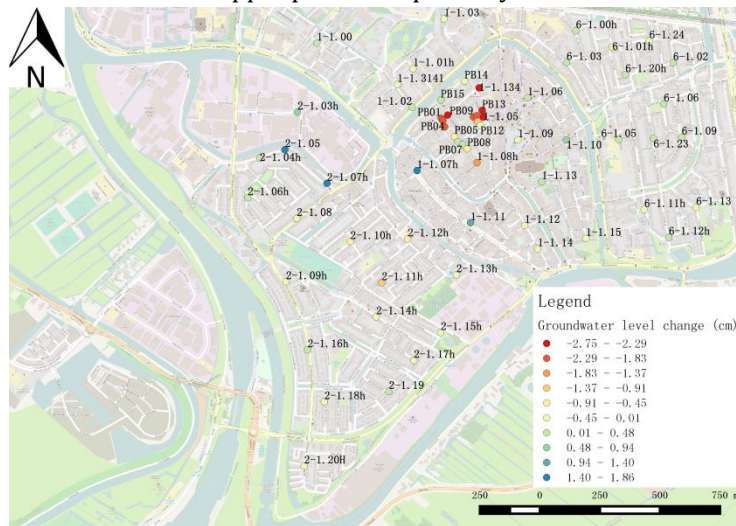


Figure 104 Average value of groundwater level change after removing 50% from hydraulic conductivity of the lower phreatic aquifer layer

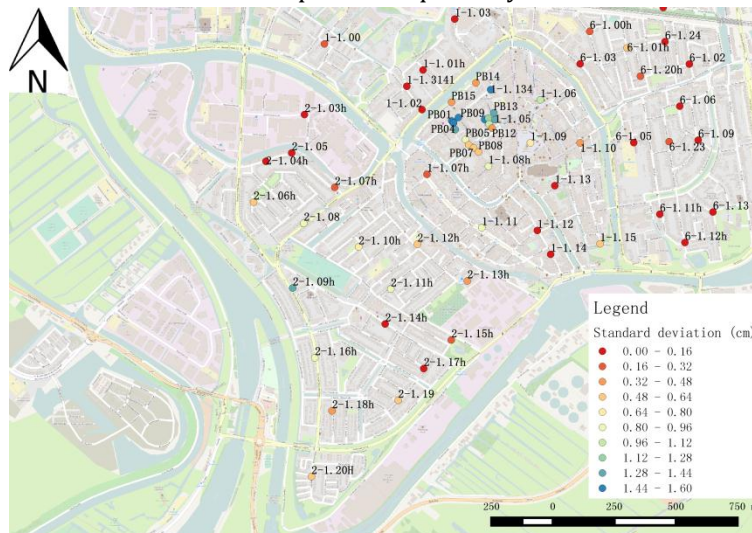


Figure 105 Standard Deviation of groundwater level change after removing 50% from hydraulic conductivity of the lower phreatic aquifer layer

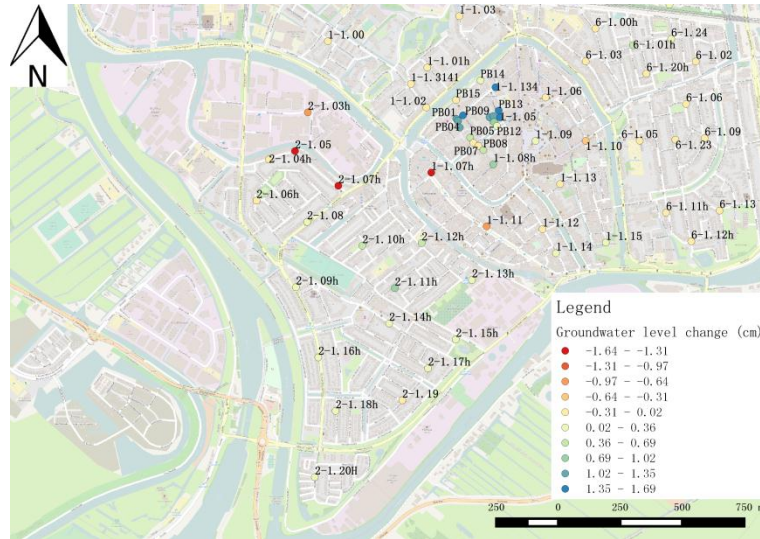


Figure 106 Average value of groundwater level change after adding 50% to hydraulic conductivity of the lower phreatic aquifer layer

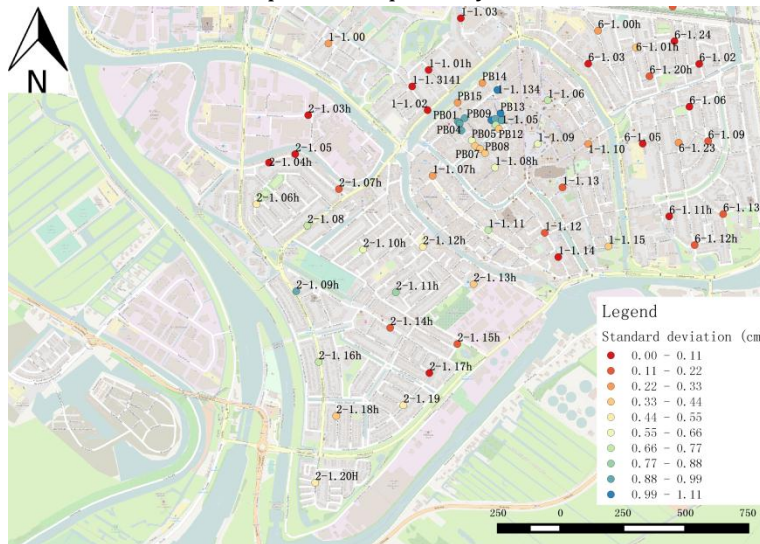


Figure 107 Standard Deviation of groundwater level change after adding 50% to hydraulic conductivity of the lower phreatic aquifer layer

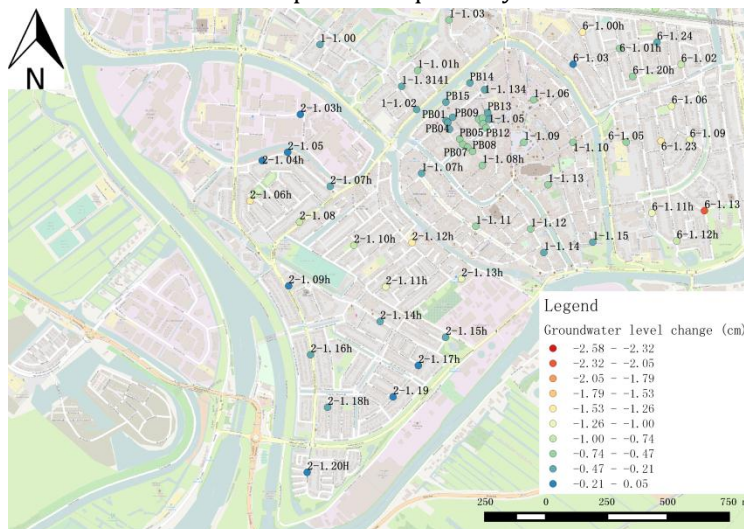


Figure 108 Average value of groundwater level change after removing 50% from storage coefficient

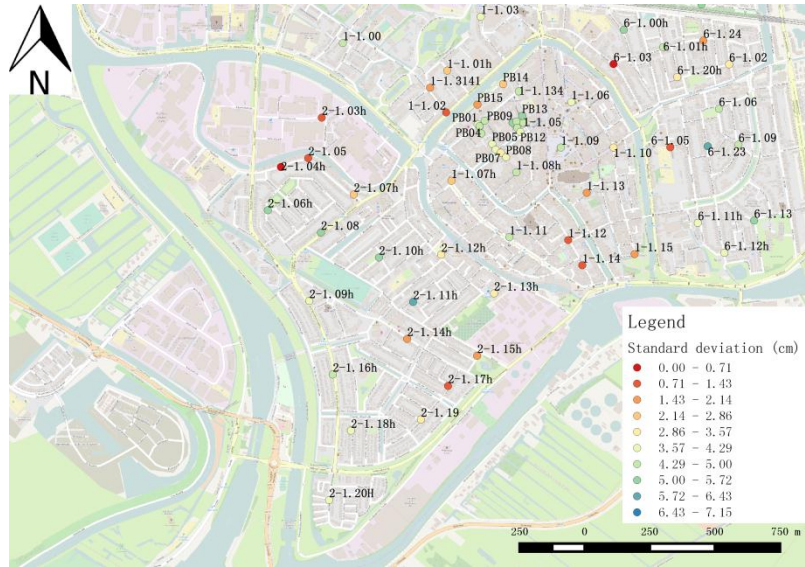


Figure 109 Standard Deviation of groundwater level change after removing 50% from storage coefficient

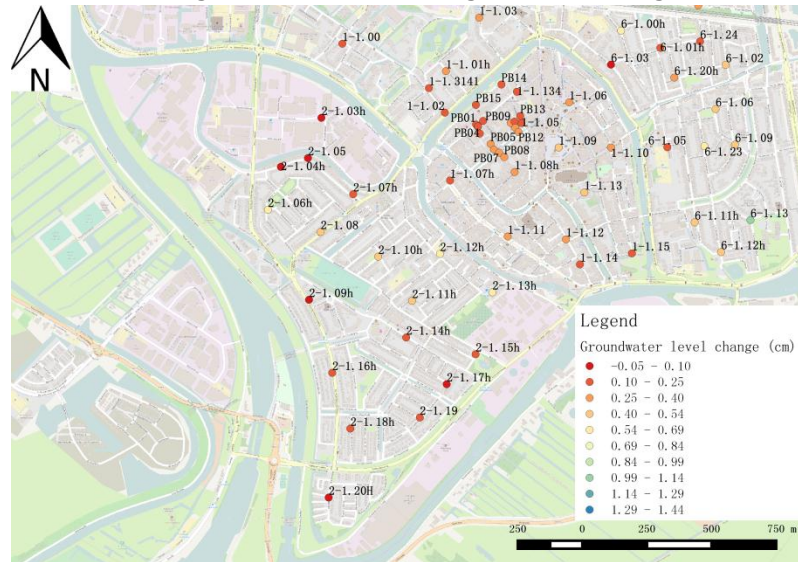


Figure 110 Average value of groundwater level change after adding 50% of amount to storage coefficient

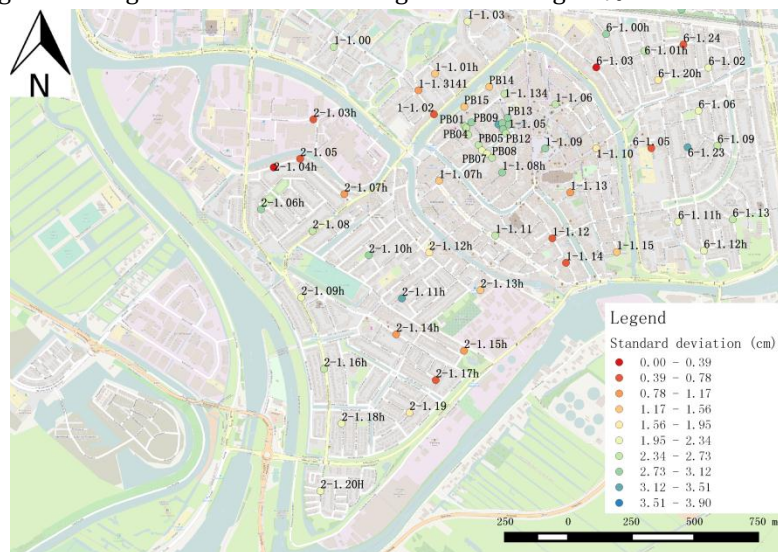


Figure 111 Standard Deviation of groundwater level change after adding 50% of amount to storage coefficient

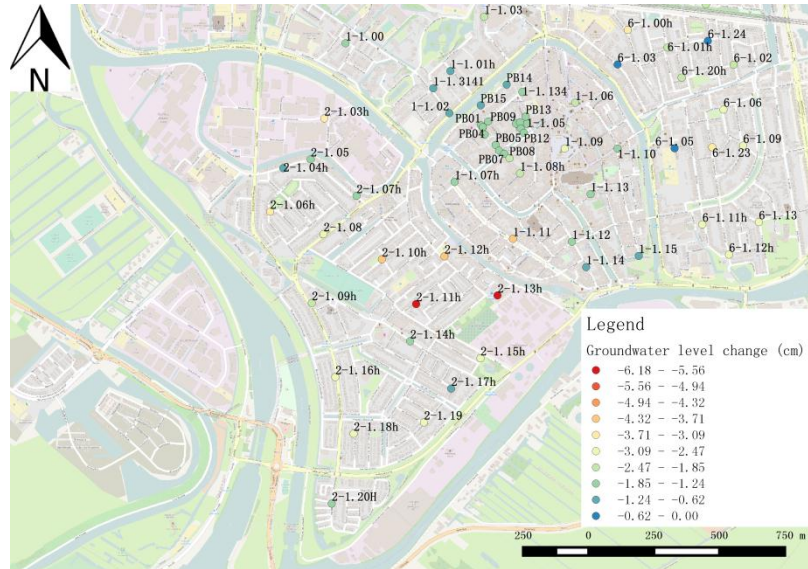


Figure 112 Average value of groundwater level change after removing 50% of value from vertical resistance

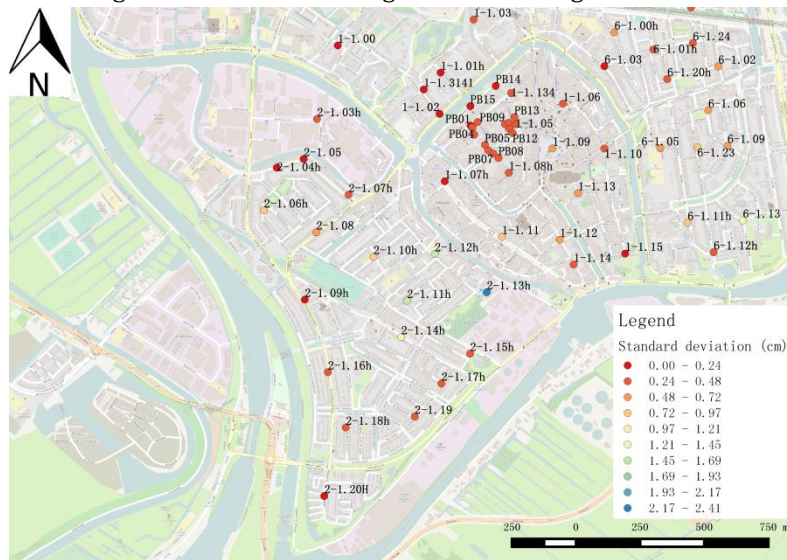


Figure 113 Standard Deviation of groundwater level change after removing 50% of value from vertical resistance

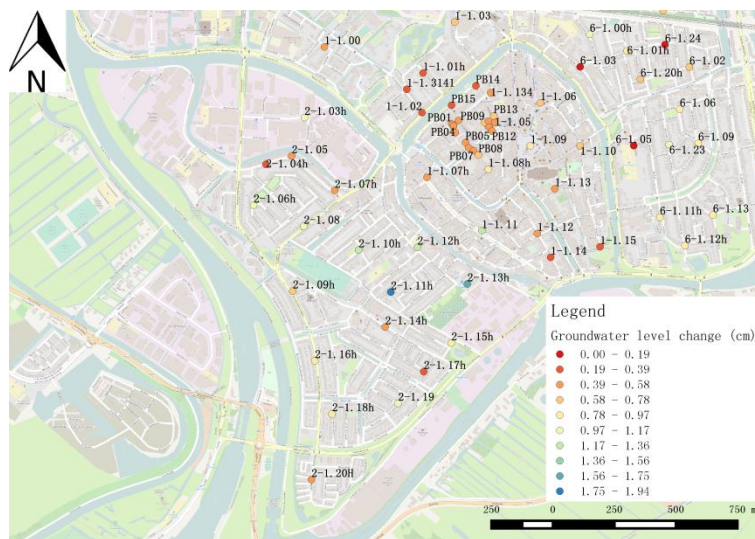


Figure 114 Average value of groundwater level change after adding 50% of value to vertical resistance

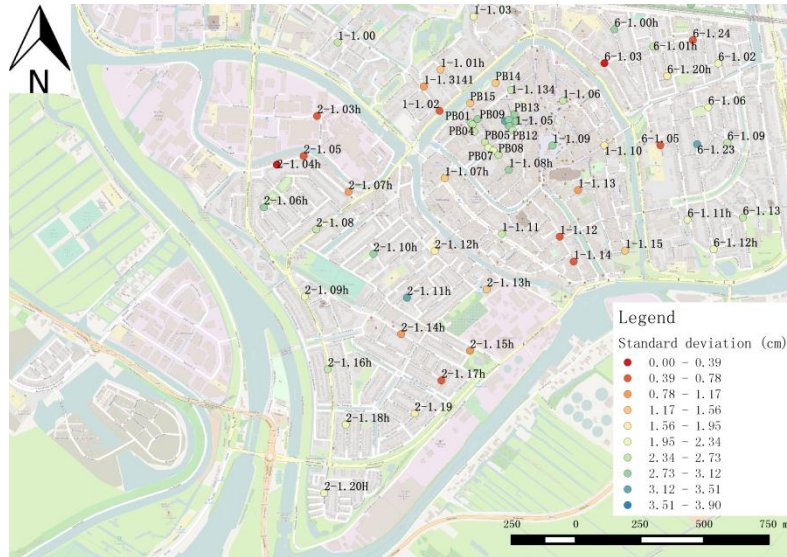


Figure 115 Standard Deviation of groundwater level change after adding 50% of value to vertical resistance

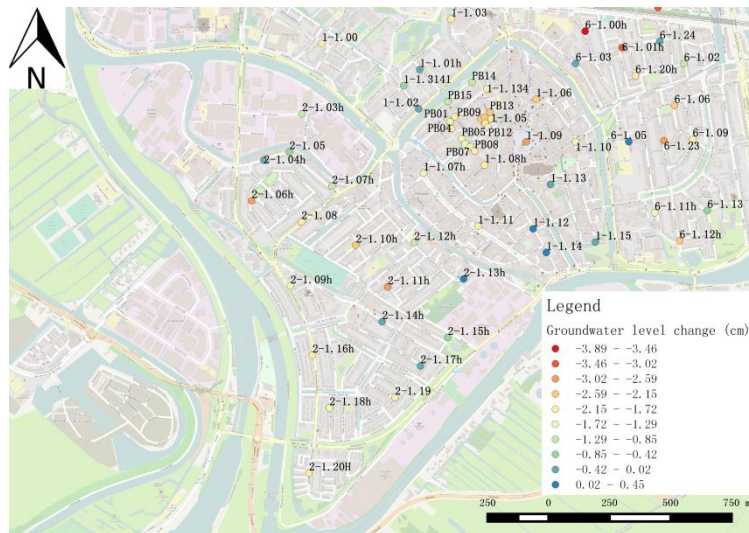


Figure 116 Average value of groundwater level change after removing 50% of calculated value from groundwater recharge

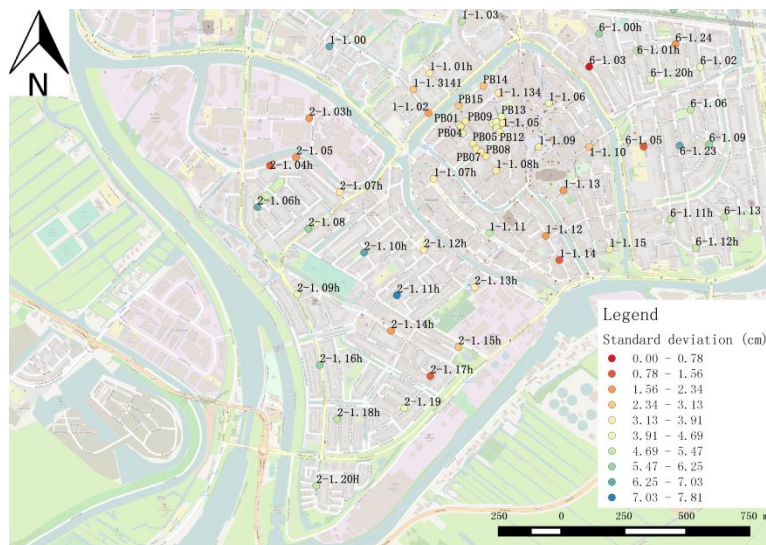


Figure 117 Standard deviation of groundwater level change after removing 50% of calculated value from groundwater recharge

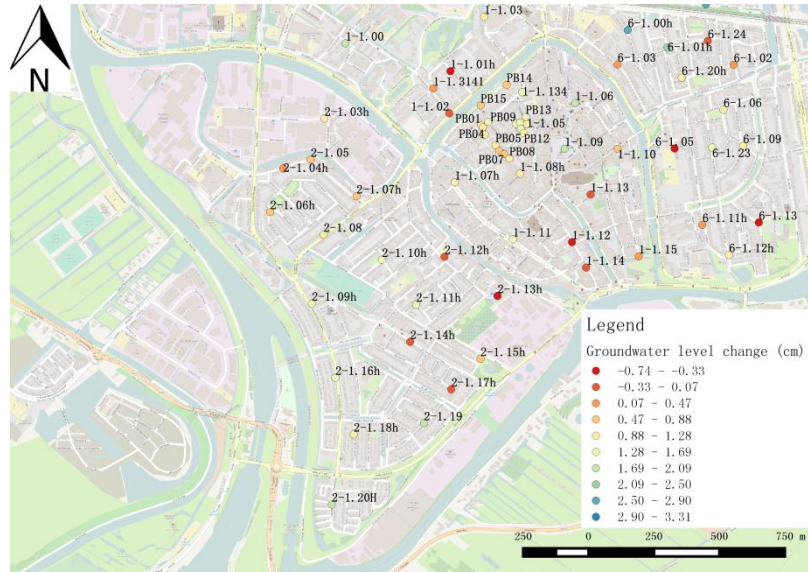


Figure 118 Average value of groundwater level change after adding 50% of calculated value to groundwater recharge

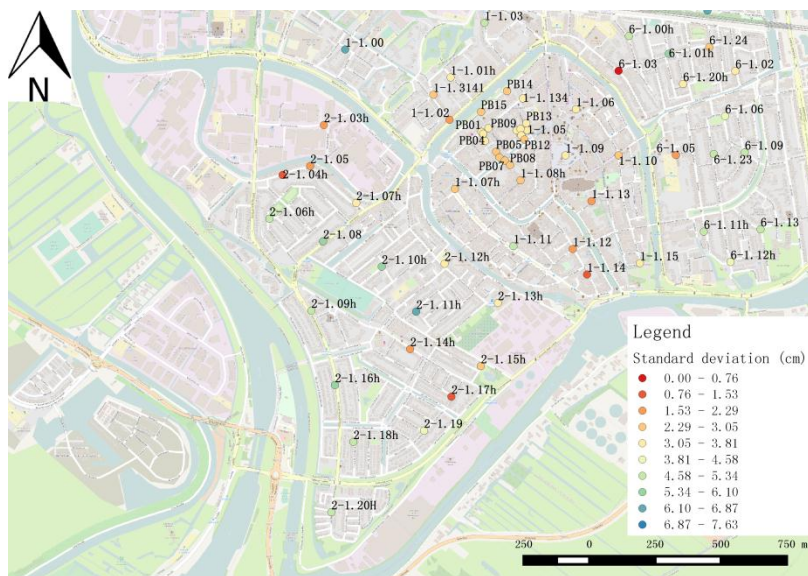


Figure 119 Standard deviation of groundwater level change after adding 50% of calculated value to groundwater recharge

Appendix 2: the mean value and the standard deviation of the level change in scenario test

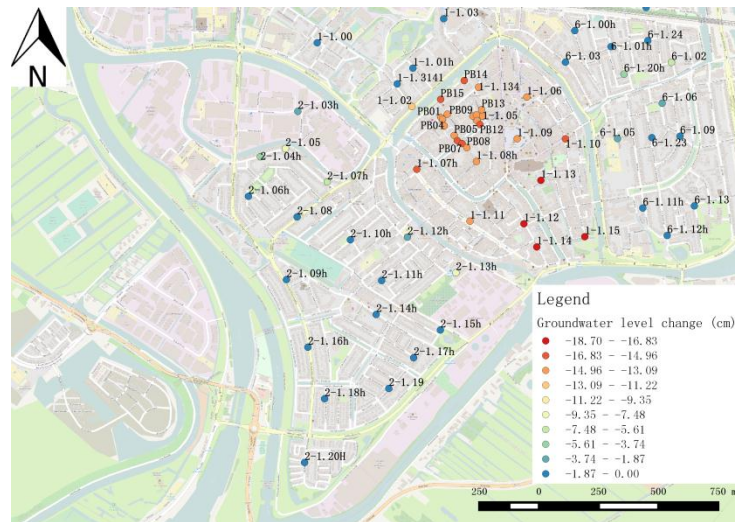


Figure 120 Mean value of groundwater level increase between Scenario 1 and null scenario

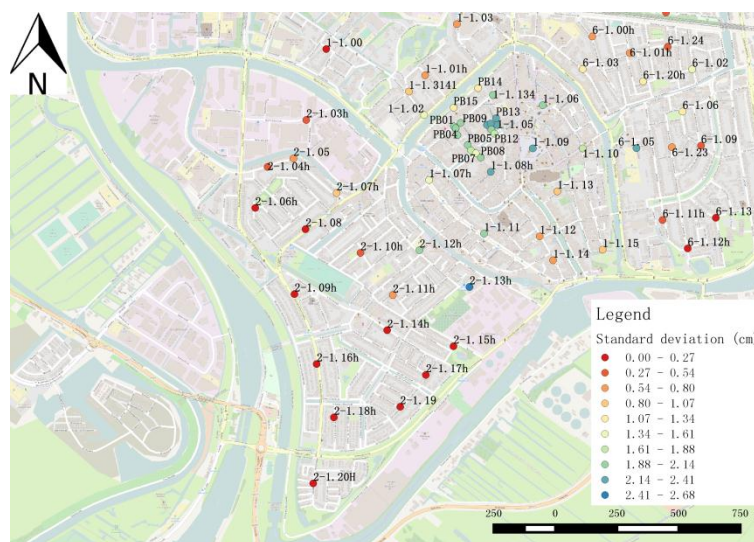


Figure 121 Standard deviation of the level difference between Scenario 1 and null scenario

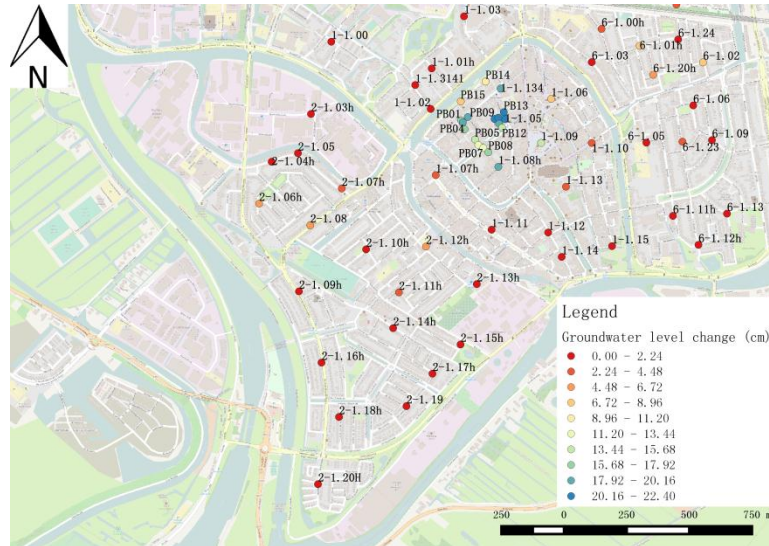


Figure 122 Mean value of groundwater level decrease between Scenario 2 and null scenario

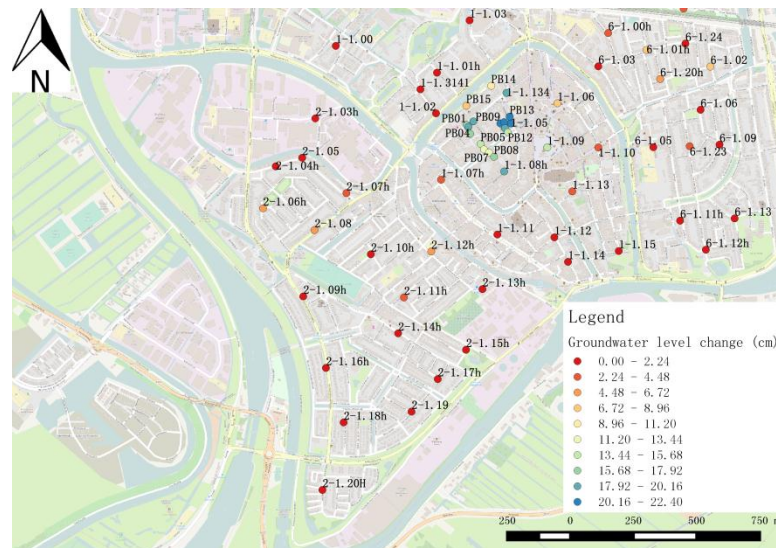


Figure 123 Standard deviation of the level difference between Scenario 2 and null scenario

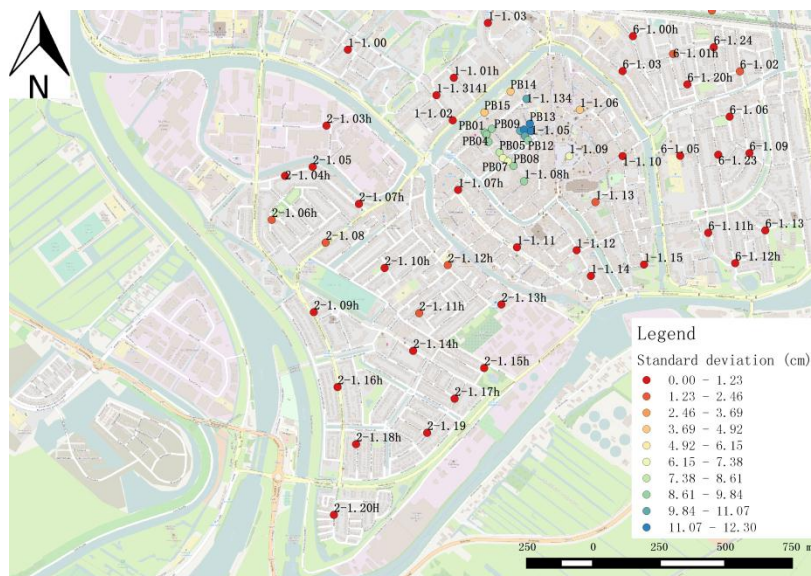


Figure 124 Mean value of groundwater level increase between Scenario 3 and null scenario

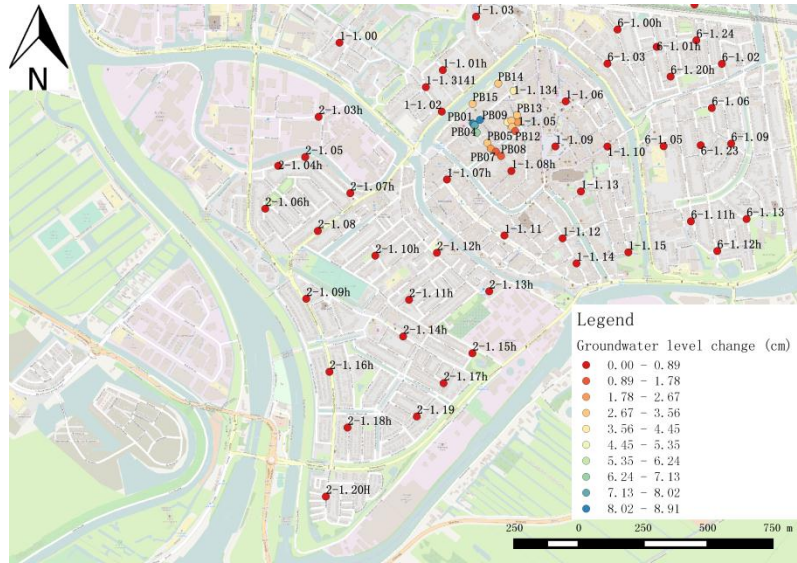


Figure 125 Standard deviation of the level difference between Scenario 3 and null scenario

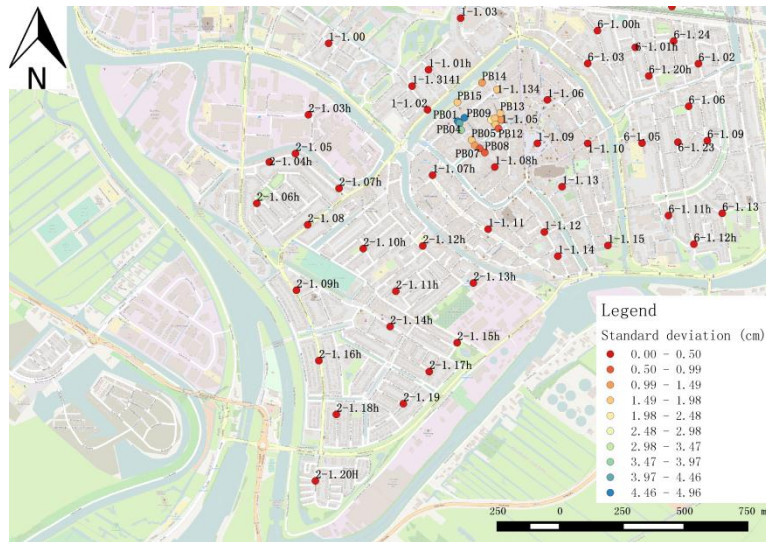


Figure 126 Mean value of groundwater level decrease between Scenario 4 and null scenario

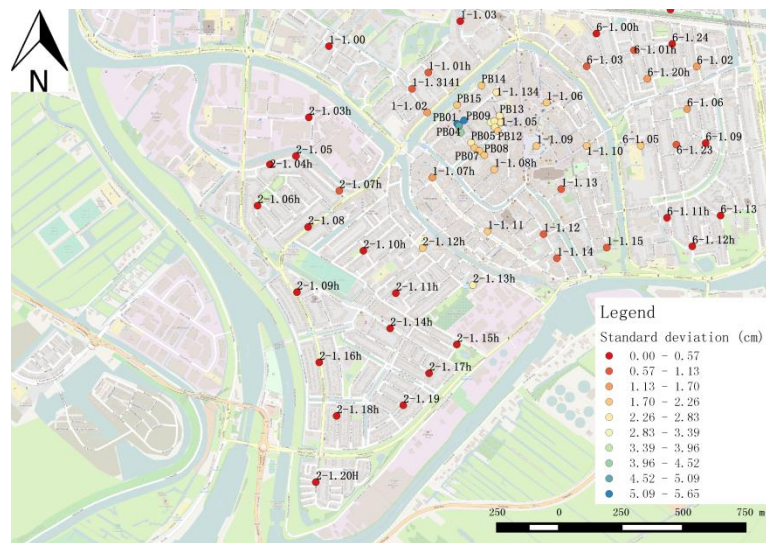


Figure 127 Standard deviation of the level difference between Scenario 4 and null scenario

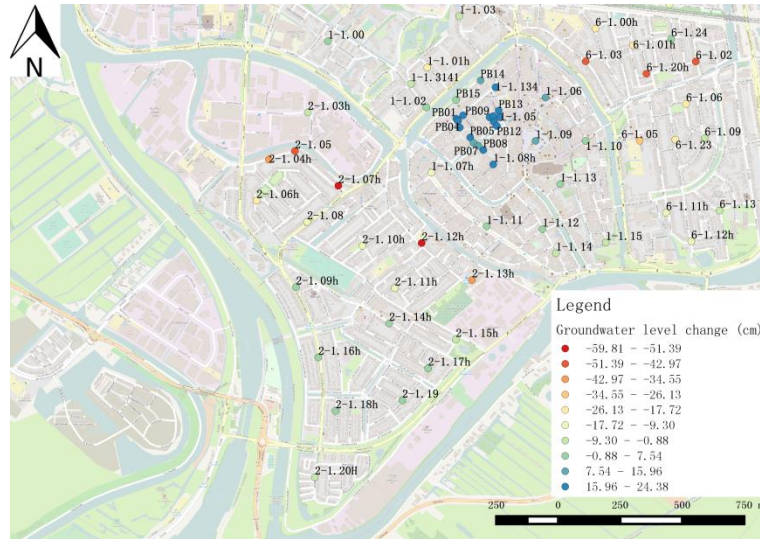


Figure 128 Mean value of groundwater level decrease between Scenario 5 and null scenario

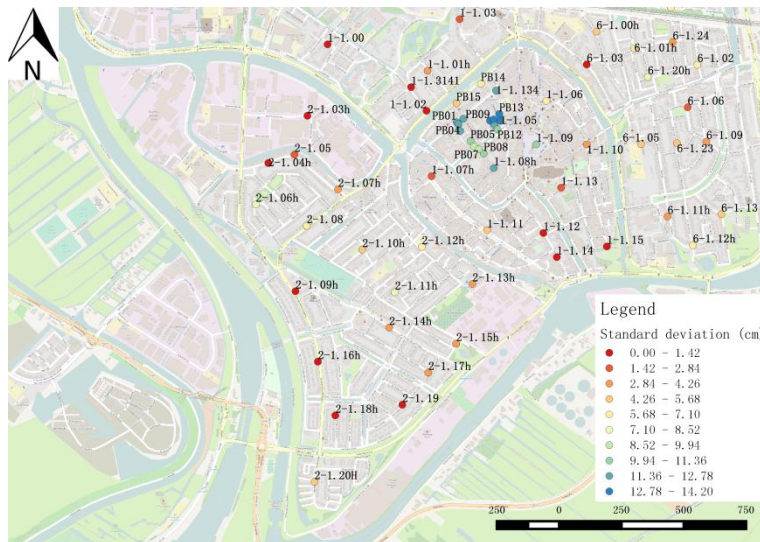


Figure 129 Standard deviation of the level difference between Scenario 5 and null scenario